ISSN 0711-6659

# canadian acoustics
# acoustique canadienne

SEPTEMBER 1992 SEPTEMBRE 1992
Volume 20 -- Number 3 Volume 20 -- Numéro 3



PROCEEDINGS ISSUE

CANADIAN ACOUSTICS WEEK
SEMAINE CANADIENNE D'ACOUSTIQUE

1992

CAHIER DES ACTES

# canadian acoustics

# acoustique canadienne

**THE CANADIAN ACOUSTICAL ASSOCIATION**
**P.O. BOX 1351, STATION "F"**
**TORONTO, ONTARIO M4Y 2V9**

**L'ASSOCIATION CANADIENNE D'ACOUSTIQUE**
**C.P. 1351, SUCCURSALE "F"**
**TORONTO, ONTARIO M4Y 2V9**

**CANADIAN ACOUSTICS** publishes refereed articles and news items on all aspects of acoustics and vibration. Papers reporting new results or applications, as well as review or tutorial papers and shorter research notes are welcomed, in English or in French. Submissions should be sent directly to the Editor-in-Chief. Complete instructions to authors concerning the required camera-ready copy are presented at the end of this issue.

**CANADIAN ACOUSTICS** is published four times a year - in March, June, September and December. Publications Mail Registration No. 4692. Return postage guaranteed. Annual subscription: $10 (student); $35 (individual, corporation); $150 (sustaining - see back cover). Back issues (when available) may be obtained from the Associate Editor (Advertising) - price $10 including postage. Advertisement prices: $350 (centre spread); $175 (full page); $100 (half page); $70 (quarter page). Contact the Associate Editor (advertising) to place advertisements.

**ACOUSTIQUE CANADIENNE** publie des articles arbitrés et des informations sur tous les domaines de l'acoustique et des vibrations. On invite les auteurs à proposer des manuscrits rédigés en français ou en anglais concernant des travaux inédits, des états de question ou des notes techniques. Les soumissions doivent être envoyées au rédacteur en chef. Les instructions pour la présentation des textes sont exposées à la fin de cette publication.

**ACOUSTIQUE CANADIENNE** est publiée quatre fois par année - en mars, juin, septembre et decembre. Poste publications - enregistrement n°. 4692. Port de retour garanti. Abonnement annuel: $10 (étudiant); $35 (individuel, société); $150 (soutien - voir la couverture arrière). D'anciens numéros (non-épuisés) peuvent être obtenus du rédacteur associé (publicité) - prix: $10 (affranchissement inclus). Prix d'annonces publicitaires: $350 (page double); $175 (page pleine); $100 (demi page); $70 (quart de page). Contacter le rédacteur associé (publicité) afin de placer des annonces.

---

# EDITORIAL

We are pleased to publish the second Proceedings Issue of *Canadian Acoustics*, containing 37 unreviewed two-page summaries of papers presented at the technical symposium of Acoustics Week in Canada 1992 in Vancouver. The papers are organized according to the technical session in which they were presented. We encourage authors to submit full versions of their work for publication as fully reviewed technical articles.

On that subject, I am increasingly concerned at the low rate at which papers are being submitted to *Canadian Acoustics* - I have received only three so far this year. This will certainly not allow the journal to continue publishing at even the absolute minimum of two papers per issue. I am actively solliciting papers for the March 1993 issue.

At the recent board of Directors' meeting it was noted that very few applications for the various CAA prizes had been received, to the point that several of these prizes will not be awarded this year. This is hard to understand, since these prizes represent "free" money to support students. Would everyone who supervises graduate students please familiarize themselves with the prizes, described at the end of each issue of the journal, and bring them to the attention of their students and encourage them to apply.

This issue marks the retirement of Winston Sydenborgh from the position of Secretary of the CAA. I guess the Post Office finally got the better of him! On behalf of all members of the Association I'd like to thank Winston for his valuable and dedicated service.

The Vancouver meeting is fast approaching. I hope to see you all there.

Nous sommes heureux de publier le deuxième Actes de l'*Acoustique Canadienne* comportant 37 résumés de deux pages non révisés des communications qui seront présentées dans le cadre du programme technique de la Semaine de l'Acoustique Canadienne 1992 à Vancouver. Les papiers sont classés par session technique dans laquelle ils seront présentés. Nous encourageons les auteurs à soumettre une version complète de leurs travaux pour publication comme article technique révisé.

A ce sujet, je suis de plus en plus inquiet de la baisse de soumission d'articles à l'*Acoustique Canadienne*; je n'ai reçu que trois articles à ce jour cette année. Ce bas taux de participation ne permettra pas de poursuivre la publication du journal même à un nombre minimal de deux papiers par numéro. Je sollicite activement la soumission d'articles pour le numéro de mars 1993.

A la réunion récente du Conseil d'administration, il a été mentionné que peu de gens ont posé leur candidature pour les prix offerts par l'ACA, au point que plusieurs des prix ne seront pas attribués cette année. Ceci est difficile à comprendre puisque ces prix représentent de l'argent "gratuite" pour encourager les étudiants. Nous invitons tous les superviseurs d'étudiants gradués à se familiariser avec les prix décrits à la fin de chaque numéro du journal et d'en informer les étudiants afin de les encourager à poser leur candidature.

Ce numéro coincide avec le départ de Winston Sydenborgh au poste de Secrétaire de l'ACA. Je devine que le bureau de poste a eu raison de lui! Au nom de tous les membres de l'Association, j'aimerais remercier Winston pour son travail consciencieux et dévoué.

Le congrès de Vancouver approche à grands pas. J'espère vous y rencontrer.

# INCREDIBLE VERSATILITY

## At Only 2.2 lbs.

RION

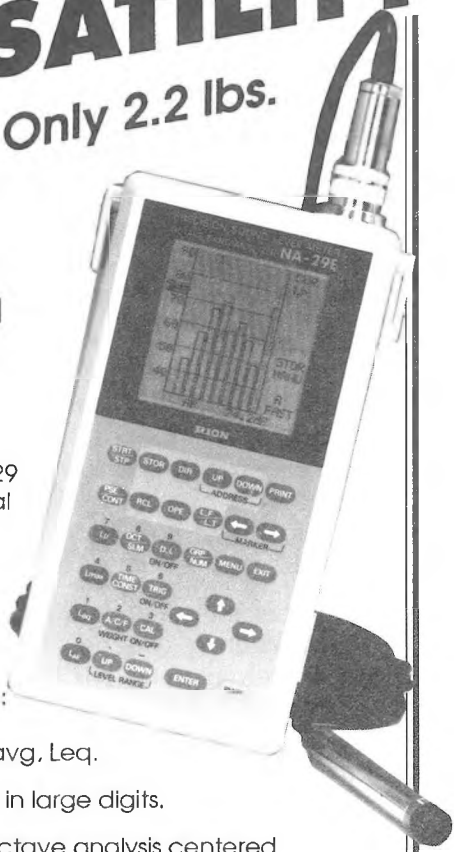

Rion's new NA-29 provides unusual capabilities for a pocket-size acoustical analyzer weighing only 2.2 lbs. It's displays include:

- ❑ Lmax, Ln, Lavg, Leq.
- ❑ Sound level in large digits.
- ❑ Real-time octave analysis centered 31.5 Hz. through 8000 Hz.
- ❑ Level vs. time, each frequency band.
- ❑ 1500 stored levels or spectra.
- ❑ Spectrum comparisons.

It also features external triggering, AC/DC outputs, and RS-232C I/O port. A preset processor adds additional versatility for room acoustics and HVAC applications. To minimize external note taking, users can input pertinent comments for each data address. Specify the NA-29E for Type 1 performance or the NA-29 for Type 2.

Our combined distribution of Norwegian Electronics and Rion Company enables us to serve you with the broadest line of microphones, sound and vibration meters, RTAs, FFTs, graphic recorders, sound sources, spectrum shapers, multiplexers, and room acoustics analyzers, plus specialized software for architectural, industrial and environmental acoustics. You'll also receive *full* service, warranty and application engineering support. Prepare for the '90s.

***Call today.*** (301) 495-7738

**SCANTEK INC.**

*Norwegian Electronics • Rion*

# PALM SIZE FFT

RION

## *Amazingly smaller and lighter than a lap-top*

Our new SA-77 FFT Analyzer is a true miniature. Yet it is very big in capability.

- 0 – 1 Hz to 0 – 50 kHz.
- Zooms to 800 lines.
- FFT, phase and PDF analysis and time waveform.
- External sampling for order analysis.
- Stores 150 screen displays plus 30K samples of time data.
- Single/double integration or differentiation.
- Arithmetic/exponential averaging or peak-hold.
- Built-in RS-232C.
- $8\frac{1}{4}$ X $4\frac{3}{8}$ X $1\frac{1}{2}$ inches.
- 23 ounces.

Call today. Discover how much noise, vibration and general signal analysis capability you can hold in the palm of your hand. And at how reasonable a cost.

**SCANTEK INC.**

*Norwegian Electronics • Rion*

# PROCEEDINGS OF ACOUSTICS WEEK IN CANADA 1992
# ACTES DE LA SEMAINE DE L'ACOUSTIQUE CANADIENNE 1992

## Table of Contents / Table de matières

MEASUREMENT / MESURE



UNDERWATER ACOUSTICS / ACOUSTIQUE SOUS-MARINE

# Modelling Auditory Scene Analysis: A Representational Approach

**Guy J. Brown and Martin P. Cooke**

Department of Computer Science, University of Sheffield

P.O. Box 600, Mappin Street, Sheffield S10 2TN, U.K.

## Introduction

Speech is normally heard in the presence of other interfering sounds, a fact which has plagued speech technology research. In this paper, a technique for segregating speech from an arbitrary noise source is described. The approach is based on a model of human auditory processing. The auditory system has an extraordinary ability to group together acoustic components that belong to the same sound source, a phenomenon named *auditory scene analysis* by Bregman [1]. Models of auditory scene analysis could provide a robust front-end for speech recognition in noisy environments [4], and may also have applications in automatic music transcription [9]. Additionally, we hope that models of this type will contribute to the understanding of hearing and hearing impairment.

## Auditory Maps

In analogy with the work of Marr [7] in vision, the modelling approach adopted here views audition as a series of representational transforms, each of which makes some aspect of the preceding representation explicit. A possible criticism of this functionalist philosophy is that the choice of representation is somewhat arbitrary. Therefore, we have attempted to justify our model by using representations that are motivated by physiological studies of the higher auditory system. Important acoustic parameters appear to be place-coded in the higher auditory system within orderly arrays of neurons, called *auditory maps*. The maps are two-dimensional, with frequency and some other parameter represented on orthogonal axes. The value of the parameter at a particular frequency is indicated by the firing rate of a cell at the corresponding position in the neural array. Parameters that appear to be coded in this manner include periodicity, intensity, frequency transition, spectral shape, interaural time difference and interaural intensity difference (see [2] for a review).

Physiological maps of this type provide a good basis for deriving useful representations of acoustic events. Hence, our approach has been to model auditory maps that provide the primitives needed for auditory scene analysis, and to demonstrate an algorithm for segregating concurrent sounds which exploits these primitives in an effective way.

## Representations For Auditory Scene Analysis

Bregman [1] has noted that mechanisms of auditory scene analysis can be broadly classified as *simultaneous* or *sequential*. Simultaneous grouping processes segregate concurrent sounds into different perceptual streams, whereas sequential grouping processes segregate acoustic components that have arisen from the same source over time. Here, primitives for simultaneous grouping are provided by auditory maps coding *periodicity*, *onsets* and *offsets*. Primitives for sequential grouping are provided by a map of *frequency transition*.

*Auditory Nerve*. The input to each auditory map is provided by a simulation of firing activity in the auditory nerve. Mechanical filtering in the cochlea is modelled by a bank of gammatone filters, with centre frequencies spaced linearly on an ERB-rate scale. Transduction by inner hair cells is simulated by the Meddis [8] hair cell model, which provides a probabilistic representation of auditory nerve activity.

*Periodicity Map*. Periodicity information is extracted from the auditory nerve by a running autocorrelation analysis at each characteristic frequency, as suggested by Licklider [6] in his "duplex" model of pitch perception. Auditory filters that are responding to the same spectral dominance give rise to a similar pattern of response in the periodicity map, providing an early opportunity for grouping channels which belong to the same acoustic source. The temporal fine structure in adjacent channels is compared by a cross-correlation metric, and channels with a similar pattern of response are combined into *periodicity groups*.

*Onset and Offset Maps*. Onsets and offsets are identified by maps that have been developed in analogy with ON-IN cells in the cochlear nucleus, which receive an excitatory input and a delayed inhibitory input. The delay before inhibition is a variable parameter which is represented along one axis of the onset map, and determines the rate of amplitude onset that the cell is most responsive to. Offset cells are modelled in a similar manner, except that excitation is delayed relative to inhibition.

*Frequency Transition Map*. An early problem facing perceptual grouping mechanisms is how to relate the auditory representation of an event at a particular time with the representation of the same event at a later time. Here, a map of frequency transition is used to solve this "correspondence problem". Each neuron in the map is tuned to a particular sweep rate, according to the orientation of its receptive field. A similar idea has recently been proposed by Mellinger [9]. When a moving dominance is aligned with a receptive field, a peak of activity occurs at the corresponding frequency and orientation in the map. Therefore, the position and direction of movement of spectral dominances can be identified by locating the maxima in the frequency transition map at each time slice.

## Modelling Auditory Scene Analysis

An algorithmic strategy for auditory scene analysis is employed, which emphasizes the time-frequency nature of the grouping process. Initially, the auditory scene is characterized as a collection of *auditory objects*, which are formed by using the frequency transition map to track periodicity groups across time and frequency. Subsequently, a pitch contour is derived for each object using the periodicity map, and auditory objects which have a similar pitch contour are grouped together. Objects can also be grouped if they start or end at the same time. In this case, the onset and offset maps are scanned to ensure that an onset or offset has occurred.

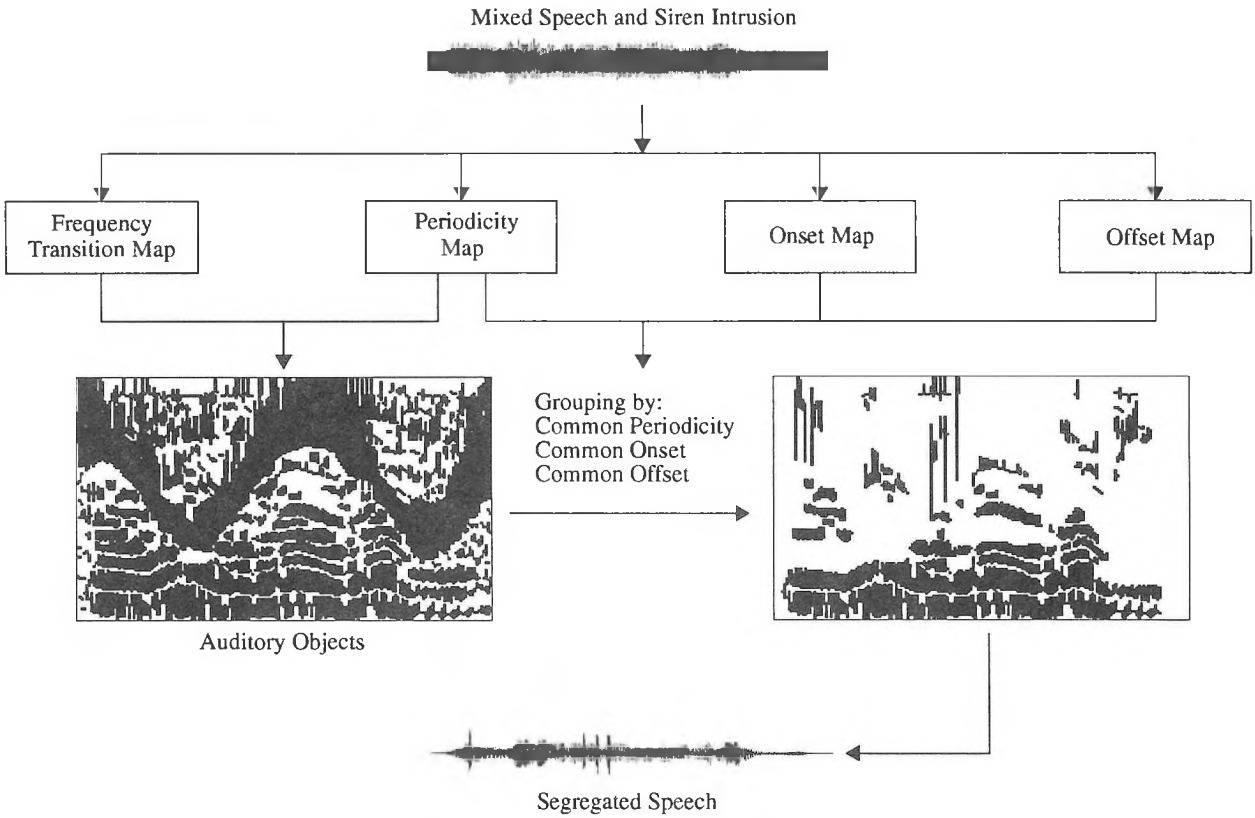


**Evaluation**

The model has been evaluated using the task of segregating speech from a wide variety of intrusions, such as "cocktail party" noise and other speech. The performance of the model has been assessed in two ways, one qualitative and the other quantitative. Firstly, given the periodicity groups that define a source, it is possible to resynthesize a waveform for the source which can be examined for intelligibility and naturalness in listening tests. The periodicity groups indicate which channels of the auditory filterbank belong to the source at a particular time, so that a resynthesized waveform can be obtained simply by summing these time-frequency regions of the (phase-corrected) gammatone filterbank output. Informally, segregated speech resynthesized in this way is highly intelligible and quite natural. Secondly, performance can be quantified by comparing the signal-to-noise ratio (SNR) before and after segregation (see [3]). On a test set of ten different noise intrusions, an improvement in SNR is obtained in each case.

**Conclusions and Future Work**

A model of auditory scene analysis has been described which uses information about periodicity, frequency transition, onset and offset to group acoustic components together. The model is able to segregate speech from a wide range of intrusive noise sources. Currently, the model is restricted to segregating periodic sounds (such as voiced speech). Additionally, the approach taken here is entirely data-driven, whereas it is known that learned (schema-driven) principles play an important role in auditory scene analysis [1]. Edelman [5] has suggested that neural maps are central to mechanisms of learning, and we are about to investigate the use of auditory maps in the formation and application of schema-driven grouping principles.

**References**

[1] A.S. Bregman (1989) *Auditory scene analysis*. MIT Press.

[2] G.J. Brown (1992) *A representational approach to auditory scene analysis*. PhD Thesis, University of Sheffield, in preparation.

[3] G.J. Brown and M.P. Cooke (1992) *A computational model of auditory scene analysis*. Proceedings of ICSLP-92, in press.

[4] M.P. Cooke (1991) *Modelling auditory processing and organization*. PhD Thesis, University of Sheffield.

[5] G.M. Edelman (1989) *Neural Darwinism: The theory of neuronal group selection*. Oxford University Press.

[6] J.C.R. Licklider (1951) *A duplex theory of pitch perception*. Experientia, **7**, 128-134.

[7] D. Marr (1982) *Vision*. W.H. Freeman.

[8] R. Meddis (1986) *Simulation of mechanical to neural transduction in the auditory receptor*. Journal of the Acoustical Society of America, **79**, 702- 711.

[9] D.K. Mellinger (1991). *Event formation and separation in musical sound*. PhD Thesis, Stanford University.

# DISCRIMINATION OF FREQUENCY TRANSITIONS AS A FUNCTION OF VARYING SPECTRAL CUES AMONG YOUNG AND ELDERLY ADULTS

**J.F. MacNeil and E.B. Slawinski**
**University of Calgary, Calgary, Alberta**

## Introduction

Next to the changes that are noted in hearing sensitivity loss, the deterioration in speech discrimination is the most commonly recognized characteristic of age-related changes in auditory function. This well-documented reduction in speech discrimination is a pivotal auditory problem associated with aging given that elderly individuals without a high sensitivity loss report difficulty in understanding speech in optimum conditions; that is, speech perception difficulties are greater than would be expected on the basis of pure tone sensitivity levels. One relevant aspect underlying the difficulties that elderly adults experience may be a function of the brevity and rapid spectral changes which characterize some speech segments. Indeed, reduced spectral and temporal resolution has been reported for elderly listeners who demonstrate normal pure tone thresholds (Cranford & Stream, 1991; Maden & Feth, 1992; Robin & Royer, 1989; Trainor & Trehub, 1989). This study investigated how various spectral characteristics influence discrimination of short duration, dynamic signals as a function of age.

## Method

Subjects

Subjects were 15 adult undergraduate students from the University of Calgary (mean age 23.8 years; range = 19-38 years) and 11 elderly subjects (mean age 71.4 years; range = 66-75 years) recruited from the community. All the young adults had normal hearing (no greater than +15 dB HL) for .5 to 8 KHz; the elderly subjects had normal thresholds up to 1 KHz with varying degrees of hearing loss from 2 KHz to 8 KHz.

Stimuli

Three continua of 17 signals increasing in 10 Hz steps were generated on a Micro Vax II computer. Stimuli were 60 ms in duration with 5 ms rise/fall times, sampled at 20 KHz, and low passed at 3 KHz To ensure that initial information was identical across continua, a 20 ms 1/3 octave band noise burst was affixed to the beginning of each signal. One continuum had a constant onset frequency of 900 Hz and diverged to varying offset frequencies ranging from 950 Hz to 1110 Hz. A second continuum had a constant rate of change of 3.4 Hz/ms, onset frequencies from 740 Hz to 950 Hz, and diverged to the same offset frequencies (950 Hz to 1110 Hz) as the first series. Onset frequencies of the third continuum ranged from 900 Hz to 1100 Hz and converged on a terminal frequency of 1110 Hz.

Procedure

Subjects were seated in an anechoic chamber and stimuli were delivered monaurally via Kross Pro/4x headphones at 65 dB SPL. A two-alternative forced-choice paradigm designed to determine the smallest discriminable differences that subjects could determine was used. Each trial consisted of two stimuli with an ISI of 500 ms and subjects responded 'same' or 'different'. The first signal in each continuum served as the 'standard' and was present on every trial, though the position as first or second member of the pair was randomly varied. The standard was paired with every other signal 6 times for a total of 96 'different' trials and 40 'same' or catch trials were included to serve as a metric of response bias for a total of 136 trials. Presentation order of of trials was randomized for each subject for each continuum.

## Results

Individual psychometric functions were calculated with probit analysis and threshold was defined as the frequency difference corresponding to the 75% correct position. Averaged psychometric functions for all three continua for both age groups are shown in Figure 1. Signals are designated as having a constant onset frequency, constant rate of change, or a constant offset frequency. Functions for the young adults are consistently to the left of those for the elderly subjects indicating a greater degree of sensitivity for discrimination of these signals.

Among the functions for the young adults, the one corresponding to the signals with a constant onset frequency has the steepest slope while the constant offset frequency signals has the shallowest slope. Among the functions for the elderly listeners, there is no difference in the functions for the constant onset frequency and the constant rate of change signals, but these are both to the left of the function for the constant offset frequency series. Neither age group asymptoted at 100 % correct performance for signals converging on the same offset frequency.

A 2 X 3 analysis of variance (ANOVA) of the threshold values revealed significant main effects for age $F(1,22) = 7.21$, $p<.05$, and signal type, $F(2,44) = 27.31$, $p<.001$. The signal type and age interaction was also significant, $F(2,44) = 4.41$, $p<.01$. Planned comparisons showed significant differences between the young and elderly adults for discrimination of signals with a constant onset frequency , $F(1,22) = 12.7$, $p<.025$, and a constant rate of change, $F(1,22) = 6.2$, $p<.025$. Young adults needed smaller differences between the constant onset frequency stimuli (M = 50 Hz, SD = 18 Hz) compared to the elderly listeners (M = 86 Hz, SD = 31 Hz). The same pattern was noticed for

signals with a constant rate of change where young adults showed smaller jnds (M = 55 Hz, SD = 28 Hz) relative to elderly listeners (M = 84 Hz, SD = 29 Hz). There were no significant differences between the age groups for the jnds associated with the discrimination of signals converging on the same offset frequency (111 Hz for the young adults versus 110 Hz for the elderly adults).

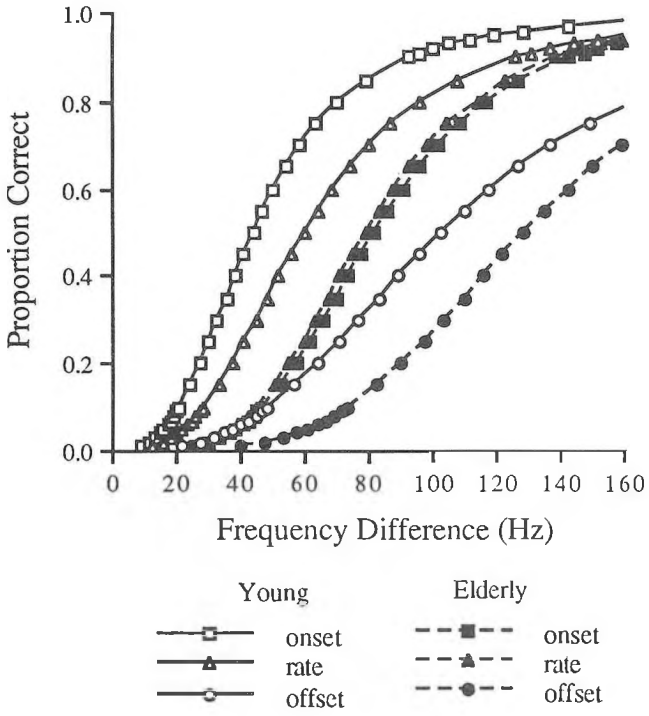


**Figure 1.** Psychometric Functions For Young and Elderly Adults for Each Signal Type.

## Conclusions

The principal finding of this study was that elderly listeners were less able than young adults to distinguish between two sequential stimuli suggesting that elderly listeners have an impaired ability to process rapid information. One important finding was that elderly listeners showed no significant differences among stimuli which had varying offset frequencies regardless of rate of change. This indicates that rate of change information is not utilized as efficiently by the elderly relative to the young adults and potentially represents a reduced ability to integrate temporal envelope modulation in addition to spectral cues when discriminating signals. It is supportive of Schouten and Pols (1989) theory of pitch extraction where the pitch of the terminal frequency is the important information. If the pitch of the terminal frequency was the only cue being used it would be expected that thresholds for signals which have varying offset frequencies would be very similar to each other. Young adults, however, showed smaller threshold values for signals which had differing offset frequencies and varying rates of change relative to signals which had only differing terminal frequencies. Among the elderly listeners pitch/timbre cues appear to be the critical component for differentiating signals.

Pure tone threshold levels are neither the limiting factor in the task, nor an accurate metric of the ability to differentiate signals. These data cannot be interpreted in terms of an associated hearing loss. There was no consistent pattern among the individual data for the elderly subjects. Two elderly listeners who had normal thresholds to 2 KHz reached threshold for the constant onset frequency stimuli when the signals were 100 Hz apart, while another elderly listener who had a moderate loss of 35 dB HL up to 2KHz achieved threshold for the same series of signals at 50 Hz difference. One elderly subject with pure tone sensitivity of 15 dB HL to 3 KHz did not reach threshold at all. The poorer performance of the elderly subjects may be a function of decreased temporal acuity among these individuals consistent with the findings of Robin and Royer (1989).

The age related results may be a function of the greater effect of masking by the noise burst on the elderly relative to the younger subjects. Though this study does not represent a typical masking paradigm (the noise burst and signal were both suprathreshold), the initial noise burst could have reduced the effective listening duration of the signal. This would have impacted upon the temporal resolution ability of the elderly subjects and impaired processing of rapid information.

## References


Cranford, J.L. & Stream, R.W. (1991). Discrimination of short duration tones by elderly subjects, *Journal of Gerontology:Psychological Sciences, 46(1)*, p37-p41.

Maden, J.P. & Feth, L.L. (1992). Temporal resolution in normal-hearing and hearing-impaired listeners using frequency-modulated stimuli, *Journal of Speech and Hearing Research, 35*, 436-442.

Robin, D.A. & Royer, F.L. (1989). Age-related changes in auditory temporal processing, *Psychology and Aging, 4 (2)*, 144-149.

Schouten, M.E.H. & Pols, L.C.W. (1989). Identification and discrimination of sweep formants, *Perception & Psychophysics, 46(3)*, 235-244.

Trainor, L.J. & Trehub, S.E. (1989). Aging and auditory temporal sequencing: ordering the elements of repeating tone patterns, *Perception & Psychophysics, 45(4)*, 417-426.



**Acknowledgements.** The authors are grateful to Geoff Smith for programming the algorithms and to Dr. J.J. Eggermont for providing the stimuli synthesis equipment.

# APPLICATION OF *FIR* DIGITAL FILTERS TO MODEL HUMAN AUDITORY PERCEPTION OF SHORT-TIME AMPLITUDE IN LOW-FREQUENCY RAPID SPECTRUM CHANGE*

**Brenda Orser**
Department of Linguistics, University of Victoria
P.O.Box 3045, Victoria, B.C. V8W 3P4 Canada

**Introduction**: FIR (finite impulse response) filters are applied using CSL,[1,2] in the quantization of the SPL amplitude component of linguistic resonant pharyngeal consonants,/ʕ/, in word-initial CV environments, Fig.1. Only the onset consonant amplitude responses are modelled, with FIR transfer functions corresponding to SPL acoustic responses: glottal excitation (forced response), Fig.2, separate from the pharyngeal transmission (natural response), Fig.3. The FIR transfer function (impulse response) system design has the following properties: pharyngeal transmission interpreted as odd amplitude/even phase; this is differentiated from glottal source characteristics: even amplitude/odd phase. This motivates a DTLTI system.

The objective of the FIR design as applied to speech transmission is to derive linguistic structure, where transmission functions correspond to both segmentation in the auditory system, and active articulatory mechanisms in speech production. The general issue is the separation of the system from the source, decoupling vocal-cavity transfer resonances from vibrations of the vocal cords.[3] The basic design problem is the filter order: specifically, determinants of the SPL amplitude constant derived from an impulse which integral to the pharyngeal transfer function will satisfy a linguistic system's transmission requirements for the auditory analysis of pharyngeal resonants. These, as transients, exhibit an increased and rapid spectrum change of amplitude in the low-mid frequency region, Fig.3. Also, the decreasing energy in the glottal excitation contrasts with the increasing energy exhibited in the transient[4,5] (Figures not incl.).

**Filters**: Neither the (temporal) rapidity of the spectral change, nor the bandwidth are modelled. These instead are derived as constants, which are linear. An FIR filter structure is implemented to obtain a linear phase and thus a constant phase shift, allowing the amplitude response to be modelled. In an FIR filter the impulse response $h(n)$ is limited to a finite number of points.[6] The impulse response is expressed as

(1) $h(n) = \alpha_n$ for $0 \le n \le k$, or (2) $h(n) = \sum_{i=0}^{k} \alpha_i \delta(n - i)$
$= 0$ elsewhere

The transfer function for (1) or (2) is expressed as

(3) $H(z) = \sum_{m=0}^{k} \alpha m_{z-m} = \alpha_0 + \alpha_1 z^{-1} + \ldots + \alpha_k z^{-k}$,

where $k$ = the number of terms, and function order. The difference equation for (3) relating the output to the input is

(4) $y(n) = \sum_{i=0}^{k} \alpha_i x\ (n\text{-}i) = \sum_{i=0}^{k} h(i)x(n-i)$

This describes a nonrecursive realization for the FIR transfer function.

One significant advantage of the FIR filter function is its capability in obtaining linear phase (or constant time delay), derived via expanding the amplitude response in a sine series. The transfer function also is expanded in sine terms; the amplitude response can then assume negative values. This method is possible because at low frequencies the amplitude response is asymptotic to $w^k$, with k odd.[7,8] This is a systemic transmission property.

The FIR filter amplitude response approximating that of an ideal differentiator is,

(5) $A(f) = w$ (6) $\beta(f) = \frac{\pi}{2} - MTw = \frac{\pi}{2} - 2\pi MTf$

where $w$ = radian frequency ($\pi$/s); $A(f)$ = amplitude response; and $\beta(f)$ = phase response, in radians: the phase associated with the noncausal function combined with the additional phase due to the added delay.[9] This method differs from stating the filter function in cosine terms, the amplitude response of which has a constant amplitude slope, and thus is predictable for any odd phase passband. Segments bearing this type of acoustic feature, and without phonatory input, are non-contrastive linguistically, and are attributed to vowel colouring, or, secondary features. The segments are contrastive only if phonatory features are added.[10,11]

Acoustic analysis using cosine terms thus does not capture the transient's amplitude change. Also, whereas the phase shift in cosine terms is ideal, the sine-type expansion allows for a real linear phase: its phase shift is constant and at 90°; also as per (6) it is given in radians, etc., and has all its poles at the origin (and therefore is stable).

The FIR filter order determines the transfer function as a real function of frequency, thus proferring stability on the linear phase characteristics. In a DTLTI system the FIR amplitude response, $A(f)$, is related as a transfer function not only to the phase response, $\beta(f)$, also to the impulse response. The latter, approximating a real function of frequency (i.e., *critical band*), should satisfy the joint requirement for transmission: linear phase and constant time delay. The impulse response is multiplied in a Hamming window function, with a 12th order bandpass filter and a low-high cutoff of .04-.13 (Figure not shown). Thus, both the fundamental and the bandwidth approximating the second formant are filtered. The research question then is, how narrow must the main lobe of the window be so as to satisfy sharp tuning, active cochlear mechanics, in the auditory system.

Summarily, the filter's input applied to the waveform gives a minimalized amplitude response, Fig. 4, D&E screens (note negative SPL value, in D). The auditory sound in E is a woody pulse - flatly-tuned and lacking resonance. This is similar perceptually to the glottal stop, [ʔ], in which there is minimal laryngeal activity, ideally -

i.e., [-voice], Fig. 2. Alternatively, broadband noise sounds, e.g., [h], can be produced by widening the bandpass cutoff and maintaining even amplitude (filters not shown). The SPL spectrum of either segment precludes mapping to complex auditory responses found in, particularly, the dorsal cochlear nucleus (DCN) responses to linear phase signals in which the amplitude is odd (nonlinear). For example, in damping (Fig.3, 650-950Hz); and in sharp tuning resolution found in transient patterns involving significant SPL peaks and troughs. Moreover, the FIR filter's amplitude response prevents lateral inhibition. Nonetheless, this does not rule out the theory that sharp tuning is due to lateral inhibition.[12] Noteably, the missing fundamental alone does not contribute to the lack of amplitude response. The damping function is missing as a factor, prevented by the technical filtering.

**Conclusion:** In applications of the preliminary filter design it is concluded that apparently the auditory system does use SPL amplitude changes of less than 3 Bark, the *critical distance*[13] across formant bandwidths. But this requires the separation of transmission frequency bands of and for transients, from those of excitation periods. Further, in regard to pharyngeal resonants, in word-initial CV environments, maintaining the amplitude generated by the fundamental neither accounts for nor preserves the apparent transient damping in the second formant region. Whereas FIR filter designs based on source-filter theory require a transfer function that will satisfy formant transitions expanded in terms of bandwidths and the fundamental, the same derivational basis is not present, thus its expansions are not possible, in a DTLTI transmission system specific to pharyngeal resonants. In this, the transfer function is a higher order, a form of transmission, which as a filter can be considered separate from the excitation (source). It should therefore be expanded functionally, as an operation on damping, to thus correspond to segmentation in the auditory system. FIR filtering, with constant phase shifts, allows for this as an operation.

Further research is required to address one of the FIR's conventional disadvantages: stability of the higher-order filter number and its concomittant increasing time delays in accounting for the observed amplitude response. This could be examined, perhaps by differencing filtering and damping in the transmission transfer functions corresponding to delays in the dorsal cochlear nucleus' complex signal processing.

**References:** *The authour wishes to thank D. Wong; Dr.'s. J.H. Esling and B.F. Carlson; and B.C. Dickson. Digital analyses were done in the Linguistics Dept., Phonetics Laboratory, University of Victoria, Canada. Spokane (Interior Salish) tape recordings (1969), provided by B.F. Carlson, were digitized with sampling @ 10k/sec.
[1]Dickson, B.C.,& J.A. Clayards, 1990, *User's Guide to the CSL Program*, Speech Technology Research, Victoria, Canada. [2]Snell, R.C., 1990, *CSL Program* Signal processing software. [3]Fant, G., 1980, The Relations between Area Functions and the Acoustic Signal, *Phonetica* 37:55-86; 1970, *Acoustic Theory of Speech Production*, The Hague: Mouton. [4]Stevens, K.N.,& S.J.Keyser, 1989, Primary Features and Their Enhancement in Consonants, *Language* 65:81-106. [5]Stevens, K.N.,& J.S.Perkell, 1977, Speech Physiology and Phonetic Features, M. Sawashima & F.S. Copper (eds.) *Dynamic Aspects of Speech Prod.*, Tokyo: U. Tokyo Press: 323-341. [6]Stanley, W., Dougherty, G.R.,& R. Dougherty, 1984. *Digital Signal Processing*, 2nd ed. Reston, VA: Reston, (incl. equations (1)-(6)). [7]ibid:223. [8]Lagerstrom, P.A., 1988. *Matched Asymptotic Expansions*. NY: Springer-Verlag. [9]Stanley, et. al., ibid:218-226. [10]Laver, J. 1980. *The Phonetic Description of Voice Quality*, Camb: Cambridge UP. [11]Esling, J.H.,et.al., 1991, Automatic procedure for laryngographic (Lx) analysis of phonation contrasts, *Proc., XIIth ICPhS*, France:Univ. de Provence:6-9; [12]Pickles, J.O. 1991. *An Intro. to the Physiology of Hearing*, 2nd ed., London: A.P. [13]Chistovich, L. 1985. Central auditory processing of peripheral vowel spectra, *Jl Acous Soc Am* 38:424-428.

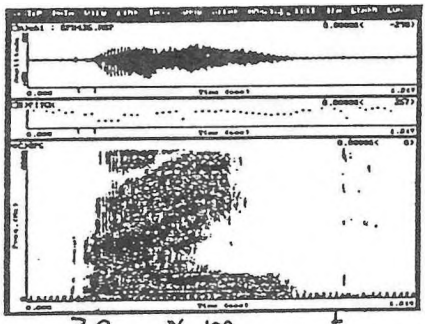

Fig. 1

/Paymt/

'angry'

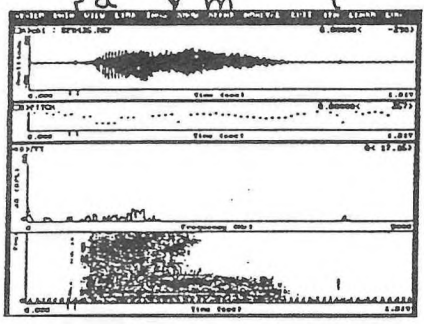


Fig. 2

[ P ]

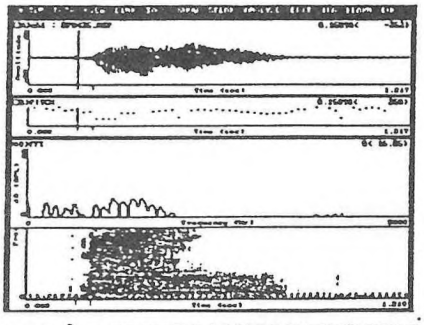

Fig. 3

[ 9 ]

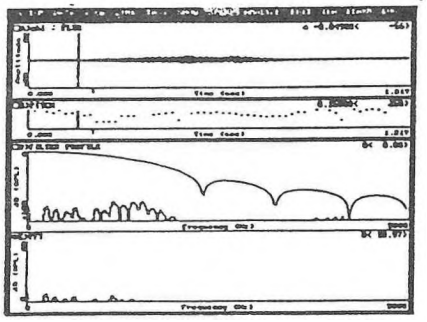

Fig. 4

D

E

# DIGITAL GENERATION OF THE HIGH QUALITY AUDIO SIGNALS WITH THE NeXT COMPUTER

**Marek Roland-Mieszkowski**
School of Human Communication Disorders, Dalhousie University
5599 Fenwick Street, Halifax, Nova Scotia, B3H-1R2, Canada.
and
**Danuta Roland-Mieszkowski**
Digital Recordings
5959 Spring Garden Rd. Suite 1103, Halifax, Nova Scotia, B3H-1Y5, Canada

## Digital methods for sinusoidal signal synthesis

A computer - based digital function generator can generate any arbitrary type of signal in the frequency range from 0 Hz to 20,000 Hz, S/N = 95 dB, and with no harmonic or intermodulation distortion (when based on 16-bit, 44.1kHz-sampling rate D/A converter). Frequency stability is determined by a quartz clock in the D/A converter which has an accuracy in the order of $1/10^7$. Generation of sinusoidal waves is of primary importance in digital synthesis, since due to the Fourier theorem any periodic wave may be constructed via additive synthesis (an addition of pure tones with appropriate amplitudes and phases). There are many alternative methods to digitally generate pure tones [1,2,3,7]. Very often real-time synthesis is accomplished by using a sine function look-up table [2,7]. A limitation to this approach is the short length of the sine table (N). In order to synthesize any arbitrary frequency using the look-up table method, one has to synthesize the values of the sine function using an interpolation process [2]. Interpolation between sine samples leads to the generation of harmonic and intermodulation distortion by this algorithm [2,7]. Another problem is that synthesis of more complex signal (combinations of several sinusoids with certain amplitudes and phases) in real time could put too much performance demand on the computer's DSP chip or microprocessor.

## Digital Function Generator software for the NeXT computer

A new high precision digital synthesis method has been developed for the generation of the high quality audio signals [7]. This method has been successfully implemented on the NeXT computer and was used with great success in teaching of acoustics, psychoacoustics, electronics and in various research projects. During the course of this research, a software package called **Digital Function Generator (DFG)** was written. At present the DFG software consists of 5 modules. The **Principles of Digital Audio** module (Fig.1) allows synthesis of pure tones and white noise. It can also be used to illustrate concepts of signal amplitude, frequency, phase, interference, coherence, incoherence, signal ramping, additive synthesis, beats, virtual pitch as well as to demonstrate quantization, dithering, aliasing / hard clipping / harmonic / intermodulation distortions, etc. The **Modulation (AM, FM & AFM)** module allows synthesis of pure tones which can be Amplitude Modulated (AM), Frequency Modulated (FM) or Amplitude and Frequency Modulated (AFM). The **Additive Synthesis** module allows very flexible synthesis of complex sounds from their Fourier components. The **Sweep Generator (AS, FS & AFS)** module is a very flexible tool for generating arbitrary amplitude (AS), frequency (FS) or amplitude and frequency (AFS) sweeps. The **Function Generator** module (Fig.2) can be used to synthesize sine, square, triangular, sawtooth, pulse and white noise signals.

## RAM-based method for sinusoidal signal synthesis

In order to generate sinusoidal signal in this method, one has to synthesize audio file, which contains appropriate samples in RAM (Random Access Memory) or on the Hard or Optical Disk. Then reading of this file in real time to the D/A converter is performed to generate the desired audio signal [6]. However there is a limit on the duration of this signal due to memory consumption = 88,200 Bytes/sec (for 16-bit, 44.1 kHz D/A converter). In many situations long durations of test signal are required. In this case the most appropriate way to generate sine wave is to construct the audio file in RAM in such a way as to be able to read this file to the D/A converter over and over again (looping) [7].

## Generation of frequencies 1Hz, 2Hz, 3Hz.....20,000Hz with the NeXT computer

NeXT computer has a 16-bit, 44.1 kHz stereo set of the D/A converters (CD-quality), available 16-bit, 44.1 kHz stereo set of the A/D converters, built in DSP processor (Motorola 56001), from 8 to 256 MBytes of RAM and from 100 MBytes to 5.6 GBytes of internal hard disk storage. This, therefore, is the best computer for audio and acoustical applications available today. With RAM buffer size N=44,100 (176,400 Bytes - which is small by the NeXT standards) the available frequencies for looping are: 1 Hz, 2 Hz, 3 Hz,.....20,000 Hz. It takes about 3 sec for Motorola 68040-based NeXT machine to generate a pure tone soundfile of this length. Once generated, this file can be played in loop from RAM indefinitely.

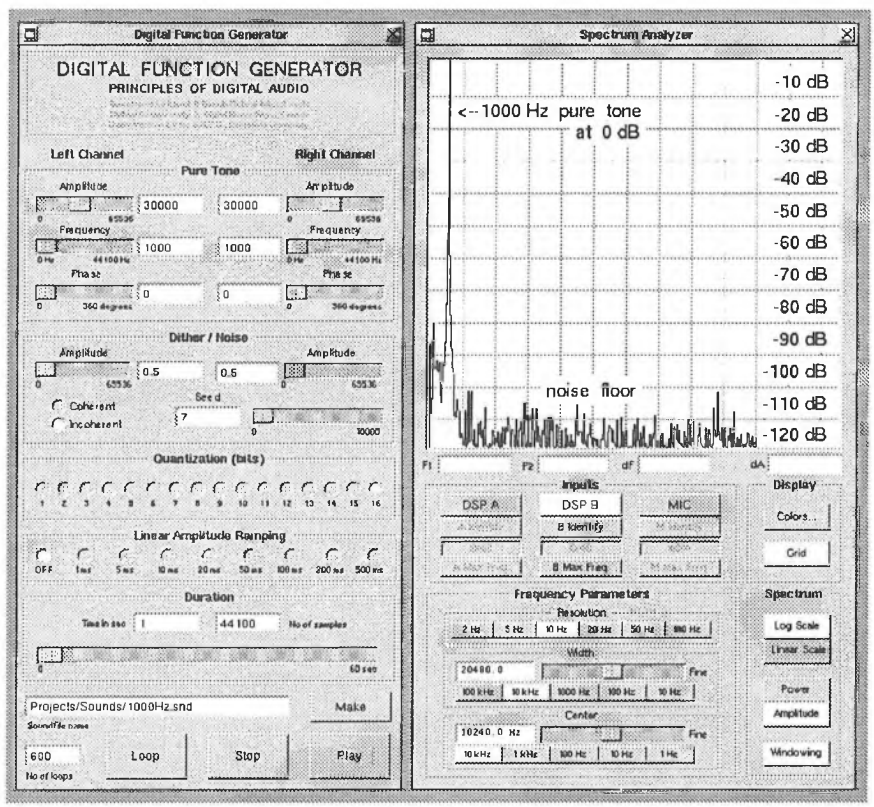


Figure 1. 1000 Hz pure tone generated with the Digital Function Generator (Principles of Digital Audio module) and displayed with the Spectrum Analyzer.

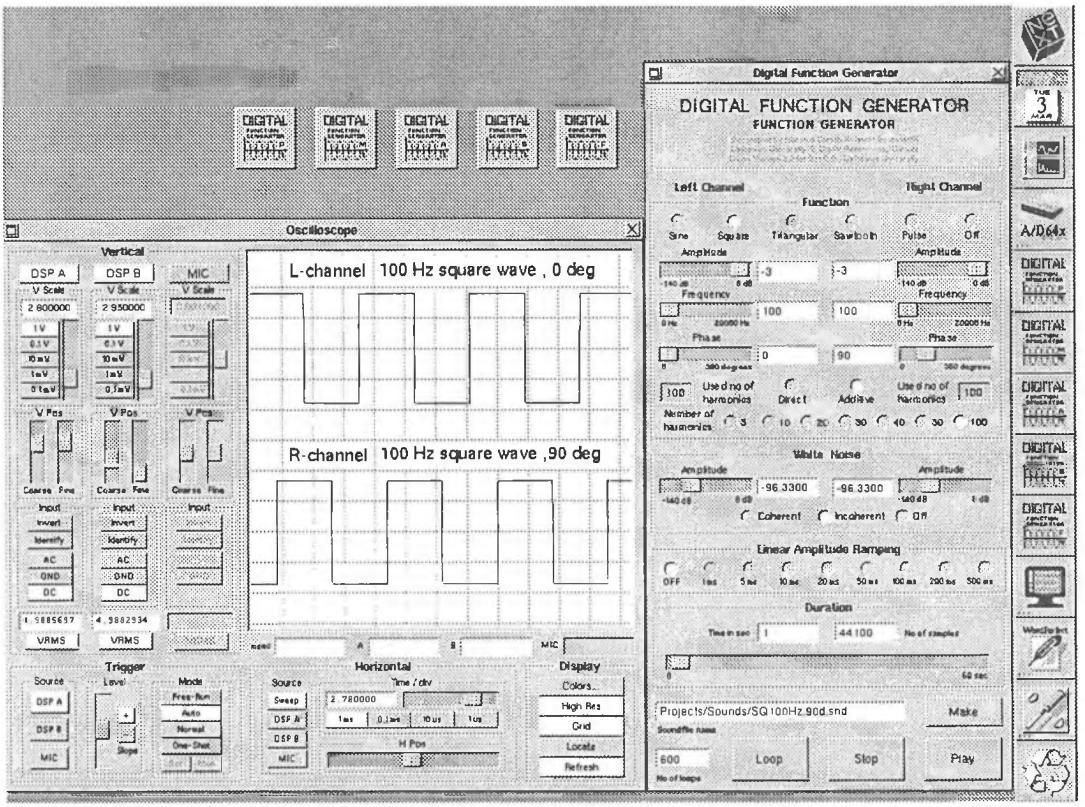


**Figure 2.** 100 Hz square wave generated with the Digital Function Generator (Function Generator module) and displayed with the Digital Oscilloscope.

With RAM buffer size N=441,000 (1,764,000 Bytes - still small by the NeXT standards), one can generate all frequencies from 0.1 Hz to 20,000 Hz with 0.1 Hz resolution. Precision of these frequencies is determined only by the precision of the D/A converter's clock which is in the order of $1/10^7$, and in the case of a 1000 Hz tone this leads to an expected error in the order of ± 0.0001 Hz. Generated soundfiles with desired frequencies can be stored on the Hard or Optical Disk and recovered into RAM prior to generation of sine tones.

### Improving DFG through the use of Digital Dither

The only harmonic and intermodulation distortion generated by the used algorithm is associated with round-off error of final amplitudes A[n] due to the signal correlated nature of quantization noise [4,5,7]. Elimination of the harmonic and nonharmonic (intermodulation) distortion (which are imposed by the resolution of the D/A converter ) may be accomplished by using Digital Dither, with a small white noise penalty (3 dB- for uniform-pdf dither) [5,8], resulting in S/N=95 dB for 16-bit dithered digital generator (theoretical S/N=98.2 dB for undithered 16-bit digital system) [4]. This technique was implemented in the DFG software to improve quality of the generated signals.

### Generating stereo signals with NeXT

The procedures outlined in ref [7] were applied for synthesis of stereo waveforms with the NeXT computer. One can generate different or similar waveforms in each channel. Phase relationship between waveforms will be maintained during playback. Since signal phase constants are arbitrary real numbers, arbitrary phase shifts between waveforms can be obtained. This could be important for some audiological and psychoacoustic tests [6,11,12].

### Conclusions

The most precise digital-domain method for the generation of arbitrary audio signals was successfully implemented on the NeXT computer. Since NeXT is a multitasking, UNIX operating system-based machine, many software applications can run on it simultaneously. DFG software by-design puts very little demand on the hardware and does not use the built-in Motorola DSP 56001 processor for sound synthesis. This allows running of the Digital Oscilloscope (Fig.2), Spectrum Analyzer (Fig.1) and Sound Recording software simultaneously with DFG. This in turn allows very sophisticated tests and demonstrations in such fields as acoustics, electronics, physics and engineering to be performed on a single NeXT computer.

### References:


[1] Leland B. Jackson, "Digital Filters and Signal Processing", Second Edition, Kluwer Academic Publishers, Boston, Dordrecht, London, 1989.

[2] Andreas Chrysafis, "Digital Sine-Wave Synthesis Using the DSP 56001", MOTOROLA Inc., Brochure No. APR1/D REV1, 1988.

[3] Waldemar Kucharski, Andrzej Czyzewski, "Implementation of Basic Methods of Sound Synthesis for IBM-PC compatibles", Proceedings of Thirty Seventh Open Seminar on Acoustics, Technical University of Gdansk, September 10-14, 1990, pp. 225-228.

[4] Marek Roland-Mieszkowski, "Introduction to Digital Recording Techniques", Proceedings from "Acoustic Week in Canada 1989"- CAA Conference,Halifax,N.S.,Canada, Oct. 16-19,1989, pp. 73-77.

[5] Robert Wannamaker, Stanley Lipshitz and John Vanderkooy, "Dithering to eliminate quantization distortion", Proceedings from "Acoustic Week in Canada 1989" - CAA Conference, Halifax, N.S., Canada, October 16-19,1989, pp.78-86.

[6] Annabel J. Cohen and Marek Mieszkowski, "Frequency synthesis with the Commodore Amiga for research on perception and memory of pitch", Behavior Research Methods, Instruments, & Computers, 1989, 21 (6), pp. 623-626.

[7] Roland-Mieszkowski, M. (1991). "Digital Generation of the High Quality Periodic Audio Signals with the aid of a D/A Converter and Computer","Acoustic Week in Canada 1991" -CAA Conference, Edmonton, Alberta, Canada, October 7-10, 1991,Published in "Canadian Acoustics" Journal, Vol.19, No.4, Sept. 1991, pp.47-48.

[8] John Vanderkooy, Stanley P. Lipshitz, "Digital Dither: Signal Processing with Resolution far below the Least Significant Bit", AES 7th International Conference,Toronto, Ontario, Canada, May 14-17, 1989, paper No. 4.E.

[9] Stanley P. Lipshitz and John Vanderkooy, "The principles of Digital Audio: a Lecture Demonstration", AES 7th International Conference, Toronto, Ontario, Canada, May 14-17, 1989, paper No. 2.B.

[10] S.P. Lipshitz and J. Vanderkooy, "Digital Dither", presented at the 81st Convention of AES, JAES (Abstracts), Vol. 34, p.1030 (1986 Dec), Reprint No. 2412.

[11] John D. Durrant and Jean H. Lovrinic, "Bases of Hearing Science", Sec. Ed., Williams & Wilkins, Baltimore/ London, 1984.

[12] Brian C. J. Moore, "An Introduction to the Psychology of Hearing", Second Edition, Academic Press Inc., New York, 1982.

# ASSESSMENT OF CONSTRUCTION NOISE FROM A HYDROELECTRIC PROJECT ON LOCAL COMMUNITIES

**D.S. Kennedy[1], N.M. Nielsen[2], A. Walkey[3], and V. Lau[1]**

[1]Barron Kennedy Lyzun & Associates Limited, #250 - 145 W. 17th St.,
North Vancouver, B.C., Canada V7M 3G4
[2]British Columbia Hydro, 6911 Southpoint Drive, Burnaby, B.C., Canada V3N 4X8
[3]Cornerstone Planning Group Limited, #22 - 1551 Johnston St., Granville Island,
Vancouver, B.C., Canada V6H 3R9

## INTRODUCTION

B.C. Hydro conducted development studies for a potential hydroelectric project on the Columbia River in Southeastern British Columbia, Canada. The proposed site of the Murphy Creek Project is located about 200 m from the nearest residences. An eight year construction period would include approximately 4 years of major activity, including about 2.5 million cubic metres of rock excavation. An initial study with a limited amount of field work was completed in 1982 to assess the effects of construction noise and vibration. Responses from the local residents and other government agencies indicated that further field tests were necessary. Community representatives were involved in drawing up the Terms of Reference for the expanded noise study, which was undertaken in the fall of 1990.

Since sound attenuation due to ground effect and shielding is difficult to estimate theoretically over irregular terrains, various source-to-receiver path attenuations were measured. Following consultation with local community representatives, it was decided to use rock drills as noise emitters and seven representative receiver locations were selected for the attenuation testing. As a possible mitigation option at the request of the communities, an alternative project site 1 km upstream from the proposed site was included in the test program. During the tests, direct community input was obtained through community meetings and interviews with key stakeholders.

Test data obtained were then supplemented by noise data from other sources and extrapolated to model a full construction site. Noise and vibration impact were assessed. Source control and moving the project site 1 km upstream were the most significant mitigation measures considered. This noise impact study integrated engineering evaluation, project economics, environmental impacts, health concerns and property issues within the framework of a community consultation process.

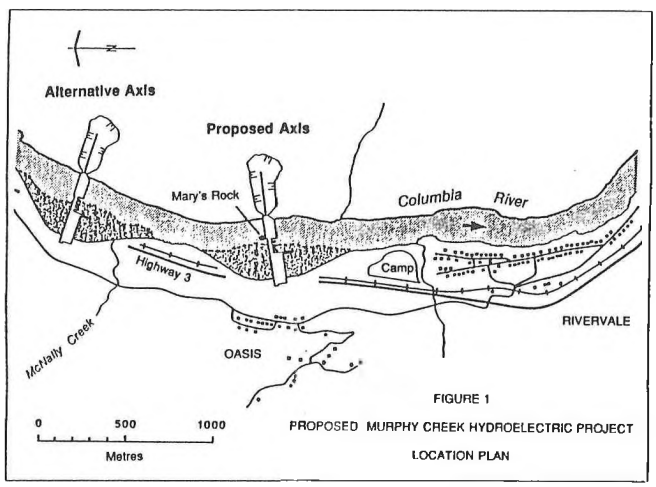


FIGURE 1
PROPOSED MURPHY CREEK HYDROELECTRIC PROJECT
LOCATION PLAN

## TEST PROGRAM

There are two possible sites for the dam construction, namely the Mary's Rock axis (originally proposed) and the McNally Creek axis. As indicated in Figure 1, the closest communities potentially affected would be Oasis and Rivervale. A field study was conducted to obtain both existing ambient sound data and reliable sound propagation data.

On the first day of testing, existing ambient sound levels at the selected receiver locations were measured continuously for 24 hours in A-weighted decibels (dBA). This information is required to fully assess the potential impact of construction noise. On the second day, drilling operations were conducted separately at the two possible powerplant sites and resulting noise was measured, both at 15m from the drills, and at various receiver locations. Both the pneumatic drill and the more time-efficient and quieter hydraulic drill were used separately as noise sources. This exercise provided source noise data for drills, and most importantly, noise attenuation values for various source to receiver paths.

Since the project would involve the realignment of the railway and the highway westward, ground vibration levels from trains passing east of Oasis were also measured. In addition, noise levels at various locations were measured during the operation of a loaded dump truck at various work areas and on designated routes. Before and throughout the test program, the procedures and significance of the above testing were explained to the residents, and their feedback was requested.

## EVALUATION METHODOLOGY AND ASSESSMENT OF IMPACT

Based upon previous experience and certain assumptions made in designing the project, B.C. Hydro personnel estimated the number and types of construction equipment that might be used during various phases and at major work areas throughout the construction project. Source levels at 15m for each type of equipment were obtained from equipment manufacturers, technical literature, and from measurements conducted by Barron Kennedy Lyzun & Associates personnel. The amount of sound attenuation that occurs between various work areas and the representative receiver locations was estimated primarily based on data from the field program. Noise levels at the receiver locations resulting from each noise source, or group of sources, were estimated by subtracting the expected attenuations from the source levels. Duty factors of the equipment and numbers of equipment were taken into account. The total project noise level at each receiver location was then calculated for each phase of the construction.

There were no local noise and vibration by-laws; hence, the most applicable assessment criteria were drawn from other sources. Since people react differently to impulsive noise than they do to non-impulsive noise, impulsive sources were evaluated separately. Criteria for low risk of complaints due to blasting peak noise levels, and for low degree of annoyance due to blasting induced ground vibration were used. Also evaluated separately were permanent changes in noise and vibration due to the proposed

highway and railway realignment. Specifically, ground vibration levels due to trains were compared to the perception threshold and the reduced comfort threshold stated in ISO Standard 2631[1].

For the total project noise assessment, noise level estimates were described in terms of the long term (i.e. several months) day-night average sound level, $L_{dn}$. For existing residences, the percentage of the population likely to be "highly annoyed" (% HA) was estimated from the total project $L_{dn}$ levels using relationships established for both non-impulsive noise (Schultz[2]) and impulsive noise (CHABA[3]). In order to assess the cumulative effect of blast noise plus other non-impulsive noise, a method recommended by the U.S. National Research Council was used (CHABA[3]). First, the above relationships were used to determine the non-impulsive level which would result in the same % HA as was estimated for impulsive blasting noise. This equivalent non-impulsive noise level was then added to the levels of other non-impulsive sources to obtain the total project $L_{dn}$ level, which allowed an estimate of % HA due to all sources.

The relationships between % HA and noise levels do not take into account the existing ambient noise levels or attitudes of the community. To account for the existing ambient, relative changes in noise levels and % HA were also reviewed. The % HA value corresponding to the existing ambient $L_{dn}$ level at each receiver location was calculated to provide further insight into the assessment results. These estimated "existing" % HA values were relatively low at approximately 5%. Since the local communities have not indicated dissatisfaction with the current noise climate, this verified that the methodology was reasonably accurate. With respect to community attitudes, it is well known that a negative attitude often leads to greater annoyance than what would otherwise occur. The community consultation effort was intended to include concerns of the residents, such that a dissatisfied community attitude would not develop. It should be mentioned that although the CHABA assessment mothod does not include every factor that may lead to annoyance, it served well for the purpose of comparing the project axes, construction phases, and receiver locations.

At the camp site proposed for the Mary's Rock axis to house construction workers (see Figure 1), land use compatibility criteria (ANSI[4]) based on total project $L_{dn}$ were used, because predictions of % HA are only valid for an existing population.

The primary conclusions arrived at were as follows. Estimated levels of noise and vibration from blasting would not exceed accepted criteria for either axis provided that a sufficient number of sequential delays are used and no nighttime blasting is allowed. With respect to ground vibration due to the realigned railway, only the Mary's Rock axis needed consideration because the McNally Creek axis would not change the distance between the railway and the communities. At the Mary's Rock axis, measured levels at a distance representing the future situation were below the reduced comfort threshold but well above the perception threshold. However, considering the relative change of +3 dB in both ground vibration and noise due to the distance reduction, the highway and railway realignments were considered to be insignificant.

Assuming a continuous work pattern of three shifts per day and seven days per week, total project noise levels for either axis were estimated for the seven receiver locations, as well as the proposed construction camp for the Mary's Rock axis. If the project is constructed at the Mary's Rock axis, noise levels at many receiver locations, primarily in Oasis, would increase during most phases of major construction by 10 dBA or more, relative to the existing ambient. Worst case increases were estimated to be 17 dBA. The estimated values of % HA vary widely from nearly unchanged at about 5% to as high as 49%, depending upon receiver location and phase of construction. If the project is constructed at the McNally Creek axis, receiver locations would be subjected to noise levels up to 6 dBA above present levels, and estimates of % HA would not exceed 10%. For the Mary's Rock axis, the construction camp site was assessed to be marginally compatible with the proposed use but building sound insulation and possibly exterior noise barriers would be required at the camp.

## MITIGATION

Source control was a significant mitigation measure considered. In the project noise estimates, it was assumed that recently manufactured equipment would be used throughout the construction project. It was expected that such conditions likely would form part of the construction contract, reinforced by on-going site monitoring. Placing further noise limits was not considered practical. With regard to blasting, sequential blasting was recommended, with maximum charge per delay required for a typical daily blast specified.

However, the most significant mitigation measure considered was moving the project to the McNally Creek axis. As indicated by the impact assessment, impact from this alternative site was relatively minor. However, 1% to 2% increase in construction costs was estimated, and a net energy loss would be incurred once the project commenced operation. An alternative work pattern with two shifts per day and five days per week was also evaluated as a mitigation measure. However, the improvements were not very significant for either axis. Since the construction equipment would be scattered over a very large area, noise barriers around the work areas would not be effective.

## COMMUNITY CONSULTATION PROGRAM

A community consultation program was designed to ensure that the concerns of the nearby residents were fully considered. It is called a community consultation program because it was targeted to deal with the concerns of the smaller, potentially directly affected communities. First, a notice about the studies for the potential hydroelectric project was placed in local newspapers. Then a meeting was held with the community association to plan for the tests, and to identify test sites and key concerns. Other efforts included an information handout delivered to all households in Oasis and Rivervale prior to the testing, as well as interviews with key stakeholders before and during the testing. After the testing, preliminary findings were reviewed with the community association. Active development of the project has now been deferred indefinitely. Any future consideration of the project would involve a review of community concerns and possible mitigation measures for perceived impacts.

## FUTURE INVESTIGATIONS

When a decision is made to resume the development of the Murphy Creek Project, results of completed studies will be reviewed and further studies may be required. Feasible target noise levels will be set in consultation with the communities, such that mitigation options can be finalized for either axis. These options include source control, building facade upgrades and exterior noise barriers, temporary or permanent relocation of residents, and compensation in the form of easements. In consideration of project economics, environmental and social factors, a project site could be determined.

## REFERENCES


1. "Guide for the Evaluation of Human Exposure to Whole-body Vibration", ISO Standard 2631-1978(E)
2. "Social Surveys on Noise Annoyance - A Synthesis", T.J. Schultz, J. Acoust. Soc. Am., 64, No. 2, 377-406, August 1978
3. "Assessment of Community Response to High-energy Impulsive Sounds", CHABA, U.S. National Research Council, 1981
4. "Sound Level Descriptors for Determination of Compatible Land Use", ANSI S3.23-1980

# Hand-Arm Vibration Associated with the Use of Riveting Hammers in the Aerospace Industry and Efficiency of "Antivibration" Devices.

**P.-É. Boileau*, H. Scory*, G. Brooks** and M. Amram*****

* IRSST, 505 De Maisonneuve O., Montréal, Qc Canada H3A 3C2

** Canadair Limitée, C.P. 6087, Montréal, Qc Canada H3C 3G9

*** École Polytechnique, C.P. 6079, Succ."A", Montréal, Qc Canada H3C 3A7

## INTRODUCTION

Riveting hammers are widely used in the aerospace industry for assembling aircraft panels. The process of riveting usually involves punching strokes on the rivet head while a bucking bar is held on the other end of the rivet for closing it up. The installation of a rivet takes only a fraction of a second but is known to subject both the operators of the riveting hammer and of the bucking bar to significantly high levels of vibration[1]. Such vibrations are susceptible to contribute to the development of vibration white finger disease of which Raynaud's phenomenon is most widely known[2].

The purpose of this work was to evaluate the exposure levels associated with the use of typical riveting hammers and bucking bars used in an assembly plant, some of these devices being characterized as "antivibration" devices, in an effort to evaluate their efficiency for reducing vibration exposure following the ISO 5349 [3] guidelines. In addition, an evaluation of specially designed vacuum pads [4], mainly aimed at reducing the noise radiated, was also attempted to establish their potential effect on hand-transmitted vibration levels.

## VIBRATION EXPOSURE LEVELS

Tables 1 and 2 present the overall frequency weighted acceleration (6.3-1250 Hz) measured on the handle of the different riveting hammer/bucking bar combinations. Riveting hammers A and B are of equivalent size but A represents a conventional hammer while B is considered "antivibration". Riveting hammers C and D are smaller and are equivalent except for the fact that the handle of D has been covered with a resilient material and incorporates a muffler to reduce the noise. The conventional bucking bar consists of a piece of steel having a mass of approximately 1 kg while the antivibration bucking bar is a commercial unit aimed at reducing vibration exposure at the bucker's hands. However, when measuring on the hammer itself, accelerometers are fixed at a point where there is no resilient material. Therefore, the levels measured on hammers C and D should be similar; only the vibrations measured on the wrist should give some indication of the efficiency of the resilient material for attenuating the vibration.

### Efficiency of Antivibration Bucking Bar

The use of an antivibration bucking bar equipped with a spring to damp the vibration is seen to represent a significant improvement over a conventional metal bar for lowering the overall frequency weighted acceleration at the bucker's hands. The vibration levels can be reduced by as much as 10 dB by using the antivibration bucking bar, bringing the levels almost equivalent to those recorded on the hammer side. The effect of the bucking bar is not apparent on the riveting hammer side except perhaps when the antivibration hammer B is being used. When using a conventional metal bucking bar, it can be expected that the bucking bar operator will be exposed to vibration levels which can be 3 to 5 times the levels recorded for the riveting hammer operator.

### Efficiency of Antivibration Riveting Hammer

A comparison of riveting hammers A and B, B being a commercial antivibration hammer equipped with an air servo installed between the handle and the vibrating parts of the tool, indicates a slight improvement of the vibration levels at the riveter's hands, the improvement being best achieved in conjunction with the antivibration bucking bar. However, the use of the antivibration hammer leads to an important increase in vibration exposure for the bucking bar operator, indicating that the blow energy , instead of being dissipated, is directly transmitted to the rivet, and consequently, to the bucking bar. On the riveting hammer side, best performance is achieved using the antivibration hammer with the antivibration bucking bar. On the bucking bar side, best performance is achieved using a conventional hammer with the antivibration bucking bar. A suitable compromise would thus appear to be the use of this latter combination such that both the riveter and the bucker would be exposed to similar vibration levels.

A comparison of hammers C and D shows no real significant difference on both the riveter's and bucker's sides.

### Efficiency of Vacuum Pads

The use of vacuum pads fixed on the structure for dampening the radiated noise is seen to have only a slight effect for reducing vibration exposure, depending on the hammer/bucking bar combination. Best improvement is seen to be achieved when conventional hammers A and C are used in conjunction with the antivibration bucking bar on both the riveter's and bucker's sides.

## CONCLUSION

The efficiency of an antivibration bucking bar, riveting hammer and vacuum pads have been evaluated during typical riveting operations in an effort to establish their efficiency for lowering exposure to hand-transmitted vibration. The use of an antivibration bucking bar has been shown to reduce exposure by as much as 10 dB at the bucker's hands while generally having no significant effect on the riveter's side. A slight decrease of vibration was noted on the riveter's side when using a riveting hammer treated against vibration at the expense of increasing exposure on the bucker's side. The best compromise appeared to be the use of a conventional hammer along with an antivibration bucking bar. The use of vacuum pads was seen to have only a slight effect on vibration exposure, although beneficial effects were only noted for certain hammer/bucking bar combinations.

## REFERENCES

[1] Dandanell, R. and Engstrom, K. Vibration Measurements and Analysis of Percussion Tools such as Riveting Hammers and Bucking Bars. U.K. Informal Group Meeting on Human Response to Vibration, Edinburgh, 21-22 September 1984. pp.13-23.

[2] Musson, Y., Burdorf, A. and van Drimmelen, D. Exposure to Shock and Vibration and Symptoms in Workers using Impact Power Tools. Annals of Occupational Hygiene, Vol. 33, No. 1, 1989. pp.85-96.

[3] International Standards Organization ISO 5349 (1986). Guidelines for the measurement and the assessment of human exposure to hand-transmitted vibration. Geneva.

[4] Amram, M., Masson, P., Brooks, G. and Boileau, P.-É. A New Vacuum-Activated Damping Device to Reduce the Noise and the Vibration in Riveting Process. Proceedings of the Canadian Acoustical Association Symposium, Vancouver, B.C., 8-9 October 1992.

Table 1. Overall frequency-weighted acceleration measured on the bucking bars

| Riveting Hammer | Without "vacuum pads" | | With "vacuum pads" | |
|---|---|---|---|---|
| | Conventional bucking bar | Antivibration bucking bar | Conventional bucking bar | Antivibration bucking bar |
| | $a_{h,w}$ ($ms^{-2}$) | | $a_{h,w}$ ($ms^{-2}$) | |
| A | 19.9 ± 0.9 | 6.0 ± 1.2 | 18.0 ± 1.0 | 4.3 ± 1.2 |
| B | 28.0 ± 2.0 | 10.6 ± 1.4 | 25.0 ± 2.0 | 10.0 ± 2.0 |
| C | 15.0 ± 1.5 | 4.6 ± 1.0 | 14.0 ± 0.7 | 2.7 ± 0.4 |
| D | 14.9 ± 1.5 | 4.2 ± 0.8 | 13.0 ± 0.7 | 4.2 ± 0.9 |

Table 2. Overall frequency-weighted acceleration measured on the riveting hammers

| Riveting Hammer | Without "vacuum pads" | | With "vacuum pads" | |
|---|---|---|---|---|
| | Conventional bucking bar | Antivibration bucking bar | Conventional bucking bar | Antivibration bucking bar |
| | $a_{h,w}$ ($ms^{-2}$) | | $a_{h,w}$ ($ms^{-2}$) | |
| A | 6.5 ± 0.4 | 7.0 ± 0.7 | 5.7 ± 0.2 | 5.8 ± 0.4 |
| B | 5.1 ± 0.4 | 3.6 ± 0.4 | 5.2 ± 1.4 | 5.1 ± 1.5 |
| C | 4.4 ± 0.3 | 4.8 ± 0.5 | 3.9 ± 0.4 | 3.3 ± 0.5 |
| D | 5.0 ± 0.4 | 5.7 ± 0.7 | 4.4 ± 0.2 | 3.9 ± 1.1 |

# Optimal use of polymetric materials in vibrating beam systems with the consideration of temperature and frequency effects.

**Li CHENG , Guy PLANTIER(*) and Marc RICHARD**

Mech. Eng. Dept., Université Laval, Québec G1K 7P4
(*) Mech. Eng. Dept., Université de Sherbrooke, Québec J1K 2R1

## 1. INTRODUCTION

Sound and vibration damping plays a critical role in numerous aspects of engineering and is increasingly addressed by legislation as well. The most commonly used damping materials are polymetric whose viscoelastic properties change a lot with temperature and working frequency. Suprisingly enough, this last point, which constitutes the main interest for chemists, has not received enough attention from researchers and engineers designing better damped structures. Quite often, the mechanical characteristics of these materials are considered to be constant. Another important problem to be tackled is the optimal use of these materials. In fact, numerous practical restrictions such as weight, cost and maintenance facilities demand that the structures be damped with partial damping coverage.The question is how to get reasonable damping performance without adding too much weight to the structures.

Theses two fundamental problems are tackled in the present work on a beam structure. First, a brief review is given to summarize the characteristics of typical polymers. Second, a preliminary model consisting of a partially covered beam is presented. The established model allows the consideration of the real variations of the characteristics of the damping materials with temperature and frequency. An iterative procedure is developped to calculate the damping factors of the whole system. Third, numerical results are presented and analyzed to show the effects of several parameters such as temperature, thickness, position, expansion of the covering layer and so on. Finally, some experimental results supporting the partial findings of the present work are illustrated. The established model presents the advantage of being sufficiently accurate and fast, and consequently constitutes the first step towards a complete model in which the optimization procedure will be included.

## 2. THEORY

### 2.1 Polymer materials

The temperature and frequency dependence of viscoelastic polymetric materials is relatively well known in the literatures [1]. Under some circumstances, the variation of the characteristics of these materials is so great that mechanical engineers have to take them into account. Two obvious observations justifing this statement are for example, mechanical systems such as space structures which suffer great temperature variations and structures driven by broad frequency excitations. Vibration damping in polymers is mainly dominated by the glass transition occuring in the amorphous portions of the polymer. For a given material, the glass transition indicates the frequency and the temperature at which the damping peak is a maximum. In the present work, the hard tan damping sheet manufactured by E.A.R (SD-40PSA) is used. The complex young's modulus comprising storage modulus and loss modulus is supposed to be frequency and temperature dependent. Measured data from the manufacturer [2] are directly used.

### 2.2 Theoretical model and formulation

The model investigated is a beam in flexural motion which is partially covered by an unconstrained viscoelastic layer. The beam is supposed to have an elstic supporting at each end. The position and the expansion of the layer are adjustable parameters in the model (fig.1).

The problem is formulated using the variationnal principle associated with the Rayleigh-Ritz method based on the following assumed displacement field [3]:

$$u(x,z) = -(z-h(f)+e_1/2)\frac{\partial w}{\partial x}$$
$$v(x,z) = 0$$
$$w(x,z) = w \quad , \qquad (1)$$

in which u,v and w are the displacements of the beam along x,y, and z axes respectivelly; $e_1$ is the thickness of the beam. h(f) can be calculated as follows:

$$h(f) = \frac{e_1^2 E_1 + e_2^2 E_2(f) + 2e_1 e_2 E_2(f)}{2(e_1 E_1) + e_2 E_2(f))} \qquad (2)$$

In the above expression $E_1$ is the Young's modulus of the beam , $E_2(f)$ and $e_2$ are respectively the storage modulus and the thickness of the viscoelastic layer. $e_2$ is equal to zero for the noncovered portion.

The variationnal principle is applied to the system with the following trial function:

$$w = \sum_{K=0}^{n} a_k (2x/L)^k \quad . \qquad (3)$$

This approach leads to the following system equation:

$$[S]\{a_k\} = \{f_k\} \qquad (4)$$

Two types of problem can be solved by using the established model: the dynamic response of the beam driven by a point-force can be obtained by solving system(4) ; free vibrational analysis of the structure can be done by neglecting the terms in the system (4)

corresponding to the excitation, the solution of this eigenvalue equation yielding the natural frequencies together with the modal damping factors.

Special attention should be paid to the treatment of the eigenvalue problem due to the fact that the system matrix [S] in which the modulus of the viscoelastic material is involved is frequency dependent. For this purpose, an iterative process is developped, the essence of which is as follows: For each seeked mode, a starting trial frequency $\omega_0$, which is necessary to determine the modulus of the viscoelastic material and consequently the matrix [S], is used. Then with the known system matrix [S], the eigenvalue $\omega_R(1+j\eta)$ of the corresponding mode is calculated by using any standard procedures. The operation repeats itself by adjusting the value of $\omega_0$ until $|\omega_0 - \omega_R| < \zeta$, with $\zeta$ being a sufficiently small quantity. In this case, $\omega_0$ is the natural frequency of the structure and $\eta$ the corresponding loss factor. The starting trial value used in the calculation is the natural frequency of the corresponding undamped beam.

## 3. PRINCIPAL FINDINGS

1). Experiments are carried out with a free-free aluminium beam(length 0.5m and thickness 4mm) covered by a layer of 1mm thickness over two-third beam length. Comparison between the measured values and the calculated ones in terms of $\omega$ and $\eta$ shows excellent agreement.

2). The consideration of the frequency variation of the polymers introduces a non-negligable weighting on the modal analysis considering the material characteristics to be constant. This is particulaly true at the vicinity of the glass transition.

3). The modal damping factors of the system depend sensitively on the working temperature. The temperature affects also the stiffness of the system via the modification of the storage modulus of the viscoelastic layer, consequently clear shift of the resonance frequencies is observed.

4). The layer position is shown to affect strongly the damping factors of low-order modes for which the wave length is long. However the high-order modes seem to be less sensitive to the layer position.

5). With the assumption of equal mass added to the beam by the viscoelastic layer, the expansion of the layer is shown to play an important role in optimizing the damping perfomance. The fully-covered beam is seldom, if ever, the best solution for all configurations tested in the present work. This observation justifies the necessity of elaborating an optimization process.


**REFERENCES**

1. B. Hartmann, Polymernews, 16,134-141, 1991
2. Technical report, E.A.R
3. L. Cheng and J. Nicolas, J. Acous. Soc. Am. 91, 1504- 1513, 1992.


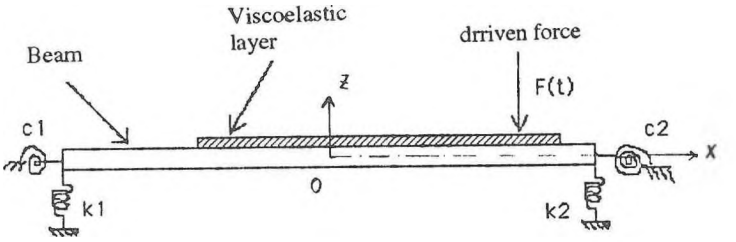


*Fig.1 Investigated beam structure.*

*Frequencies in Hz*

| Mode | calculated | measured | difference in % |
|---|---|---|---|
| 3 | 95.63 | 95.82 | 0.2 |
| 4 | 265.53 | 264.64 | 0.3 |
| 5 | 521.35 | 520.85 | 0.1 |
| 6 | 863.33 | 856.65 | 0.8 |
| 7 | 1294.78 | 1285.45 | 0.7 |
| 8 | 1813.06 | 1792.51 | 1.1 |
| 9 | 2416.68 | 2393.00 | 1.0 |

*Damping factors in %*

| Mode | calculated | measured | difference in % |
|---|---|---|---|
| 3 | 0.999 | 1.124 | 12.5 |
| 4 | 1.000 | 0.933 | 6.7 |
| 5 | 0.988 | 0.954 | 3.4 |
| 6 | 1.131 | 1.235 | 9.2 |
| 7 | 1.117 | 1.123 | 5.4 |
| 8 | 1.135 | 1.250 | 10.1 |
| 9 | 1.170 | 1.27 | 8.5 |

*Comparison of the measured and calculated natural frequencies and damping factors.*

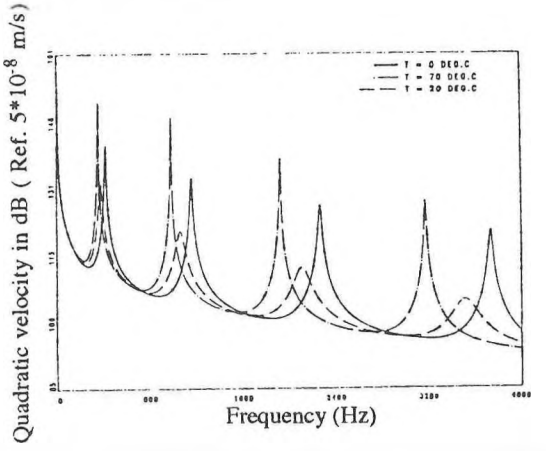


*Fig.3 An example of the forced response of a partially covered beam working at different temperatures.*


**ACKNOWLEDGEMENTS**

Authors thank M. Ph. DECOURT for participaping the work during his four month's training period.

# SCALE-MODEL EVALUATION OF THE PERFORMANCE OF SUSPENDED BAFFLE ARRAYS IN TYPICAL FACTORY SOUND FIELDS

**Murray Hodgson**

Occupational Hygiene Programme / Department of Mechanical Engineering,
University of British Columbia,
2324 Main Mall, Vancouver, BC V6T 1Z4.

## 1. Introduction

Sound fields in industrial buildings are often controlled by the installation of arrays of baffles (rectangular pieces of sound-absorptive material) suspended from the building roof. Several researchers have measured the performance, in particular the absorption coefficient, of baffle arrays in reverberation rooms - that is, in a diffuse sound field. Unfortunately, the sound fields in most industrial buildings are non-diffuse for reasons related to the room shape, surface absorption and the presence of fittings (machines, stockpiles and other obstacles in the room). The performance of absorptive materials in a non-diffuse sound field may be very different from that in a diffuse sound field. In order to determine the performance of baffles in non-diffuse fields such as those found in typical factories, reverberation times and steady-state sound pressure levels were measured in a 1:8 scale model with variable dimensions, and containing various arrays of baffles. The experimental results were then predicted using a ray-tracing model, with the input parameters describing the baffle array varied in order to obtain a best fit. In this report, the results for the preliminary series of tests are described and summarized, with emphasis on the experimental work.

## 2. Scale model

The 1:8 scale model of an idealized typical industrial workroom was built. In its various factory configurations it had a length of 30 mFS (FS = full-scale equivalent value), a width of 15 mFS and variable height (5, 10, 15 mFS). A second configuration, with dimensions of 15 mFS cube was also tested to simulate reverberation-room tests with a diffuse sound field. The floor of the model was made of painted concrete. Its walls were made of varnished 12 mm plywood. Its roofs were of varnished 3 mm plywood. The average absorption coefficient of these surfaces was about 0.06 at all test frequencies, values typical of real factories at all but the lowest frequencies. In its factory configurations two roofs were used; one was flat, the other singly pitched with a 1:3 slope and the roof apex parallel to the long dimension of the model. The model was tested when both empty and fitted with 12 2mFS-cube varnished wood boxes located randomly over the floor area. In its reverberation-room configuration the model always contained 6 of these boxes located on the floor to promote sound-field diffuseness.

## 3. Measurements made

Measurements were made of sound decay / reverberation time and of sound propagation (the variation with distance of the difference between the sound pressure level and the source sound power level) in third-octave bands from 800-20000 Hz (100-2500 HzFS). The sound source was a 75 mm diameter tweeter loudspeaker. For sound propagation testing a rigid cone narrowing from 75 mm to 3 mm was attached to the tweeter. This resulted in a compact source which was omnidirectional even at the highest test frequencies. Its constant output sound power was measured in an anechoic chamber. A B+K 4135 1/4" microphone was used as the receiver. In each test, sound decays were measured at 4 source/receiver positions and the results averaged. For sound propagation testing the source was located 5 mFS from one end wall, at half width and at a height of 1 mFS. The receiver was at half width and at a height of 1.5 mFS; sound pressure levels were measured at source/receiver distances of 1, 2, 5, 10, 15, 20, 25 mFS. Octave-band sound propagation values were derived from the third-octave results. Measurements were made using a Nortronics 830 real-time analyser. The temperature and relative humidity were measured for each test in order to determine the applicable air absorption.

## 4. Baffles and baffle arrays

Scale-model baffles were made from 6 mm (48 mmFS) thick Armstrong AF530 mineral wool. The absorption coefficent of this material was measured in a full-scale reverberation room to increase monotonically from 0.27 to 0.76 over the test frequency range. This is reasonably close to the absorption of typical unfaced full-scale baffles. The baffles had dimensions of either 1.2 x 1.2 mFS or 1.2 x 0.6 mFS. Arrays of baffles were assembled, by stringing the baffles on wires, using two baffle patterns, refered to as 'square' and 'staggered' as illustrated below:

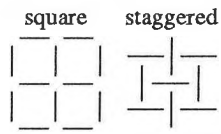


Four densities of baffles were tested; these are referred to as 1/4, 1/2, 1/1 and 2/1. For example, 1/2 indicates that the array contained 1 $mFS^2$ of baffle material per 2 $mFS^2$ of roof area. In both the flat and pitched-roof cases, the top surface of the baffle array was in the same horizontal plane as the tops of the side walls.

## 5. Test configurations

Measurments were made for configurations corresponding to various combinations of the variable model, baffle and array parameters. The configurations corresponded to variations of at most one parameter from a reference configuration. The test-parameter values were as follows, with those constituting the reference configuration in bold characters: Roof shape: **flat**, pitched; Roof height: **5**, 10, 15 mFS; Baffle dimensions: **1.2 mFS high x 1.2 mFS wide**, 1.2 mFS high x 0.6 mFS wide, 0.6 mFS high x 1.2 mFS wide; Baffle pattern: **square**, staggered; Baffle density: 1/4, **1/2**, 1/1, 2/1. In each case the model was tested when both empty and fitted.

First, reverberation times were measured in the model without baffle arrays, and with each test baffle array, in its reverberation-room configuration. These results were used to determine the 'approximate-diffuse-field' absorption coefficients of the varnished-wood model surfaces and of each baffle array. Secondly, reverberation times and sound propagation levels were measured in each test configuration in order to determine how these variables varied with each of the above model and baffle parameters, and how this differed in the empty and fitted cases.

## 6. Results

The experimental results reveal many complicated phenomena. Following are the main preliminary conclusions suggested by these results. Space limitations prohibit more than one result from being illustrated.

General comments - It was generally found that trends were easier to discern at middle and high frequencies, and in the fitted cases. At low frequencies wave effects result in complicated trends. Fittings have the effect of diffusing the sound field, resulting in more regular trends. It was clear that the effect of the introduction

of baffles on the sound field is generally different in the empty and fitted room, different in a diffuse field and in a non-diffuse field and strongly dependent on frequency. Of considerable interest is the fact that its effect was generally different for reverberation time and for sound propagation.

Baffle density - Fig. 1 shows the variation of measured reberberation times with baffle density in the fitted 5 mFS-high flat-roof model with 1.2 x 1.2 mFS baffles in a square pattern. Figure 2 shows the corresponding sound propagation result for the 1000 HzFS octave band. Introduction of the lowest density of baffles into the empty or fitted model significantly reduced the reverberation time. Doubling the density had a similar effect. However, subsequent density increases either were ineffective or, in the empty model at mid frequencies, increased reverberation times. Increasing the baffle density generally resulted in lower sound propagation levels at all frequencies and source/receiver distances.

Room height - As expected, increasing the height of the roof and its suspended baffle array resulted in higher reverberation times, whether the room is empty or fitted. Regarding sound propagation, levels tend to decrease, as expected, by up to a total of 3 dB. However, in most cases levels increase at large source/receiver distances. This suggests that the baffle arrays are acting not only to increase the absorption of the ceiling, but also as a fitted layer.

Roof shape - Roof shape had little effect on the reverberation time and sound propagation levels.

Baffle pattern - Baffle pattern had little effect on the reverberation time and sound propagation levels.

Baffle dimension - Baffle dimension had a small effect on the results. 1.2 mFS square baffles generally resulted the lowest reverberation times and sound propagation levels. 1.2 mFS high x 0.6 mFS wide baffles generally resulted in the highest values.

## 7. Prediction work

The prediction phase of the work involved modelling each test configuration using ray-tracing techniques and predicting the octave-band reverberation times and sound propagation levels. Baffle arrays were modelled by increasing the absorption coefficient of the ceiling. The known prediction parameters (dimensions, source and receiver positions, non-baffle-surface absorption coefficients, fitting density and absorption coefficients, air absorption exponents) were input. The unknown ceiling/baffle absorption coefficients were varied until a best fit with the experimental results was obtained. This established the effective absorption coefficient of the array for that configuration. In general measured sound propagation levels were thus predicted to within ±2 dB, reverberation times very closely. As an example, Table 1 shows the best-fit coefficients for the empty and fitted flat-roof model with 1.2 mFS-square baffles with 1/2 density in a square pattern, for the three test roof heights - 5, 10 and 15 mFS. Also shown are the best-fit 'approximate-diffuse-field' coefficients determined from reverberation time measurements in the cubic model using the Eyring theory. The non-diffuse coefficients may be significantly lower or higher than the diffuse values. In general, and ignoring many interesting effects, the coefficients are higher for reverberation time than for sound propagation. They also tend to be higher in the fitted model. They tend to decrease with increasing roof height.

Table 1 - Best-fit baffle-array absorption coefficients (see text for details)

| Case | Roof height | Reverberation time 125 | 250 | 500 | 1000 | 2000 | Sound propagation 125 | 250 | 500 | 1000 | 2000 |
|---|---|---|---|---|---|---|---|---|---|---|---|
| Eyring | | 0.28 | 0.28 | 0.20 | 0.51 | 0.61 | 0.28 | 0.28 | 0.20 | 0.51 | 0.61 |
| Empty | 5 | 0.37 | 0.42 | 0.34 | 0.67 | 0.82 | 0.39 | 0.28 | 0.27 | 0.39 | 0.38 |
| | 10 | 0.23 | 0.14 | 0.17 | 0.34 | 0.37 | 0.16 | 0.09 | 0.17 | 0.50 | 0.15 |
| | 15 | 0.18 | 0.13 | 0.18 | 0.33 | 0.15 | 0.18 | 0.13 | 0.18 | 0.33 | 0.15 |
| Fitted | 5 | 0.37 | 0.42 | 0.49 | 0.67 | 0.82 | 0.38 | 0.31 | 0.30 | 0.42 | 0.44 |
| | 10 | 0.33 | 0.34 | 0.42 | 0.55 | 0.58 | 0.34 | 0.25 | 0.31 | 0.30 | 0.17 |
| | 15 | 0.28 | 0.33 | 0.44 | 0.58 | 0.62 | 0.29 | 0.20 | 0.21 | 0.37 | 0.16 |

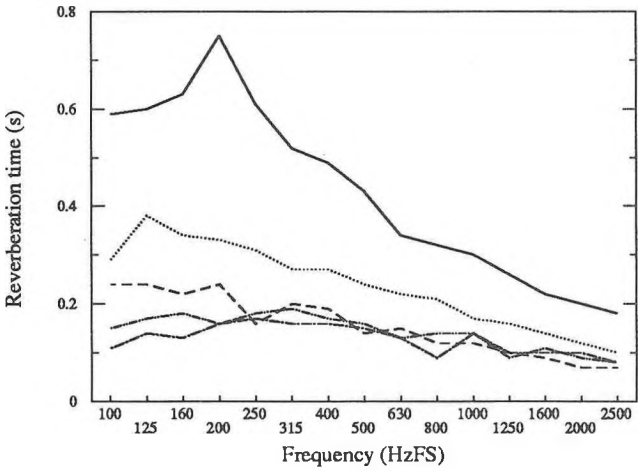


Fig. 1

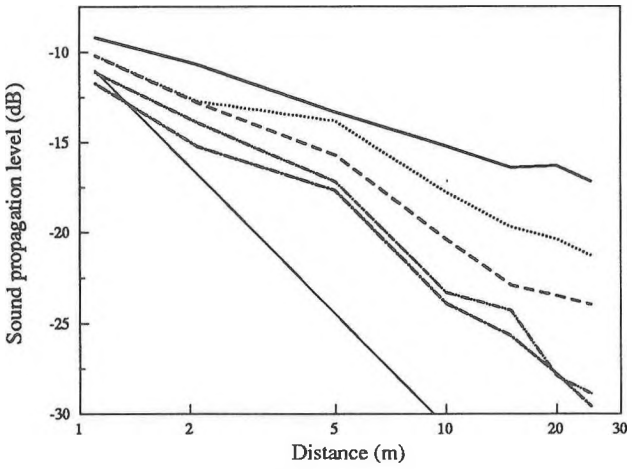


Fig. 2

Variation of measured reverberation time (Fig. 1) and 1000 HzFS octave-band sound propagation (Fig. 2) with baffle density (see text for details): (——) free field; (▪▪▪▪▪▪) no baffles; (·····) 1/4; (– – – –) 1/2; (—··—) 1/1; (—▪—) 2/1.

# OPTIMISATION DE L'ISOLATION AU BRUIT D'IMPACT DES PLANCHERS À OSSATURE D'ACIER

MIGNERON, Jean-Gabriel, *Labo. d'acoustique, CRAD, 1636 Félix-Antoine Savard, Université Laval, Québec, Qué., G1K 7P4*

LECLERC, Dominique, *Acoustec Inc. 925 Newton, suite 103, Québec, Qué., G1P 4M2*

Cette recherche, subventionnée par la SCHL, a porté sur l'optimisation de l'isolation aux bruits d'impact des planchers à ossature d'acier utilisés pour la construction d'immeubles à logements. Les bruits d'impact constituent, en effet, le principal problème d'intimité acoustique dans ce genre de construction résidentielle multiple, avec des planchers sur poutrelles d'acier, tout particulièrement lorsqu'on est en présence d'une finition de planchers dure, comme le bois franc, la céramique, voire même le linoléum.

Les objectifs principaux de la recherche ont été doubles, soit de mettre au point et de vérifier l'efficacité de différents types de planchers flottants et, ensuite, de renforcer l'isolation des plafonds contre les bruits d'origine vibratoire (bruits d'impact), transmis à travers la charpente d'acier. Il est à noter ici que la réduction de la propagation des bruits d'impact est également bénéfique à l'isolation conventionnelle aux bruits aériens. Pour les planchers flottants, on a pu vérifié le choix des différents matériaux, l'épaisseur du plancher, le panneau de plancher comme tel (masse, raideur, présence éventuelle de lambourdes), de même que les dispositifs amortissants. En tout, 16 échantillons de plancher ont été testés. Par ailleurs, pour le renforcement des plafonds, les liaisons mécaniques entre la structure et les fourrures du plafond ont été vérifiées, ainsi que la désolidarisation périphérique et le montage des panneaux de gypse (influence de la masse et d'un éventuel amortissement) et ce, pour 5 types de plafonds différents. Finalement, dans la dernière partie du projet, différentes finitions de plancher ont été ajoutées sur certains planchers flottants, les mêmes mesures étant reprises pour deux types de plafonds différents, soit un plafond conventionnel et un plafond désolidarisé, afin de vérifier l'isolation globale aux bruits d'origine vibratoire produit par la combinaison de ces traitements.

## TESTS SUR LES PLANCHERS FLOTTANTS

Toute l'étude des planchers flottants et de l'isolation des plafonds aux bruits d'impact a été réalisée à l'aide d'un montage expérimental conçu de manière à s'approcher le plus possible des conditions réelles de construction. Ce montage s'apparente à une chambre réverbérante de 60m³, dont le toit est constitué par une dalle de béton de 100mm d'épaisseur, coulée sur une ossature d'acier constituée de poutrelles de type "Hambro", avec des portées de 5m. Cette chambre expérimentale permet de réaliser tous les tests en laboratoire, en plus d'obtenir des niveaux s'approchant de ceux qu'il serait possible de mesurer in-situ.

Plusieurs informations sur les planchers de finition flottants, destinés à renforcir l'isolation aux bruits d'impact des planchers à ossature d'acier, peuvent se dégager de cette étude. Les principaux résultats de mesures sont reproduits dans le tableau N°1. Tout d'abord, l'augmentation de la masse surfacique du panneau flottant provoque un certain accroissement de l'indice IIC. De plus, lorsque l'on ajoute des lambourdes à un même panneau et que l'on utilise le même matériau résilient, on augmente d'environ 5 dB l'isolation aux bruits d'impact (indice IIC). Par ailleurs, si l'on ajoute de la laine minérale dans les espaces d'air entre les lambourdes, dépendamment de la masse surfacique du type de panneau et du matériau résilient utilisé, il est également possible d'augmenter d'environ 4 à 6 dB l'indice IIC obtenu.

*TABLEAU N°1: principaux résultats relatifs aux planchers*

| N° | Description de l'échantillon de planchers flottants | Épaisseur du plancher flottant (mm) (masse surfacique du plancher , kg/m²) | Indice IIC | Pertes moyennes aux fréq. dominantes de la dalle 125-250 Hz (dB accél.) |
|---|---|---|---|---|
| 0 | Dalle de béton seulement | ---- | 39 | ----- |
| 1 | Contre-plaqué 19mm<br>Duralux 10mm | 29<br>(11.4) | 40 | 28.3 |
| 2 | Contre-plaqué collé 16mm<br>Gypse firecode 16mm<br>Duralux 10mm | 42<br>(18.9) | 40 | 24.5 |
| 3 | Contre-plaqué collé 16mm<br>Gypses firecode 2x16mm<br>Duralux 10mm | 58<br>(30.0) | 43 | 27.2 |
| 4 | Contre-plaqué, gypse firecode,<br>contre-plaqué (collés 3x9mm)<br>Duralux 10mm | 38<br>(16.9) | 41 | 26.2 |
| 5 | Contre-plaqué, gypse firecode,<br>contre-plaqué (collés 3x9mm)<br>Duralux 18mm | 44<br>(16.9) | 44 | 29.7 |
| 6 | Contre-plaqué, gypse firecode,<br>contre-plaqué (collés 3x9mm)<br>Duralux 10mm<br>Duralux 10mm | 48<br>(16.9) | 46 | 30.6 |
| 7 | Contre-plaqué 19mm<br>Lambourdes collées 19mm<br>Bandes Duralux 10mm | 48<br>(11.4) | 45 | 39.0 |
| 8 | Contre-plaqué, gypse firecode,<br>contre-plaqué (collés 3x9mm)<br>Lambourdes collées 19mm<br>Bandes Duralux 10mm | 57<br>(16.9) | 47 | 34.6 |
| 9 | Contre-plaqué 19mm<br>Lambourdes collées 19mm<br>Blocs isolants CDM 10mm | 48<br>(11.4) | 40 | 36.3 |
| 10 | Contre-plaqué, gypse firecode,<br>contre-plaqué (collés 3x9mm)<br>Lambourdes collées 19mm<br>Blocs isolants CDM 10mm | 57<br>(16.9) | 44 | 37.2 |
| 11 | Contre-plaqué 19mm<br>Lambourdes collées 19mm<br>Laine minérale 25mm<br>Blocs isolants CDM 10mm | 48<br>(11.4) | 46 | 38.3 |
| 12 | Contre-plaqué, gypse firecode,<br>contre-plaqué (collés 3x9mm)<br>Lambourdes collées 19mm<br>Laine minérale 25mm<br>Blocs isolants CDM 10mm | 57<br>(16.9) | 48 | 37.1 |
| 13 | Contre-plaqué 19mm<br>Lambourdes collées 19mm<br>Laine minérale 25mm<br>Blocs isolants CDM 20mm | 58<br>(11.4) | 46 | 37.9 |
| 14 | Contre-plaqué, gypse firecode,<br>contre-plaqué (collés 3x9mm)<br>Lambourdes collées 19mm<br>Laine minérale 25mm<br>Blocs isolants CDM 20mm | 67<br>(16.9) | 47 | 37.3 |
| 15 | Contre-plaqué 19mm<br>Lambourdes collées 19mm<br>Laine minérale 25mm<br>Bandes Duralux 18mm | 54<br>(11.4) | 47 | 39.2 |
| 16 | Contre-plaqué, gypse firecode,<br>contre-plaqué (collés 3x9mm)<br>Lambourdes collées 19mm<br>Laine minérale 25mm<br>Bandes Duralux 18mm | 63<br>(16.9) | 48 | 37.9 |

Un autre élément important dans la conception d'un plancher flottant concerne le choix du matériau résilient.

Comme on peut le constater, le caoutchouc granulaire (Duralux) a une résilience supérieure aux coussins de liège et caoutchouc agglomérés (CDM-12) et cette résilience se répercute directement sur la valeur de l'indice IIC. De plus, l'épaisseur optimale du matériau varie dépendamment du matériau retenu. Dans le cas du caoutchouc granulaire, plus l'épaisseur augmente, plus l'isolation aux bruits d'impact augmente, tandis que pour les coussins antivibratoires, une augmentation de l'épaisseur de 10 à 20mm, ne change sensiblement pas l'indice IIC.

## EXPÉRIMENTATION RELATIVE AUX PLAFONDS

La seconde partie de l'étude a permis de mettre en évidence l'influence de la finition du plafond sur l'isolation aux bruits d'impact des planchers à ossature d'acier. Parmi les 5 types de plafonds testés, celui qui s'avère le moins performant acoustiquement est un plafond conventionnel, soit celui qu'on retrouve le plus souvent dans ce type de construction (type 1). Le fait d'ajouter de la laine minérale dans l'espace d'air au-dessus du plafond (type 2), augmente quelque peu la valeur de l'indice IIC. Par ailleurs, l'augmentation de la masse, c'est-à-dire lorsqu'on double le plafond d'une seconde feuille de gypse (type 4), accroît significativement l'isolation aux bruits d'impact. Par contre, lorsqu'on sépare les deux feuilles de gypse à l'aide de barres résilientes, les résultats sont égaux ou inférieurs à ceux sans barres résilientes (type 3). L'ajout de barres résilientes pour doubler un plafond ne semble donc pas influencer l'isolation aux bruits d'impact.

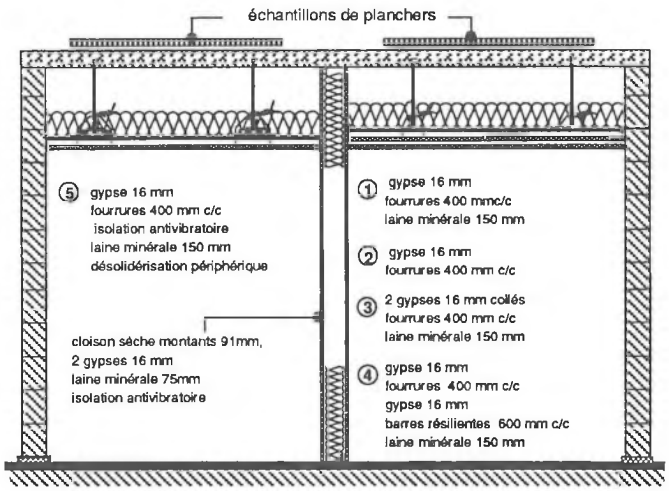


*Dispositif expérimental utilisé pour les plafonds*

En ce qui concerne le plafond avec isolation anti-vibratoire et désolidarisation périphérique (type 5), les résultats sont nettement supérieurs à ceux obtenus pour un plafond conventionnel. Avec le plafond conventionnel, les vibrations de la dalle de béton sont directement transmises aux panneaux de gypse du plafond; pour les fréquences inférieurs à 630 Hz, les vibrations peuvent même se trouver amplifiées. Par contre, le plafond muni d'un système anti-vibratoire atténue grandement les vibrations provenant de la dalle de béton. Cette atténuation vibratoire se répercute également sur un mur mitoyen, comme le montre le croquis du dispositif expérimental employé pour les tests relatifs aux plafonds, de même que les spectres d'accélération reproduits dans le graphique ci-dessous.

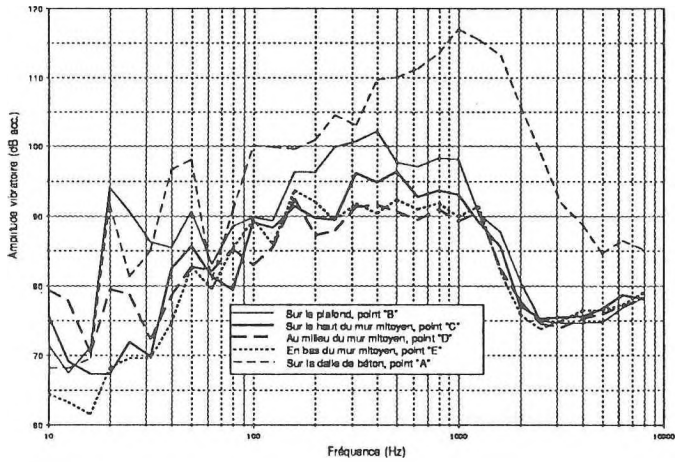


*Atténuation vibratoire due à la désolidarisation du plafond*

*TABLEAU N°2: principaux résultats relatifs aux finitions*

| N° échantillon | Type de planchers flottants avec leurs revêtements de finition | Indice IIC (Plafond N°1) | Indice IIC (Plafond N°5) |
|---|---|---|---|
| 17 | Céramique collée<br>Contre-plaqué 16mm<br>Gypse 16mm<br>Lambourdes 19mm<br>Bandes Duralux 12mm | 61 | 58 |
| 18 | Tapis<br>Duralux 6mm<br>Contre-plaqué 16mm<br>Gypse 16mm<br>Lambourdes 19mm<br>Bandes Duralux 12mm | 77 | 80 |
| 19 | Bois franc<br>Contre-plaqué 16mm<br>Gypse 16mm<br>Lambourdes 19mm<br>Bandes Duralux 12mm | 57 | 56 |
| 20 | Tapis<br>Duralux 12mm | 79 | 83 |

## CONCLUSION

Comme on peut le constater dans le tableau N°2, il est difficile d'obtenir un indice IIC-65 lorsqu'on utilise une finition de plancher dure, comme la céramique ou le bois franc, peu importe le type de plafond construit. Par contre, avec une finition de tapis et sous-tapis de qualité, l'indice IIC augmente considérablement. Lorsqu'on met en oeuvre ce type de finition, un plafond désolidarisé est supérieur à un plafond conventionnel. Par contre, avec une finition de plancher dure, les modes vibratoires semblent se combiner et ainsi réduire légèrement l'isolation aux bruits d'impact pour le plafond désolidarisé. Ce point resterait, cependant, à vérifier sur un échantillon de plus grandes dimensions.

## RÉFÉRENCES

ACOUSTEC Inc.: Optimisation de l'isolation aux bruits d'impact des planchers à ossature d'acier utilisés pour la construction d'immeubles à logements, 192p., SCHL, 6585/C52, 1992.

MIGNERON, J.-G. et coll.: Qualité acoustique, isolation et intimité des immeubles d'habitation en copropriété, 325p., CRAD/SCHL, 6585/M12-4, 1989.

MIGNERON, J.-G.: Tests d'isolation au bruit d'impact sur six échantillons de planchers, 17p., CRAD/Dôme Const. 1988.

# CONTROLE DU BRUIT DES THERMOPOMPES EN MILIEUX RÉSIDENTIELS

MIGNERON, Jean-Gabriel, ABONCE, Ramon et LEMIEUX, Pierre, *Laboratoire d'acoustique, CRAD, 1636 Félix-Antoine Savard, Université Laval, Québec, Qué., G1K 7P4*

Les installations de pompes à chaleur domestiques se sont multipliées ces dernières années, notamment avec les coûts croissants de l'énergie. Les thermopompes sont généralement localisées à l'endroit extérieur le plus pratique pour être relier au reste de l'installation de chauffage et ventilation. Il en résulte souvent une perturbation par le bruit pour tout le voisinage résidentiel. Toutes les thermopompes, même si elles ne comprennent pas d'unité de compresseur intégrée, sont bruyantes. Elle comportent toutes un puissant ventilateur qui fait circuler l'air extérieur pour assurer le refroidissement des serpentins, en plus de ce bruit, il faut compter le bruit propre au compresseur et le bruit de circulation du gaz réfrigérant. Les municipalités du Québec recoivent de plus en plus de plaintes, surtout estivales, relatives à ce type d'équipement résidentiel.

La présente recherche, subventionnée par la SCHL, comportait ainsi plusieurs objectifs: analyser le mode de rayonnement acoustique des thermopompes les plus couramment utilisées dans les secteurs résidentiels, étudier la possibilité d'un traitement acoustique simple destiné à confiner le bruit produit par ce type d'équipement, vérifier dans quelle mesure ce traitement acoustique devait être adapté à chacune des différentes machines et, finalement, s'assurer que le traitement acoustique éventuel ne réduirait pas les capacités thermiques de la machine, que ce soit en mode chauffage ou en mode climatisation. Une première étape portait sur la vérification in-situ du mode de rayonnement acoustique des principales marques de thermopompes rencontrées dans la région de Québec. Cent vingt cinq thermopompes ont été ainsi identifiées, soit à cause de leur visibilité à partir de la rue ou bien de leur bruyance audible. Après analyse de la distribution par marques des 125 thermopompes de l'échantillon, on a pu constater une nette prédominance de la marque TRANE, avec 38 unités, suivie par les marques CARRIER, YORK et LENNOX, avec respectivement 28, 18 et 10 unités.

## ÉCHANTILLON ET MESURES SUR LE TERRAIN

Une première mesure du niveau de pression acoustique a été relevé à 1m de distance de chaque unité; 80 dossiers de référence ont été ouverts, avec des machines pour lesquelles les niveaux de bruit obtenus se situaient entre 52.5 et 70.6 dB(A). Parmi cet échantillon de 80 thermopompes, 20 d'entre elles, choisies parmi les plus bruyantes, ont été étudiées plus en détail. Les mesures acoustiques ont porté essentiellement sur la détermination de la puissance acoustique, ainsi que sur deux analyses spectrales de référence au 1/3 d'octave, la première faite de face et la seconde sur le dessus de la machine (bruit du ventilateur).

Les résultats des mesures du niveau global de bruit en dB(A), réalisées à 1m de distance de chaque unité, permettent de confirmer que *la plupart des thermopompes peuvent être considérées comme bruyantes* (mis à part les hauts-de-game et les derniers modèles). En plus de cette première constatation, les données correspondants aux 80 thermopompes mesurées montrent qu'il existe certaines marques et modèles plus bruyants. D'autre part, il a été constaté que la localisation de la thermopompe par rapport à la maison, constituait souvent une des raisons de son impact sur voisinage.

## ÉTUDE DU DISPOSITIF DE RÉDUCTION DE BRUIT

Une thermopompe de marque TRANE a été choisie pour une analyse détaillée de faisabilité d'un dispositif de silencieux. Non seulement cette marque semblait la plus répandue, mais il était encore possible de trouver un ancien modèle, relativement plus bruyant que ceux des séries les plus récentes. Le modèle retenu était une machine de 2 tonnes, largement répandue et relativement bruyante.

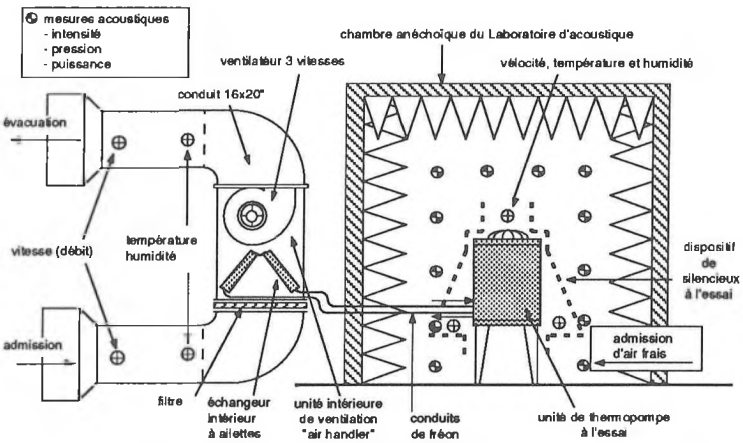


La thermopompe expérimentée a été installée dans les nouvelles chambres de mesure du Laboratoire d'acoustique de l'Université Laval. L'unité de thermopompe a été montée dans la chambre anéchoïque et le dispositif de circulation de l'air, dans la grande chambre réverbérante voisine. Le montage expérimental a permis de réaliser simultanément des mesures acoustiques et des mesures thermiques. Le "air handler" a été monté en position vertical; deux conduits perpendiculaires d'entrée et de sortie d'air ont été utilisés, afin de recirculer l'air dans les coins opposés de la chambre. Le silencieux expérimenté sur l'unité extérieure devait rencontrer quatre objectifs: contrôler le bruit produit le plus près possible de la source, avec une enceinte collée sur l'enveloppe extérieure de la thermo-pompe, réduire le niveau et modifier la directivité de la source principale de bruit constituée par le ventilateur supérieur, réduire la radiation latérale du bruit par les quatre faces d'aspiration et, enfin, permettre une bonne circulation de l'air dans la thermopompe, en assurant, si possible, la séparation de l'air aspiré et refoulé.

Pour des raisons pratiques, le silencieux placé à la sortie du ventilateur n'a pas été modifié, seule sa longueur aurait pu d'ailleurs faire l'objet d'un changement. Les variations possibles du dispositif de silencieux concernaient le traitement des quatre faces d'aspiration, ceci selon trois étapes d'intervention différentes. Les mesures acoustiques correspondantes ont porté sur la détermination de la puissance acoustique globale de la thermopompe et l'analyse de la composition spectrale du bruit produit sur les

*Réductions moyennes de bruit en dB(A), obtenues pour les trois modèles de silencieux expérimentés.*

| Modèle de thermopompe expérimenté | Admission d'air sans traitement | Admission d'air avec traitement | Réduction de bruit à l'admission | Refoulement d'air sans traitement | Refoulement d'air avec traitement | Réduction de bruit au refoulement | Pour toute la thermo-pompe |
|---|---|---|---|---|---|---|---|
| Marque "TRANE" | 68.7 | 57.0 | 11.7 | 68.3 | 61.3 | 7.0 | 11.4 |
| Marque "YORK" | 74.6 | 57.6 | 17.0 | 77.2 | 59.7 | 12.5 | 16.4 |
| Marque "LENNOX" | 72.5 | 62.4 | 10.1 | 72.2 | 59.7 | 12.5 | 11.6 |

différentes faces de la machine. Pour tenir compte d'une éventuelle directivité des différentes sources de bruit, les mesures ont toutes été relevées en pression et en intensité acoustique. Cette précaution n'a pas permis de mettre en évidence une directivité particulière du rayonnement acoustique de la machine. Le calcul détaillé de la puissance acoustique a ensuite permis de préciser l'efficacité de chacune des étapes du traitement acoustique.

Les mesures aéroliques avaient comme objectif de déterminer si le traitement acoustique de la thermopompe pouvait avoir une incidence quelconque sur le rendement thermique de la machine et de chiffrer les éventuelles modifications du comportement theermomécanique. Ces mesures ont porté sur la détermination détaillée des vitesses de l'air dans les différentes parties de la thermopompe et sur la vérification des écarts de température entre les flux d'air aspiré et refoulé. Des mesures similaires ont été relevées du côté du "air handler", surtout en regard des différentes vitesses et du différentiel de température. La constance du débit d'air, avec ou sans silencieux est une condition essentielle pour l'efficacité des dispositifs étudiés. Il faut cependant remarquer que l'enceinte de la thermopompe et la disposition de ses éléments constituent déjà une limitation significative pour la circulation de l'air, en particulier, l'orientation, la dimension et la nature des grilles d'entrée et de sortie d'air.

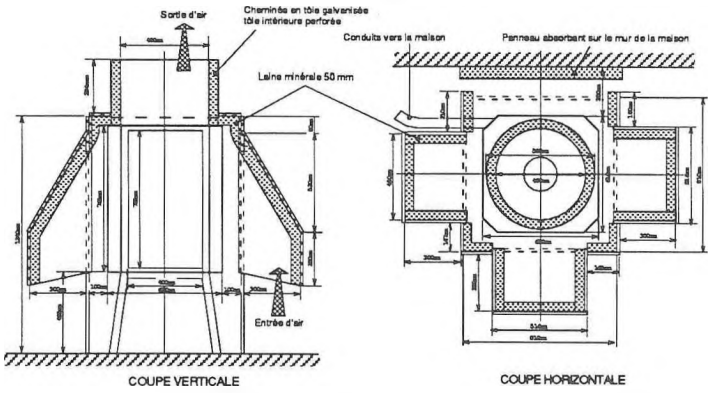


*Croquis du silencieux réalisé pour la thermopompe YORK*

Afin de compléter cette expérience détaillée de laboratoire, deux autres silencieux ont été conçus et installés sur des machines différentes, soit une thermopompe de marque YORK de 3 tonnes, avec grilles d'aspiration sur les quatre faces latérales et refoulement par un ventilateur localisé sur le dessus de la machine, et une thermopompe de marque LENNOX, également de 3 tonnes, avec grilles d'aspiration sur deux des faces latérales et refoulement par les deux faces opposées. Cette dernière thermopompe était très différente des deux autres modèles, puisque complètement fermée sur les dessus, sa circulation d'air se faisant horizontalement, selon une diagonale.

## CONCLUSION

Les unités extérieures de thermopompes résidentielles constituent une source de bruit continu importante, dommageable pour l'environnement des milieux résidentiels. Les niveaux de bruit produits sont relativement variables, suivant la puissance des machines, leur technologie, leur degré d'usure, et leur disposition autour de la résidence. Il faut éviter, en tout premier lieu, la proximité des fenêtres du voisinage et les réflexions nuisibles, sur un mur de façade ou sur un sol trop dur. Néanmoins, quelles que soient les situations, *il est toujours possible de construire un véritable dispositif de silencieux autour d'un thermopompe donnée.* Cette disposition étant préférable à l'érection d'un écran absorbant; car l'écran s'opposera à la libre circulation de l'air autour de la machine.

Un dispositif de silencieux efficace doit être installé le plus proche possible du coffret de la thermopompe et comporter, en plus d'une enveloppe centrale isolée, des silencieux appropriés pour les entrées et les sorties d'air de la machine. Malheureusement, ce dispositif ne peut être universel, il doit être conçu et construit, en fonction des dimensions et des caractéristiques de la thermopompe considérée. Si nécessaire, il doit être complété par un traitement absorbant du mur le plus proche, de façon à contrôler les réflexions acoustiques. On peut être assuré qu'*un silencieux bien construit n'affectera pas le rendement thermique de la thermopompe*, quel que soit le point de vue de l'installateur sur ce sujet. Il est même probable que ce rendement thermique se trouve accru, du fait d'une meilleure séparation des flux d'air, à l'aspiration et au refoulement.

## RÉFÉRENCES


AIR CONDITIONING & REFRIGERATION INST.: Directory of certified unitary air-conditioners, unitary air-source heat-pumps, sound-rated outdoor unitary equipment, ARI, Arlington VA, 1989.

ASHRAE: "Measurement of sound power radiated from heating refrigeration and air conditioning equipment", ASHRAE:, Standard 36-62, Atlanta GA, 1962.

FRASER, J. and QUIRT,J., D.: "Enclosures to reduce noise from heath pumps: four case studies", pp.19-28, in Can. Acoustics, Vol.13 Nº 3, 1985.

GCPM & ASS.: Guide des Thermopompes au Québec, 160 p., ABC Publication, Montréal, 1988.

HAROLD, R.,G.: "ARI sound rating and certification of residential outdoor air conditioning units", pp. 249-258, in Noise-Con. 83 proceed., MIT, Cambridge Mass., 1983.

MARSH, A.: "Noise control for roof-mounted air conditioning condensing units", pp. 269-276, in Noise-Con. 83 proceed., MIT, Cambridge Mass., 1983.

MIGNERON, J.-G., ABONCE, R. et LEMIEUX, P.: Analyse du rayonnement acoustique des thermopompes en milieux résidentiels, étude de faisabilité pour un dispositif de réduction de bruit,191p., CRAD/SCHL, Nº6585/M12-4, 1991.

# VIBRATIONS AND SOUND RADIATION OF A CYLINDRICAL SHELL UNDER A CIRCUMFERENTIALLY MOVING FORCE

**Raymond Panneton, Alain Berry, Frédéric Laville**
GAUS, Mechanical Engineering
University of Sherbrooke, Sherbrooke (Quebec) J1K 2R1

## 1. INTRODUCTION

Vibrations and sound radiation by finite cylindrical shells have been extensively studied in the past few years. Usually, the authors have studied the vibrations and the sound radiation by cylinders in the case of a non-moving harmonic driving force [1]. Most papers dealing with a moving force on a cylindrical shell (axially [2] or circumferientially [3]) were only concerned about the mechanical vibrations. This is a presentation of the work under progress to develop a model including both the vibrations and the sound radiation of a simply supported cylindrical shell excited by a circumferentially moving radial point force. The motivation behind this work is the modelisation of the "pressure screens" used in the pulp and paper industry. The theoretical formulation presented in section 2 is based on a variational approach. The case of a homogeneous cylindrical shell in air is treated as a first step towards more complex structures. Numerical results in terms of quadratic velocity and radiated sound power are presented, and principal phenomena related to the moving force rotational speed are discussed in section 3.

## 2. THEORETICAL FORMULATION

The studied system consists of a baffled thin cylindrical shell with the simply supported boundary conditions (Fig. 1). In the case of a finite cylinder, and with a variational approach, one can find the governing equations of motion for the studied system using the Hamilton's function, which has the form:

$$H = \int_{t_o}^{t_1} \left\{ T_{shell} - E_{shell} - E_{fluid} + E_{force} \right\} dt \tag{1}$$

where $T_{shell}$ and $E_{shell}$ are respectively the shell kinetic and deformation energy, $E_{fluid}$ is the energy related to the exterior acoustic pressure field, and $E_{force}$ is the energy of the rotational driving force. Using the thin shell theory and under Donnell's assumptions, the three first terms are expressed as in reference [1]. The energy term related to the radial force is

$$E_{force} = \int_V \left\{ \overrightarrow{P(M)} \right\}^t \left\{ \overrightarrow{U(M)} \right\} dV \tag{2}$$

where $V$ is the volume of the cylinder, $F(M)$ is the radial force at a point M on the shell, and $U(M)$ is the displacement of point $M$. A radial point force located at $x_o$ and travelling around the circumference is expressed as:

$$P(M,t) = P(x,\varphi,t) = \frac{P}{aL}\delta(x - x_o)\delta(\varphi - \Omega \cdot t) \tag{3}$$

where $\delta$ is the Dirac distribution, and $\Omega$ is the rotational speed of the force. Applying the Poisson's summation formula on (3) one can separate the space and time variables:

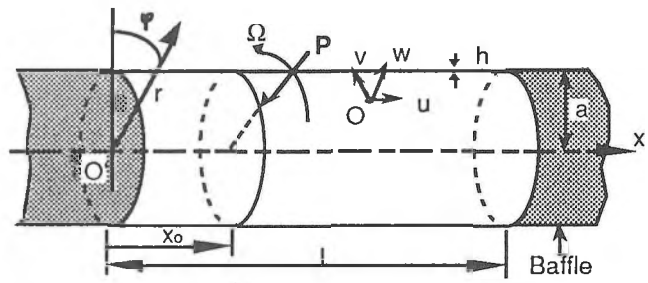


Fig. 1: Schematic of the cylindrical shell excited by a circumferentially moving radial point force

$$\left\{ \begin{array}{c} P(M,t) = \sum_{N=-\infty}^{\infty} P(M)P(t) \\ P(M) = \dfrac{P}{2\pi a \cdot L}\delta(x - x_o)\cdot e^{-jN\varphi} \\ P(t) = e^{jN\Omega t} \end{array} \right\} \tag{4}$$

Integrating $P(M)$ in (2) and developing on the modes of a simply supported *in vacuo* circular cylindrical shell, one can minimize this energy function with respect to the modal amplitudes and obtain the expression of the generalized force vector:

$$P^{\alpha}_{Nnmj} = \frac{1}{2}\delta^{\alpha}_{Nn} P \sin\left(\frac{m\pi x_o}{L}\right) \tag{5}$$

where

$$\delta^{\alpha}_{Nn} = \left\{ \begin{array}{ll} 0 & n \neq N \\ 0 & n=N=0, \alpha=0 \\ 2 & n=N=0, \alpha=1 \\ -j & n=N\neq 0, \alpha=0 \\ 1 & n=N\neq 0, \alpha=1 \end{array} \right\}$$

Applying the same development for the three first energy terms of equation (1) gives finally, for an $e^{jN\Omega t}$ rotational excitation, the following modal equation of motion:

$$m_{nmj}\left(\omega^2_{nmj}(1-j\eta) - (N\Omega)^2\right)a^{\alpha}_{nmj} - j(N\Omega)\sum_{q=1}^{\infty}\sum_{k=1}^{3} Z_{nmq}\, a^{\alpha}_{nqk} = P^{\alpha}_{Nnmj} \tag{6}$$

where $N\Omega$ represents the $N^{th}$ harmonic of the rotational speed, $n$ the circumferential order, $m$ and $q$ the longitudinal orders, $j$ and $k$ the type of mode (torsional, radial, axial), $\omega_{nmj}$ the eigen-angular frequencies, $a^{\alpha}_{nmj}$ the modal amplitudes, $\eta$ the structural damping, and $Z_{nmq}$ the modal radiation impedances.

For a better understanding of equation (6), let's neglect $Z_{nmq}$. Then, one can observe that maxima for modal amplitudes will occur when

$$\Omega = \Omega_c = \frac{\omega_{nmj}}{N}; \quad N=n \tag{7}$$

where $\Omega_c$ is named the critical speed. In fact, there are as many critical speeds as eigen-angular frequencies.

## 2. NUMERICAL RESULTS

The results for a 0.003 m thick steel shell with a length of 1.2 m and a radius of 0.48 m are presented in Figs. 2, 3 and 4 for two different rotational speeds (25 Hz and 75 Hz), for the first longitudinal order ($m$ =1), and for the type of mode (torsional, radial, axial) having the lowest eigen-angular frequency.

Fig. 2 represents critical speeds versus circumferential orders. As one can see, the first critical speed occurs at 28 Hz, for the fifth circumferential order and the first longitudinal order (i.e. mode (5,1)).

Because the 25 Hz rotational speed is very close to the first critical speed of 28 Hz associated with the mode (5,1), the quadratic velocity amplitude presents a significant single peak for the 25 Hz fifth harmonic (i.e. 125 Hz or the fifth '+' in Fig. 3). Since only frequencies around mode (5,1) (75-250 Hz) are very excited, a low sound power will be radiated (see Fig. 4).

If the rotational speed is increased up to 75 Hz, one can predict, by looking at Fig. 2, that a first peak will occur at its third harmonic (mode (3,1)) and a second at its sixteenth harmonic (mode (16,1)). The result predicted is verified in Fig. 3. The bandwidth excited is now very large and the final result will be an important increase of the radiated sound power (see Fig. 4).

For the 75 Hz rotational speed, the previous results include only the first longitudinal order. If the $m$ first longitudinal orders are included, the quadratic velocity and the radiated sound power will be radically different because more than two critical speeds will occur.

For the 25 Hz rotational speed, including $m$ longitudinal modes will not change appreciably the curves because no other critical frequency will occur.

Finally, as one can see, on Fig. 3 and 4, or by the mean of equation (6), to obtain the quadratic velocity and the radiated sound power at 2000 Hz, for a radial force rotating at 25 Hz, the circumferential order has to be equal to 80 ($80^{th}$ harmonic). In that case, we need to ensure that thin shell theory is still applicable by using the following criteria:

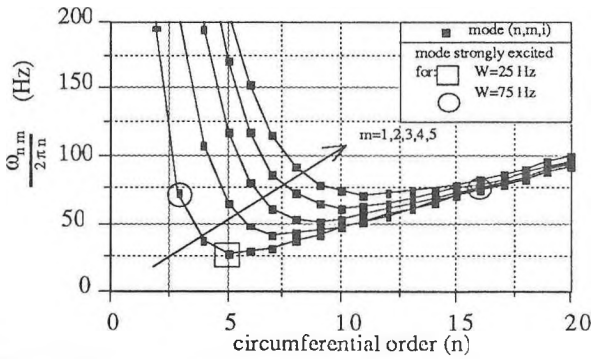


Fig. 2: Critical speed versus circumferential orders

$$n < 0.2\,\pi \left(\frac{a}{h}\right) \tag{8}$$

## 3. CONCLUSION

The model developed in the case of a simply supported cylindrical shell has allowed us to draw some preliminary conclusions useful in design such as the low level of sound radiation when the force rotational speed is lower than the critical frequency associated with the first mode. The use of the variationnal approach will allow the integration of more complex parameters such as stiffeners, visco-elastic layers, internal pressure and heavy fluid.


## ACKNOWLEDGEMENTS

This work was supported by N.S.E.R.C. (Natural Sciences and Engineering Research Council of Canada), I.R.S.S.T. (Quebec Occupational Health and Safety Institute), and Andritz Sprout Bauer inc.


## REFERENCES


[1] B. Laulagnet, J.L. Guyader, "Sound radiation by finite cylindrical ring stiffened shells", J.S.V., **138**(2), pp. 173-191, 1990

[2] P.Mann-Nachbar, "On the role of bending in the dynamic response of thin shells to moving discontinuous loads", J. Aerospace Sc., pp.648-657, june 1962

[3] S.C. Huang, W. Soedel, "On the forced vibration of simply supported rotating cylindrical shells", J.A.S.A., **84**(1), pp. 275-285, July 1988


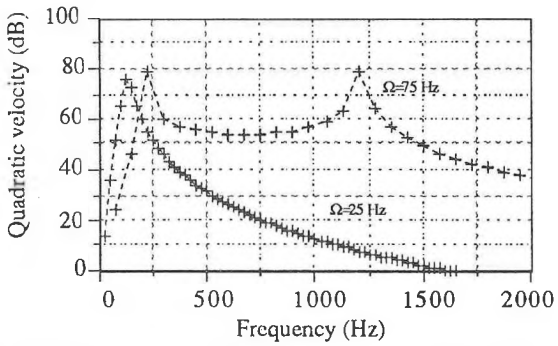


Fig. 3: Quadratic velocity (each '+' corresponds to an harmonic of the 25 or 75 Hz rotational speed)

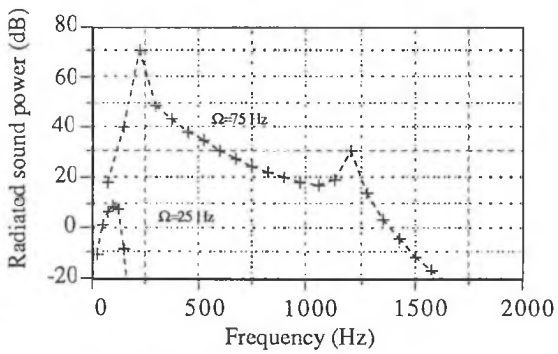


Fig. 4: Radiated sound power (each '+' corresponds to an harmonic of the 25 or 75 Hz rotational speed)

# Insertion Loss of Multi-Chamber Mufflers

**R. Ramakrishnan and A. Misra**
Ontario Hydro
700 University Avenue
Toronto, Ontario

## 1.0 Introduction

Expansion chamber mufflers are commonly used as noise control devices in piping systems, when the application of passive silencers is not possible. Single expansion chamber mufflers has been studied extensively [1, 2, 3]. Lamancusa [4] conducted a parametric study on the transmission loss of double expansion mufflers. However, insertion loss is more meaningful than transmission loss for the effect of the inlet and tail pipe lengths are properly taken into account. A parametric study on the insertion loss of two chamber and three chamber mufflers was conducted and preliminary results of our study are presented in this paper. The results of this paper assume anechoic termination at the tail pipe exit and hence the tail pipe effects are neglected. Further, the damping due to the flow medium and the pipe walls is negligible.

## 2.0 Solution Procedure

The details of two chamber and three chamber mufflers are shown in Figure 1. Standard solution methods usually evaluate the transmission loss of the muffler, which is the amount of sound transmitted through the muffler installed in an infinitely long pipe. Insertion loss on the other hand reflects the actual attenuation provided by the muffler. The insertion loss is defined by,

$$I.L. = 20 \log \left| \frac{P_{o,w}}{P_{o,n}} \right|, \quad dB \qquad (1)$$

where, $p_{o,w}$ is the sound pressure downstream of the muffler with the muffler in place and $p_{o,n}$ is the sound pressure at the same location without the muffler.

Three conventional methods can be used to evaluate the insertion loss of the mufflers: plane wave analysis (one dimensional wave propagation model); transfer matrix methods; and numerical schemes such as finite element methods. Plane wave analysis [1, 4] is easy to apply, but the valid frequency is limited to the size of the muffler components. Munjal [2] has used transfer matrix methods extensively and in this paper, we have applied finite element discretization to evaluate the insertion loss.

Craggs [3] developed a finite element code to solve for the insertion loss of reactive mufflers. Misra and Ramakrishnan [5] used an existing standard structural finite element package with acoustic elements, ABAQUS, [6] to solve for the acoustics of complex heat transport piping systems. Details of the finite element formulation and its acoustical application are given in references 5 and 6. In the present paper, the outlet of the muffler system is assumed to be anechoically terminated and hence the effect of the tail pipe is neglected. The preliminary results focus on the effects of: the inlet pipe length; and the lengths and cross sectional sizes of the two chamber and three chamber muffler elements. Both one dimensional and two dimensional elements ( the chosen examples are axi-symmetric) are used to evaluate the applicable frequency range of the one dimensional models. Comparison with transmission loss results of Lamancusa [4] for a two chamber muffler is also presented to highlight the limitations of transmission loss calculations.

## 3.0 Results and Discussion

The insertion loss results were calculated for four (4) two chamber and for four (4) three chamber mufflers. The details of the mufflers are outlined in Table 1. The results for Case 1. are shown in Figure 2. The insertion loss evaluated using a plane wave model, One-D acoustic elements as well as the transmission loss are presented in Figure 2a. The plane wave predictions agree very well with the finite element results. Even though the spectral trend is similar, the transmission loss fails to account for the resonances of the inlet pipe ( 3 m for Case 1.), where as the insertion loss properly accounts for the reduced noise loss at the various inlet pipe frequencies. If source frequencies happen to match with the inlet resonances, the muffler would have negligible effect. The transmission loss calculations would not have recognized the shortcoming of the muffler. The insertion loss values are seen to be higher than the transmission values. The effective bandwidth between the two predictions seems to be comparable if one neglected the inlet pipe effects. The insertion loss evaluated using One-D and Two-D acoustic elements in ABAQUS is shown in Figure 2b. The two results agree well with each other up to about 110 Hz and start to diverge even though the loss spectra are similar. The wave length at 110 Hz is 3 m. The expansion chamber dimension becomes comparable to the wavelength and the Two-D effects (higher order axial and radial modes) become important.

The insertion loss results for double expansion chamber mufflers are presented in Figure 3. The effect of the inlet pipe is reflected in the dip around 55 Hz. The width of the passband and the magnitude of the maximum insertion loss are used to evaluate the muffler performance. The maximum insertion loss was 49 dB with a passband of 40 Hz was calculated for Case 1. The effect of changing the length is seen in Cases 2 and 4. The maximum insertion loss reduced to around 41 dB with a passband of 20 Hz (one half of the value of Case 1). Reducing the area ratio of even one chamber reduced the maximum insertion loss by about 5 dB. This behaviour is similar to single chamber mufflers, except that the insertion loss of double chambers can be as high as 50 dB for an expansion ratio of 16. The maximum insertion loss of a single expansion chamber of comparable dimensions is about 25 dB [5].

The insertion loss results for triple chamber mufflers are presented in Figure 4. The results are very similar to the double chamber mufflers. The maximum insertion loss is much higher for triple chamber than for double chamber mufflers. The maximum insertion loss is 74 dB with a passband of 40 Hz for Case 1. If the dominant lengths are modified (Case 2 and Case 4), the maximum insertion loss reduces by 9 dB to 64 dB with halving of the passband to 20 Hz.

## 4.0 Conclusions

Preliminary results of the insertion loss of double and triple expansion chamber mufflers were presented. The behaviour of the mufflers was seen to be similar to that of a single chamber muffler. The main salient result was that the amount of insertion loss can be substantially increased by the use of the more chambers if possible. The passband width can be better controlled with two and three chamber mufflers as compared to the single chamber muffler. The triple chamber muffler therefore offers the maximum performance as compared to a single chamber muffler of comparable overall dimensions.

## References

1. D. Davis, G. Stokes, D. Moore and G. Stevens, " Theoretical and Experimental Investigation of Mufflers with comments on Engine Exhaust Muffler Design," NACA Report 1192, 1954.

2. M.L. Munjal, *Acoustics of Ducts and Mufflers*, Wiley-Interscience, New York, 1987.

3. A. Craggs, " A Finite Element Method for Damped Acoustic Systems: an Application to Evaluate the Performance of Reactive Mufflers," Journal of Sound and

Vibration, Vol. 48 pp. 377-392, 1976.

4 J.S. Lamancusa, "The Transmission Loss of Double Expansion Chamber Mufflers with Unequal Size Chambers," Applied Acoustics Journal, Vol. 24, pp. 15-32, 1988.

5. A. Misra and R. Ramakrishnan, "Application of ABAQUS to Acoustical Modelling," Proceedings, ASME PVP Conference, Vol. 235: Design and Analysis of Pressure Vessels, Piping and Component, 1992.

6 ABAQUS Theory Manual, Version 4.8, Hibbitt, Karlsson and Sorenson Inc., Providence, Rhode Island, 1989.

**Table 1. Details of Muffler Parameters**

| | Double Chambers | | | Triple Chambers | | |
|---|---|---|---|---|---|---|
| | $L_1$ | $L_2$ | $d_2/d_1$ | $L_1$ | $L_2$ | $d_2/d_1$ |
| Case 1 | 1 | 1 | 4 | 1 | 1 | 4 |
| Case 2 | 2 | 1 | 4 | 2 | 1 | 4 |
| Case 3 | 1 | 1 | 3 | 1 | 1 | 3 |
| Case 4 | 1 | 2 | 4 | 1 | 2 | 4 |
| $L_1$ = 3 m, $d_1$ = .305 m | $L_2$ = 1, $d_2/d_1$ = 1 | | | $L_2$=1, $L_4$=1, $L_6$=1, $d_2/d_1$=4, $d_4/d_1$=4 | | |

**Figure 1. Details of Expansion Chamber Mufflers**

a) Double Chamber Muffler

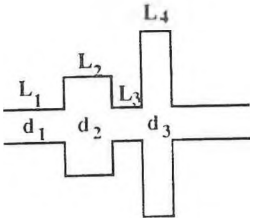


b) Triple Chamber Muffler

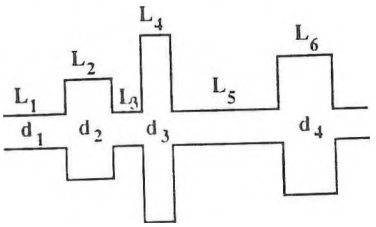


**Figure 2. Compariosn of Insertion Loss Results**

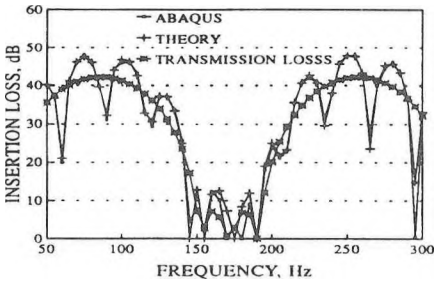


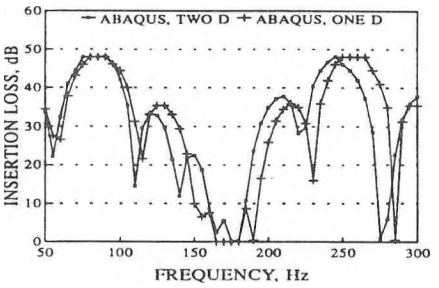


**Figure 3. Insertion Loss Results for Double Chamber Muffler**

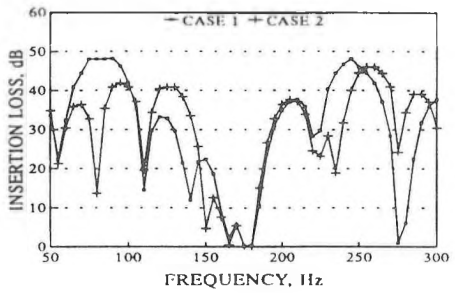


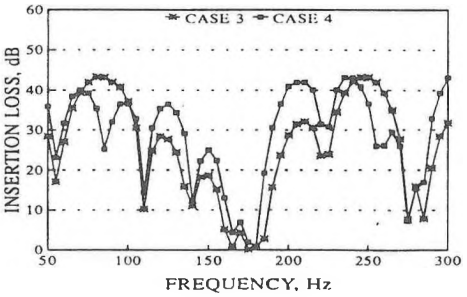


**Figure 4. Insertion Loss Results for Triple Chamber Muffler**

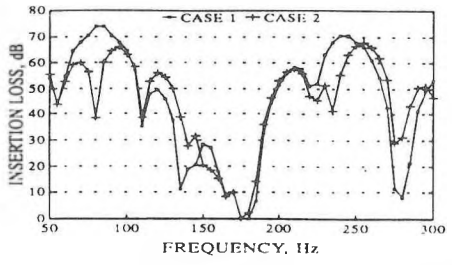


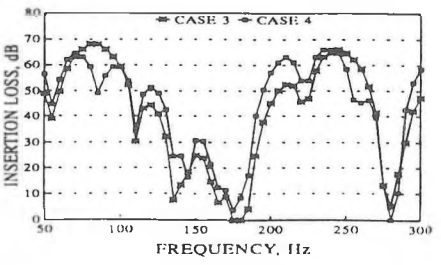

# Finite Element Modelling of Machinery Vibration Isolation Systems

**D.C. Stredulinsky**
Defence Research Establishment Atlantic, P.O. Box 1012, Dartmouth, Nova Scotia B2Y 3Z7

## Introduction

Vibration isolation of ship machinery is needed to achieve low radiated and habitable space noise levels. Shipboard isolation systems can be more difficult to design than similar systems on land due to space restrictions, weight limitations and ship motion considerations. Supporting foundation structures are often lightweight and relatively flexible and can influence the isolation system effectiveness. DREA is enhancing an in-house finite element vibration and strength analysis code VAST [1] to facilitate the analysis of passive vibration isolation systems. This paper describes the application of VAST to two problems. The first examines a simple machine decoupled from a flexible foundation structure using sixteen resilient isolators. The second considers the prediction of the natural frequencies of vibration of a helical compression spring isolator.

## Modelling capabilities

The amplitudes of machinery vibration are normally small and it is generally sufficient to consider the isolation system dynamics using three-dimensional linear elastic models. Finite element analysis (FEA) methods can be used to predict isolation characteristics in the lower frequency range and are well suited for modelling the complex structural geometry. Upper frequency limits are dependent on the size of the structure (whether modelling an entire ship or a smaller component) and the degree of discretization that can be achieved with available computer resources. Machine, raft and supporting structure flexibility can be modelled as well as multiple degrees of freedom (DOF) at resilient isolator interfaces. Rotations and moments may in some cases be as important as translations and forces for transmission of vibrational energy. Wave effects within isolation mounts can be included using detailed finite element models of the resilient components.

The VAST code is presently being enhanced to include frequency dependent complex stiffness properties. This should improve capabilities to model 'rubberlike' materials and viscoelastic damping materials which are often used in vibration isolation systems.

## Machine on multiple isolators with beam foundation

This example considers the application of VAST to the analysis of a simple machine consisting of a rectangular steel block (2489mm long, 508mm wide and 348mm tall) mounted on 16 isolation mounts (each with a vertical stiffness of 840N/mm and a horizontal stiffness of 420N/mm) modelled by massless beam elements of solid circular cross-section which were clamped to the support beams and pinned to the machine. The two steel support beams were 2845mm long with a 51mm wide by 152mm deep solid rectangular section. The material properties used for the machine and support beams were: a Young's modulus of $2.07 \times 10^5$MPa; a Poisson's ratio of 0.3; and, a density of 7874kg/m$^3$. The ends of the support beams were rigidly clamped. A harmonically varying machine excitation force was applied to the centre of the top face of the machine mass. The effect of a non-vertical excitation force was considered by applying the force obliquely with equal components in the $x$, $y$, and $z$ directions. The finite element model is shown Figure 1. The machine mass consisted of sixteen brick elements (8-noded). One 2-noded beam element was used for each mount and nine 2-noded beam elements were used for each support beam.

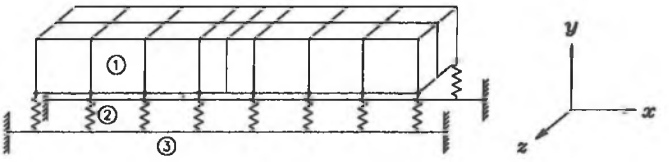


Figure 1: FE Model of machine on beam foundation and multiple isolators (1 = machine, 2 = isolator, 3 = support beam)

The first 50 undamped natural frequencies and mode shapes of the system were predicted and used in a forced response analysis over the frequency range of 1 to 1600 Hz. The decoupling of the machine mass and the support beams caused localization of vibration modes. Some modes involved mainly motion of the machine mass and others involved mainly motion of the support beams. The lowest six modes were essentially machine rigid body modes (5.4 Hz to 15 Hz). The next twelve modes (39 Hz to 298 Hz) were vertical and horizontal support beam bending modes which occurred in pairs. The remaining modes (300 Hz to 1650 Hz) included machine bending modes, higher order beam bending modes, and torsional and longitudinal deformation modes in the beams and machine.

This problem was originally considered by Snowdon [2] (for vertical motion only and a rigid machine). He specified complex stiffnesses for mounts and beams. The present VAST program cannot handle damping of this type and, instead, a viscous damping was assumed (with a damping ratio of 0.05 for the first mode and 0.01 for higher modes). The vertical force transmissibility at one end of the support beams is plotted as a function of the machine excitation forcing frequency in Figure 2 (a different transmissibility was obtained for each support due to the unsymmetric loading; only one is shown). Peaks in transmissibility occurred near natural frequencies of both machine and beam vibration modes, giving significantly greater force transmission to the supports at higher frequencies compared to a case which modelled the machine and beams as rigid structures (shown by the dashed line in Figure 2).

## Modelling of a spring isolator

The previous problem considered a system in which each isolator was assumed to be massless. Resonances within mounts can affect the isolation characteristics and this second example considers the prediction of the natural frequencies of a helical compression spring with closed ground ends, compressed between two rigid surfaces. This type of spring was modelled by

Table 1: VAST natural frequency predictions for the helical spring (Hz)

| Mode: | 1 | 2 | 3 | 4 | 5 | 6 | 7 | 8 | 9 | 10 |
|---|---|---|---|---|---|---|---|---|---|---|
| Beam model | 1089 | 1206 | 1475 | 1495 | 1898 | 2097 | 2189 | 2734 | 3020 | 4889 |
| Solid model | 1086 | 1193 | 1450 | 1475 | 1850 | 2088 | 2194 | 2713 | 2810 | 4661 |
| Dev.(%) | 0.3 | 1.1 | 1.7 | 1.4 | 2.6 | 0.4 | -0.2 | 0.8 | 7.5 | 4.9 |

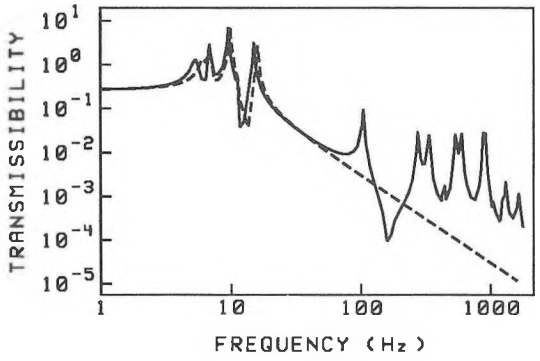


Figure 2: Vertical force transmissibility to the clamped end of one support beam

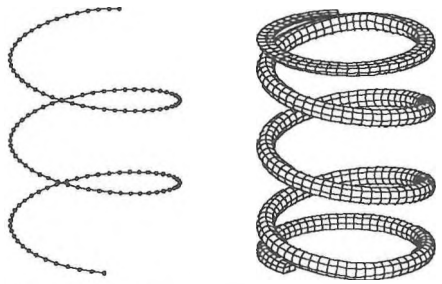

a) Beam (126 el.) b) Solid (944 elements)

Figure 3: FE Models of helical compression spring

Pearson [3] using a beam element transfer matrix method and assuming clamped ends and pinned points where the tip of the spring wire contacts the adjacent coil. A finite element model was constructed using 2-node general beam elements along the spring wire centre-line (shown in Figure 3a). A solid model was constructed using 20-noded brick elements (shown in Figure 3b) to provide an improved model of the end coil boundary conditions.

The details of the springs and the comparison to Pearson's results can be found in Reference [4] where it is shown that the beam element models were reasonably accurate in predicting the first eight to ten modes. The beam and solid FE model predictions are given in Table 1. The springs considered by Pearson and modelled in this example were much smaller (19 to 25mm long, 14mm O.D) and have much higher natural frequencies than those likely to be used in isolation systems.

Although the solid element models can provide more accurate high frequency predictions, the resulting finite element models become too large to include in overall isolation system models which involve many isolators, machinery rafts and the supporting structure.

## Concluding Remarks

This paper has demonstrated that the VAST finite element program, and FEA methods in general, provide a useful tool for the analysis of machinery vibration isolation systems; however, the enhancement of capabilities for modelling of damping is desirable. Damping properties can vary significantly between different components of the isolation system and can include viscous, structural and frequency dependent damping found in 'rubberlike' materials which can be included using a complex stiffness. A direct frequency response method is being implemented in VAST [5] which will allow modelling of frequency dependent complex stiffness properties for materials.

Component mode synthesis methods [6] are also being implemented in VAST which may allow analysis of larger system models and efficient reanalysis for the evaluation of structural modifications such as changing some of the natural frequencies of the isolation system components to avoid coincidence with machine excitation frequencies. Power flow finite element methods [7] are in the early stages of development and potentially offer a useful finite element based technique for higher frequency analysis.

## References


[1] 'Vibration and Strength Analysis Program (VAST)', Version #6.0, Martec Limited, Halifax, Nova Scotia, September 1990.

[2] Snowdon, J. C., 'Isolation of Machinery Vibration from Nonrigid Substructures Using Multiple Antivibration Mountings', ASME Applied Mechanics Division Serial AMD Vol. 1, 1973, pp. 102-127.

[3] Pearson, D., 'Modelling the Ends of Compressional Helical Springs for Vibration Calculations', Proceedings of the Institution of Mechanical Engineers, Vol. 200 C, 1986, pp. 3-11.

[4] Stredulinsky, D. C., 'Isolation of Structure-borne Sound from Ship Machinery: A Literature Review and Possibilities for Finite Element Modelling', DREA Technical Memorandum 91/208, May 1991.

[5] Stredulinsky, D. C., 'Finite Element Modelling of Helical Compression Springs', DREA Technical Memorandum 92/211, April 1992.

[6] Smith, M.J., and Hutton, S.G., 'Implementation of Component Mode Synthesis in the VAST program', DREA Contractor Report 90/449, September 1990.

[7] Burrell S.C. and Chernuka M.W., 'Extension of Power Flow Finite Element Analysis to Ship Structures', DREA Contractor Report 90/410, December, 1990.

# PERFORMANCE OF COMBUSTOR WITH ACOUSTIC AUGMENTATION OF PRIMARY ZONE AIR-JET MIXING

**P.J. Vermeulen, J. Odgers, V. Ramesh and B. Sanders**
**Department of Mechanical Engineering**
**The University of Calgary**
**Calgary, Alberta, Canada T2N 1N4**

**Introduction** - Earlier work[1] established that the dilution-air mixing processes of a small tubular combustor of normal design could be beneficially controlled by acoustic means; specifically a desired exit-plane temperature distribution may be achieved. From these results it was inferred that the entrainment rate and mixing of the dilution-air jets was increased by the acoustic pulsation. These encouraging results promoted detailed investigations into acoustically pulsed free-jet mixing[2], and showed that the entrainment and entrainment coefficient of the jet could be considerably increased, by up to 6 times. Also, work on acoustically pulsed jet mixing with a confined crossflow[3], showed that mixing was significantly increased and penetration at least 100% increased.

The success of these activities has now resulted in the technique being applied to the air jets of the combustor primary zone of Ref. 1, because of the potential for control and improvement in combustor performance. These novel experiments were designed to examine the effectiveness and control by the acoustic drive, by means of temperature profile measurements in the combustor exit plane, and by combustion products measurements across the mid-plane diameter of the combustor secondary zone, Fig. 1, ie., just downstream of the primary zone. Tests were made over representative ranges of overall equivalence ratio $\phi_o$ (or air/fuel ratio A/F), reference Mach number $M_r$ (load) and acoustic driver power $\dot{W}$.

**Experimental** - The method, Fig.1, channels air from upstream of the combustor inlet via six by-pass tubes connecting to a split manifold (3 separate segments) which feeds the 20 primary zone air-jet holes in the flame tube. Ten pairs of radial tubes cross the combustor annulus to connect the air holes of the flame tube to the manifold segments surrounding the combustor casing. Each manifold segment is connected by a driver tube to a 300W loudspeaker which provides the acoustic driving and control.

Figure 2 presents typical combustor exit plane local average dimensionless temperature contour maps, for symmetrical driving of all primary zone air jets, by the three-drivers at an average power of 151W per acoustic driver. $T_3$ is the exit plane local average temperature, $T_{3m}$ is the exit plane mean temperature and $T_2$ is the combustor inlet temperature. This clearly shows that the acoustic drive produced a more uniform exit plane temperature pattern, resulting in up to 35% improvement in mixing relative to the "no-drive" state. The figure shows maximum effects for A/F = 56.2, a rich condition at about ¼ maximum air mass flow rate $\dot{M}_a$, and $p_2, T_2$ are inlet pressure and temperature respectively.

Figures 3 and 4 show the typical effect of acoustic drive on the distributions across the combustor diameter of local equivalence ratio $\phi$ (stoichiometric A/F/actual A/F) and the gas temperature $T_g$. In general, all the combustion parameters measured tended to increase with acoustic drive and as shown $\phi$ became distinctly richer and $T_g$ became more uniform.

**Conclusions** - The acoustic drive produced a more uniform exit plane temperature pattern, resulting in up to 35% improvement in mixing relative to the "no-drive" state. The effects depended on air/fuel ratio and in general, improved relative to "no-drive" with richening. The effects of acoustic drive were controllable by means of the driving power, but saturated at about 150W when a single acoustic driver was used.

The acoustic drive enriches the primary zone and causes the primary zone temperature distribution to be more uniform.

Increased penetration of the primary zone air jets by the acoustic drive increased the combustor flow blockage and this constitutes the control mechanism. Overall, acoustic modulation improved mixing and produced favourable general progressive control over the combustor exit plane temperature pattern.

**References**

1. Vermeulen, P.J., Odgers, J. and Ramesh, V., "Acoustic Control of Dilution-Air Mixing in a Gas Turbine Combustor", Trans. ASME, Journal of Engineering for Power, Vol. 104, No. 4, Oct. 1982, pp. 844-852.

2. Vermeulen, P.J., Rainville, P. and Ramesh, V., "Measurements of the Entrainment Coefficient of Acoustically Pulsed Axisymmetric Free Air Jets", Trans. ASME, Journal of Engineering for Gas Turbines and Power, Vol. 114, No. 2, April 1992, pp. 409-415.

3. Vermeulen, P.J., Grabinski, P. and Ramesh, V., "Mixing of an Acoustically Excited Air Jet with a Confined Hot Crossflow", Trans. ASME, Journal of Engineering for Gas Turbines and Power, Vol. 114, No. 1, Jan. 1992, pp. 46-54.

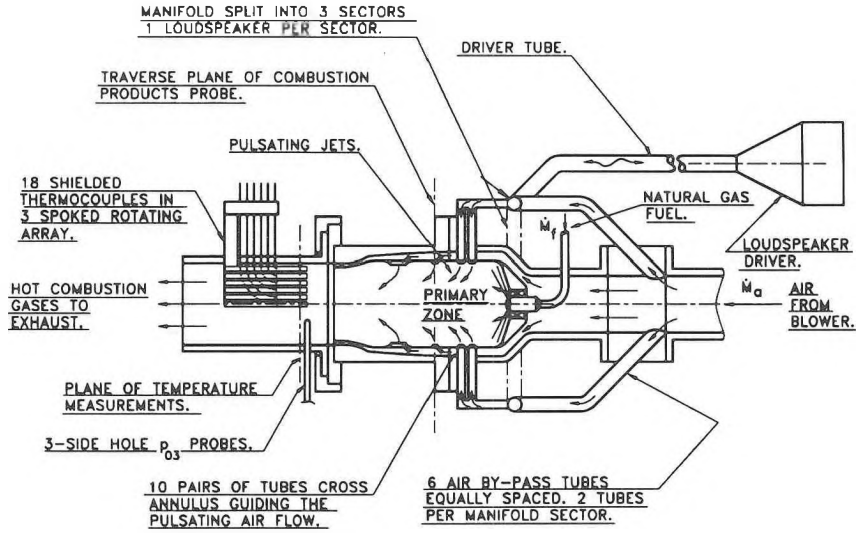


Fig. 1 Method for Acoustic Control of Combustor Primary Zone Air-Jet Mixing.

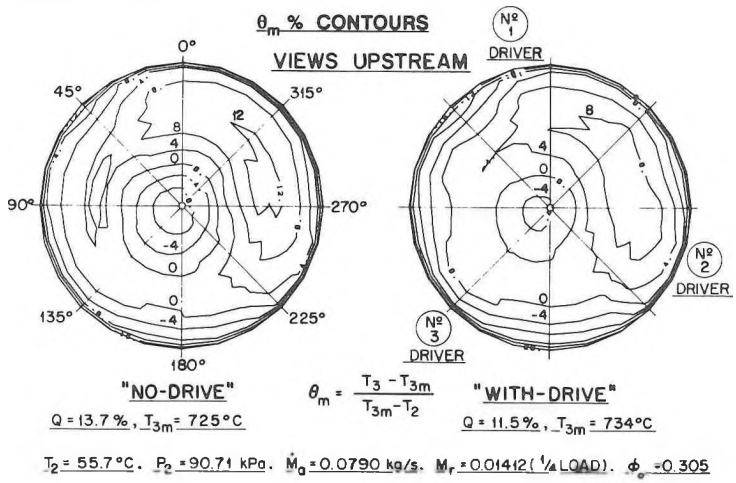


Fig. 2 Typical Exit Plane Local Average Temperature Contour Maps, 3 Drivers 151W Each, 227 Hz.

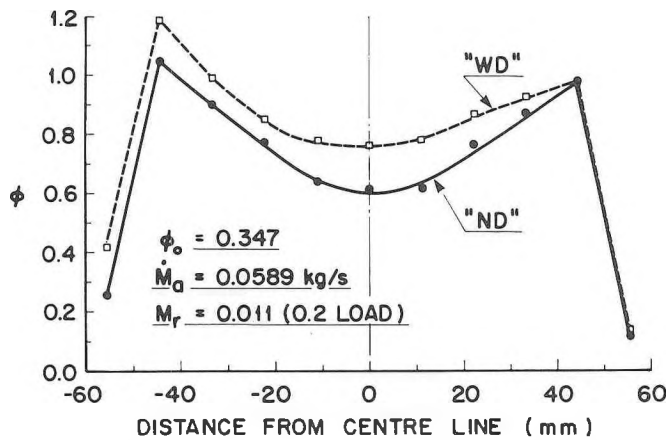


Fig. 3 Typical Downstream Primary Zone Local Equivalence Ratio Distribution, 3 Drivers, 94W Total Power, 225 Hz.

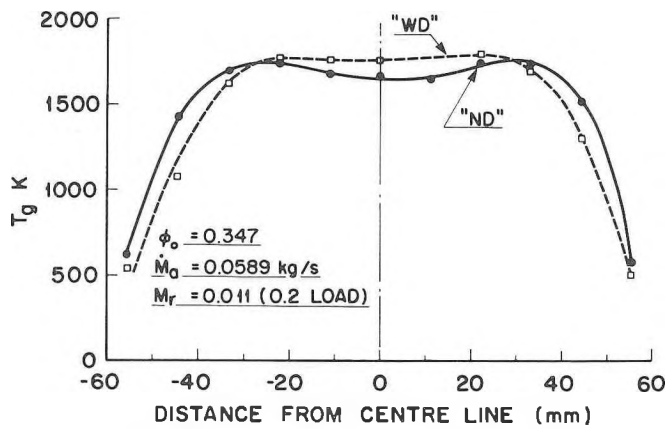


Fig. 4 Typical Downstream Primary Zone Local Gas Temperature Distribution, 3 Drivers, 94W Total Power, 225 Hz.

# Blachford

# *"The ABC's of noise control"*

### *H.L. Blachford's Comprehensive Material Choices*

Noise treatments can be categorized into three basic elements: Vibration Damping, Sound Absorption and Sound Barriers.

### *Vibration Damping*

It is well known that noise is emitted from vibrating structures or substrates. The amount of noise can be drastically reduced by the application of a layer of a vibration damping compound to the surface. The damping compound causes the vibrational energy to be converted into heat energy. Blachford's superior damping material is called **Aquaplas** and is available either in a liquid or a sheet form.

**AQUAPLAS DL** is a liquid damping material that can be applied with conventional spray equipment or troweled for smaller/thicker application.

It is water-based, non-toxic and provides economical and highly effective noise reduction from vibration.

**AQUAPLAS DS** is an effective form of damping material provided in sheet form for direct application to your product. Available with pressure sensitive adhesive for ease of application.

### *Sound Barriers*

Sound Barriers are uniquely designed for insulating and blocking airborne noise. The reduction in the transmission of sound (transmission loss or "TL") is accomplished by the use of a material possessing such characteristics as high mass, limpness, and impermeability to air flow. Sound barriers can be a very effective and economical method of noise reduction.

Blachford Sound Barrier materials:

BARYFOL®

Limp, high specific gravity, plastic sheets or die cut parts. Can be layered with other materials such as acoustical foam, protective and decorative facings to achieve the desired TL for individual applications.

### *Sound Absorption*

Blachford's **CONAFLEX** materials provide a maximum reduction of airborne noise through absorption in the frequency ranges associated with most products that produce objectionable noise. Examples: Engine compartments, computer and printer casings, construction equipment cabs, ...etc.

Available with a wide variety of surface treatments for protection or esthetics. Material is available in sheets, rolls and die-cut parts — designed to meet your specific application.

### *Suggest Specific Material or Design*

Working with data supplied by you, or generated from our laboratory, **H. L. Blachford** will make engineeri recommendations on treatment methods which may include specific material proposals, design ideas, or modifications to components. Recommendations are backed by documentation which can include written progress reports containing summarization of goals and results, conclusions, data, test procedures and background.

### *A Quality Supplier*

The complete integration of:

- Experience
- Advanced engineering
- Quality-oriented manufacturing technology
- Research and development
- Problem solving approach to noise control

Result in:

## Comprehensive Noise Control Solutions

MISSISSAUGA (416) 823-3200
MONTREAL (514) 938-9775
VANCOUVER (604) 263-1561

ECKEL

# Noise Control Products & Systems

## for the protection of personnel... for the proper acoustic environment...

### engineered to meet the requirements of Government regulations

**Eckoustic® Functional Panels**

Durable, attractive panels having outstanding sound absorption properties. Easy to install. Require little maintenance. EFPs reduce background noise, reverberation, and speech interference; increase efficiency, production, and comfort. Effective sound control in factories, machine shops, computer rooms, laboratories, and wherever people gather to work, play, or relax.

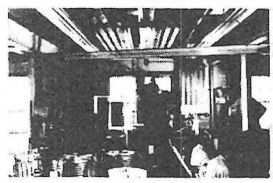

**Eckoustic® Enclosures**

Modular panels are used to meet numerous acoustic requirements. Typical uses include: machinery enclosures, in-plant offices, partial acoustic enclosures, sound laboratories, production testing areas, environmental test rooms. Eckoustic panels with solid facings on both sides are suitable for constructing reverberation rooms for testing of sound power levels.

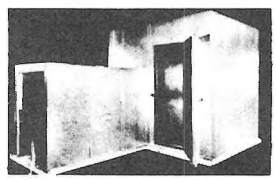

**Eckoustic® Noise Barrier**

● **Noise Reduction Curtain Enclosures** ● **Machinery & Equipment Noise Dampening**

The Eckoustic Noise Barrier provides a unique, efficient method for controlling occupational noise. This Eckoustic sound absorbing-sound attenuating material combination provides excellent noise reduction. The material can be readily mounted on any fixed or movable framework of metal or wood, and used as either a stationary or mobile noise control curtain.

**Acoustic Materials & Products** for dampening and reducing equipment noise

**Multi-Purpose Rooms**

Rugged, soundproof enclosures that can be conveniently moved by fork-lift to any area in an industrial or commercial facility. Factory assembled with ventilation and lighting systems. Ideal where a quiet "haven" is desired in a noisy environment: foreman and supervisory offices, Q.C. and product test area, control rooms, construction offices, guard and gate houses, etc.

**Audiometric Rooms:**
**Survey Booths & Diagnostic Rooms**

Eckoustic Audiometric Survey Booths provide proper environment for on-the-spot basic hearing testing. Economical. Portable, with unitized construction.

Diagnostic Rooms offer effective noise reduction for all areas of testing. Designed to meet, within ±3 dB, the requirements of MIL Spec C-81016 (Weps). Nine standard models. Also custom designed facilities.

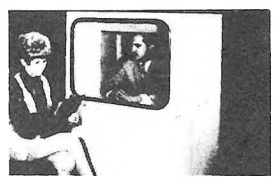

**An-Eck-Oic® Chambers**

Echo-free enclosures for acoustic testing and research. Dependable, economical, high performance operation. Both full-size rooms and portable models. Cutoff frequencies up to 300 Hz. Uses include: sound testing of mechanical and electrical machinery, communications equipment, aircraft and automotive equipment, and business machines; noise studies of small electronic equipment, etc.

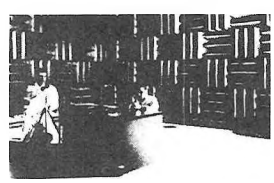

For more information, contact

**ECKEL INDUSTRIES OF CANADA, LTD.,** Allison Ave., Morrisburg, Ontario • 613-543-2967

**ECKEL INDUSTRIES, INC.**

# Can an inactivated hearing aid act as a hearing protector?

**R. Hétu[1], H. Tran Quoc[1], Y. Tougas[2]**
1 Groupe d'acoustique de l'université de Montréal, Montréal, Québec
2 Département d'audioprothèse, Collège de Rosemont, Montréal, Québec

According to the jurisprudence on discrimination due to hearing impairment, any assessment of employability must take into account to what extent a hearing aid may restore hearing capabilities [1]. In noisy working environments, the possibility of further hearing loss due to amplification of the ambiant noise through the hearing aid should then be considered. This potential damage could possibly be controlled by turning the hearing aid off during noisy periods and turning it on to facilitate communication during quiet intervals. However, little is known about the effectiveness of hearing aid earmolds as ear protectors when the aid is inactivated.

Only one study has been conducted on attenuation of hearing aid earmolds [2]. The findings showed a mean attenuation of less than 10 dB below 2 kHz with six models of earmolds coupled with a behind-the-ear hearing aid. However, questions concerning the validity of this data can be raised. The subjects were fitted with an aid earmold in the tested ear and with a foam earplug and earmuff on the non-tested ear. The influence of the non-tested ear on the hearing threshold measurements in the occluded condition may have contaminated the data. Another source of uncertainty is related to the earmold impressions obtained, based on a comparison of attenuation data from the conventional earmolds (fabricated from impressions) with data from an earmold made out of a foam plug equipped with a tube. The author of the study explains the relatively poor attenuation he measured with conventional earmolds, by the influence of leaks around the molds when inserted in the ear. It has indeed been shown that a difference of only 0.5 mm between measured ear canal dimensions and earplug size exert a considerable effect on the sound pressure level in the ear canal [3]. Furthermore, there are other factors that need to be investigated, such as earmold venting, length of the earmold canal, and earmolds of in-the-ear and in-the-canal model of aids. This study was undertaken to assess the effectiveness of various models of inactivated hearing aids as hearing protectors. Insertion loss was measured in a free field using an acoustic head simulator specifically designed for hearing protector evaluation.

## Method

Equipment and procedure

Experiments with hearing aid earmolds were carried out in a hemi-anechoic chamber using the acoustic head simulator designed by Kunov and Giguère [4]. This acoustic test fixture (ATF) approximates the physical dimensions and the acoustical eardrum impedance of the median human adult. The ATF includes a mechanical reproduction of the human circumaural and intraaural tissues. The acoustic isolation of the head simulator is greater than the bone conduction limitations to hearing protection.

A pink noise generator (BK-1405) was directed to an attenuator (HP-350D), a power amplifier (BGW-750D) and a loudspeaker (JBL-2445J) coupled with an exponential horn. The ATF, the left ear of which was equipped with the large KEMAR pinna, was facing the horn at a distance of 25 cm. The sound pressure level was picked up in the Zwislocki coupler from the left ear of the simulator by means of a condenser microphone (BK-4134) connected with a real time analyzer (BK-2123) by means of a preamplifier (BK-AO009). The ATF was installed on a platform that allowed a 360° rotation.

A wide band noise was presented at an overall level of 100 dB SPL as measured at the center of the ATF position in its absence. The hearing aid earmolds were evaluated in terms of their insertion loss, that is, the difference between the unoccluded ear sound-pressure level and the occluded ear sound-pressure level. Insertion loss was measured in third-octave bands between 0.125 and 8 kHz, with the hearing turned-off.

Three types of hearing aids, behind-the-ear (BTE), in-the-ear (ITE) and in-the-canal (ITC) aids were tested. The BTE was a Phonak PICO C-S-T aid , the ITE was a Starkey CE7 and the ITE, a Starkey INTRA III aid. The influence of the following factors was investigated: the type of aid, the effect of venting, the type of earmold associated with a BTE aid (inlcuding the shape, the material, the length of the earmold canal). The interaction between these factors and the horizontal angle of sound incidence was also examined.

Reliabitity of insertion loss measurements

The standard error of measurement (Se) has been assessed by replicating the insertion loss measurements with the three models of unvented aids. Se amounted to ±1.5 dB on an average across different frequency bands. The reproducibility of earmold properties was appraised by replicating the impressions and ordering, on two separate occasions, lucite earmolds for a BTE aid at a earmold laboratory. The difference in measurements of insertion loss from these two earmolds was smaller than 3 dB in any frequency band.

## Results

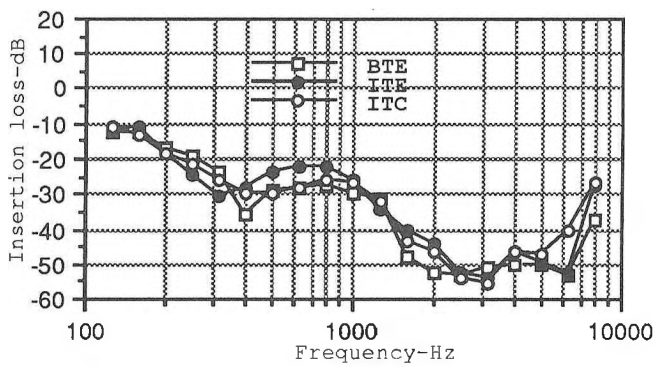


Figure 1. Insertion loss from unvented earmolds of three types of hearing aids measured with a 100 dB SPL wide spectrum noise at azimuth 0°.

Figure 1 compares insertion loss from the three types of aids tested. With all three types, insertion loss values come close to bone conduction limitations to hearing protection in the 1.5-6 kHz band. It drops to 25-30 dB between 0.3 and 1 kHz and to 13 dB or less below 0.2 kHz. The amount of insertion loss is maximal at 0° incidence of incoming noise. It is minimal at 270°, with a drop of 20 dB at 0.8 kHz.

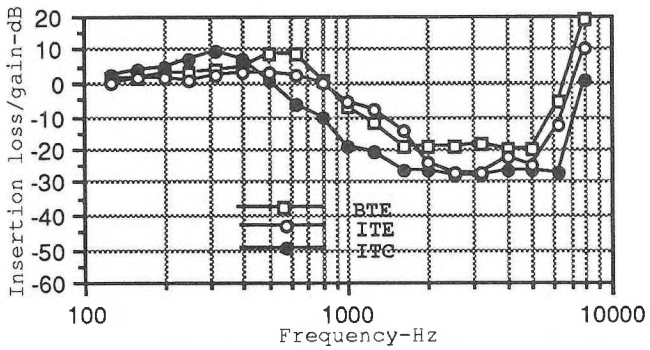


Figure 2. Insertion loss from vented earmolds of three types of hearing aids (vent diameter: 1/8", 1/8" and 1/16" for the BTE, ITE and ITC respectively).

As shown in Figure 2, when the earmolds are vented, insertion loss is considerably reduced in the mid-frequencies and amplifications occur in the lower and higher frequencies. Even a small diameter vent makes an inactivated hearing aid a poor hearing protector at frequencies below 1 kHz. Amplification of the ambiant noise has been measured with a vent diameter as small as 1/32". As expected, our data shows that the smaller the diameter of the vent, the lower the frequency of maximum amplification.

Comparison of a skeleton with a shell earmold of a BTE aid showed insertion loss differences smaller than the error of measurement. The length of the shell earmold canal had no significant influence on insertion loss as long as it extended to 0.8 cm. The material used to make the earmolds affected insertion loss to a certain degree. Silicone was compared to lucite using shell and skeleton molds. The silicone molds gave less insertion loss across the whole frequency range tested. But the difference varied when making the comparison with two shapes of molds, presumably because of a variation in the density of the silicone. This observation raises questions about the reliability of this material when used for earplugs.

A comparison between insertion loss of earmolds and standardized real-ear attenuation at threshold (REAT), measured with conventional hearing protection devices [5], has been made using the Schroeter and Poesselt model [6]. It provides corrective factors for insertion loss measurements that take into account the effect of bone conduction and of the physiological masking artifact of the REAT procedure as well as the occlusion effect of earplugs. The corrected insertion loss values thus obtained show a close correspondance with the mean attenuation data collected in standardized laboratory conditions with conventional hearing protectors.

Table I presents corrected insertion loss results for molds of three types of hearing aids, an E-A-R foam plug with a plastic tube coupled with a BTE aid, and a standard E-A-R foam plug. The corrected insertion loss values for the plug are within 2 dB of those reported by Giguère and Kunov [7], except at 6 and 8 kHz. The discrepancy at these frequencies is explained by free-field measurements in the present study as opposed to diffuse field in the other investigation. The data in Table I indicates that inactivated unvented hearing aids could act as effective hearing protective devices. Sound attenuation should be comparable to or even greater than a well-fitted foam plug above 0.25 kHz. In the lower frequencies, corrected insertion loss values are closer to those reported for earmuffs [7].

*Work supported the I.R.S.S.T. (grant #N/D PE-90-13).*

Table I. Corrected insertion loss values (dB), measured in a free field at an angle of sound incidence of 0°, for four types of hearing aid earmolds and a conventional foam earplug.

| Frequency Hz | BTE Lucite shell | ITE | ITC | E-A-R earmold +BTE | E-A-R plug |
|---|---|---|---|---|---|
| 125 | 10.2 | 9.2 | 9.3 | 7.3 | 19.6 |
| 250 | 17.2 | 19.3 | 22.0 | 11.6 | 27.6 |
| 500 | 27.2 | 27.7 | 21.5 | 16.4 | 27.6 |
| 1000 | 30.1 | 26.8 | 26.3 | 29.6 | 31.3 |
| 2000 | 52.5 | 46.4 | 44.2 | 33.0 | 36.4 |
| 3150 | 51.0 | 55.3 | 54.3 | 46.1 | 45.4 |
| 4000 | 50.2 | 46.7 | 46.2 | 39.2 | 45.8 |
| 6300 | 53.2 | 40.2 | 52.8 | 42.2 | 37.8 |
| 8000 | 37.0 | 26.6 | 27.3 | 29.4 | 34.8 |

## Discussion

According to the present results, BTE, ITE and ITC hearing aids can be used as effective hearing protective devices when turned off. This should be the case, however, only if the mold is unvented and if it is fitted optimally. This latter condition implies excellent impression quality and reliable earmold production. As reported above, silicone molds may have inadequacies in this respect, but a more thorough investigation would be needed on this question.

Although a BTE aid can be coupled with a foam earplug equipped with a tube, for sound attenuation purposes, it is preferable to use a conventional lucite shell or skeleton earmold (Table I).

REAT measurements are considered an accurate indication of the effectiveness of optimally fitted hearing protective devices [5]. The corrected insertion loss results obtained in the present study provide satisfactory estimates of mean REAT data [7]. The present results should thus provide a correct estimate of the sound attenuation that hearing aid users can expect if they wear a properly fitted mold. In light of our findings, a hearing impaired worker could indeed use a passive hearing aid to protect him/herself when the ambiant noise is excessive.

## References

1- Canadian Human Rights Reporter, 1987, 8: Ruling 628.

2-Frank, T. Attenuation characteristics of hearing aid earmolds. Ear and Hearing, 1980, 1(3): 161-166.

3-Smith, S.C., Borton, T.E., Patterson, L.B., Mozo, B.T. and Camp, R.T. Insert hearing protector effects. Ear and Hearing, 1980, 1(1): 26-32.

4-Kunov, H. and Giguère, C. An acoustic head simulator for hearing protector evaluation. I: Design and construction. J. Acoust. Soc. Am. 1989, 85: 1191-1196.

5-ANSI S12.6-1984. Method for the measurement of the real-ear attenuation of hearing protectors. New York: American National Standards Institue, Section 1.2.

6-Schroeter, J. and Poesselt, C. The use of acoustical test fistures for the measurement of hearing protector attenuation. Part II: Modeling the external ear, simulating bone conduction, and comparing test fixture and real-ear data. J. Acoust. Soc. Am. 1986, 80: 505-527.

7-Giguère, C. and Kunov, H. An acoustic head simulator for hearing protector evaluation. II: Measurments in steady-state and impulse noise environments. J. Acoust. Soc. Am. 1989, 85: 1197-1205.

# PRELIMINARY SIMPLIFIED MODELS FOR PREDICTING SOUND PROPAGATION CURVES IN FACTORIES

**Murray Hodgson**

Occupational Hygiene Programme / Department of Mechanical Engineering,
University of British Columbia,
2324 Main Mall, Vancouver, BC V6T 1Z4.

## 1. Introduction

Predictions of factory noise levels are based on predictions of the factory sound propagation curve - the variation with distance from an omnidirectional point source of the sound pressure level minus the source sound power level; $SP(r)=L_p(r)-L_W$. While more accurate approaches such as ray tracing exist [1], from a practical point of view there is considerable scope for developing simplified empirical prediction methods. In fact, several such models exist [2]. However, these have short-comings which warrant the development of a new model. The approach taken here was to predict the slope(s) and absolute level(s) of the sound propagation curve, approximated by one or more straight-line segments. With this in mind, octave-band sound propagation measurements were made in a number of empty and fitted factories. The curves were approximated by one or two straight-line segments. The intercepts and slopes of the segments were then determined. In this paper the development of preliminary simplified prediction models from the results is discussed.

## 2. Factories and measurements

Test factories were chosen to be of modern steel-deck construction. Eleven were nominally empty. A further 13 were fitted; the fittings were compact and fairly uniformly distributed over the factory floor areas. Four of the fitted factories contained a sound-absorptive ceiling treatment. The factories had a wide range of dimensions, with aspect ratios varying from low to high.

In each factory the sound propagation curves were measured in octave bands from 125-4000 Hz. An omnidirectional loudspeaker radiating random noise was located near one end of the building. Octave-band sound pressure levels were measured at a number of distances away from the speaker. From these and the octave-band source sound power levels the sound propagation curves were determined. Observation of the shapes of the curves revealed certain consistent characteristics, as illustrated in Fig. 1. In the case of smaller factories, with major dimension less than about 50 m, the slopes of the curves were approximately constant. In larger factories, the slopes were approximately constant to source/receiver distances of about one half of the length; at larger distances the slopes increased sharply, particularly in fitted factories.

## 3. Best-fit procedure and results

It was apparent that the measured sound propagation curves could, with good accuracy, be approximated by a single straight-line segment in the case of smaller factories, and by two straight-line segments in the case of larger factories. With this in mind, all measured curves were approximated in this way using regression techniques. To date results have only been analysed for the initial portion of the curves for the larger factories. In any case, for each segment the SP value at r=1m (the 'intercept') and the slope in dB/dd (dd=distance doubling) were determined. The averages and standard deviations of the values in each octave band were calculated separately for the empty, fitted and fitted+absorptive cases.

Table 1 shows the results for the intercept. This varies with frequency from -11.1 to -11.6 dB in empty factories, from -7.8 to -9.7 dB in fitted factories and from -7.5 to -9.7 dB in fitted+absorptive factories. Also shown in Table 1 are the changes in intercept when fittings are 'added' to the average empty factory (increase of 1.7-3.3 dB), or when an absorptive treatment is 'added' to the average fitted factory (little change).

Table 2 shows the corresponding results for the initial slope. This varies with frequency from 1.9-2.6 dB/dd in empty factories, from 3.4-4.3 dB/dd in fitted factories and from 4.0-5.0 dB/dd in fitted+absorptive factories. Also shown in Table 2 are the changes in slope when fittings are 'added' to the average empty factory (increase of 1.3-1.7 dB/dd), or when an absorptive treatment is 'added' to the average fitted factory (increase of 0-1.5 dB).

## 4. Preliminary prediction model

From the above results it is possible to develop preliminary empirical models for predicting the initial sound propagation curves in empty and fitted factories, without and with absorption. Two types are proposed - frequency-independent models based on the average octave-band results, and frequency-dependent, octave-band models. They are as follows:

Frequency-independent models

Empty: $SP_E(r) = -11.4 - 18.6 \log r$

Empty+absorption: $SP_{EA}(r) = -11.4 - 26.2 \log r$

Fitted: $SP_F(r) = -13.7 - 31.3 \log r$

Fitted+absorption: $SP_{FA}(r) = -13.7 - 38.9 \log r$

Frequency-dependent model

$$SP(r) = (I_E + \Delta I_F) - 8.5\,(S_E + \Delta S_F + \Delta S_A) \log r$$

| Band | $I_E$ | $\Delta I_F$ | $S_E$ | $\Delta S_F$ | $\Delta S_A$ |
|---|---|---|---|---|---|
| 125 | -11.6 | 1.9 | 2.2 | 1.7 | 0.6 |
| 250 | -11.3 | 2.1 | 2.1 | 1.7 | 1.0 |
| 500 | -11.5 | 2.6 | 2.2 | 1.3 | 1.5 |
| 1000 | -11.1 | 3.3 | 1.9 | 1.5 | 1.4 |
| 2000 | -11.4 | 2.4 | 2.1 | 1.3 | 0.6 |
| 4000 | -11.2 | 1.7 | 2.6 | 1.7 | 0 |

## 5. Conclusion

Models have been developed for predicting the initial sound propagation curves. While this has yet to be analysed in detail, the proposed models predict the average initial curves with good accuracy; typically within 1 dB. It would be of interest to combine the models into one model which includes the absorption coefficent of absorptive treatments and some measure of the fitting density as parameters. Clearly, models based on average results are of limited accuracy. It is important to extend the models to account for variations of sound propagation with room dimension or other applicable parameters. It also remains to extend them to predict the final part of the curves in the case of large factories.

## References

[1] M.R. Hodgson, Canadian Acoustics **19**(1) 15-23 (1991).

[2] M.R. Hodgson, J. Acoust. Soc. Am. **88**(2), 871-878 (1989).

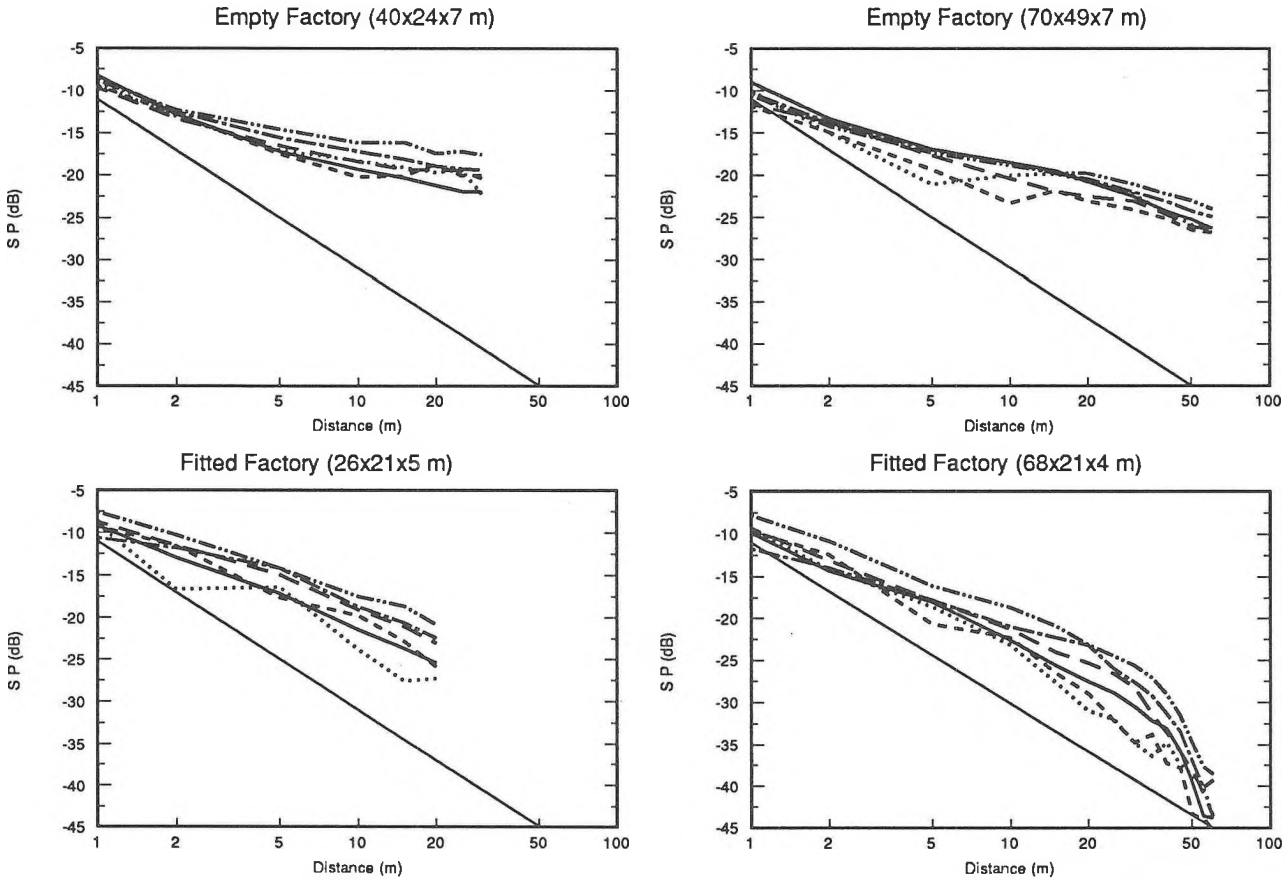


Fig. 1. Measured octave-band sound propagation curves for typical small and large, empty and fitted factories: (——) free field; (·····) 125Hz; (– – –) 250 Hz; (— —) 500 Hz; (—·—) 1000 Hz; (— — —) 2000 Hz; (————) 4000 Hz.

Table 1. Averages, standard deviations and changes (Δ) of octave-band intercepts (SPs at 1m) in dB for the measured factories.

| Band (Hz) | Empty | Fitted | Fitted+ Absorption | Δ(E→F) | Δ(F→F+A) |
|---|---|---|---|---|---|
| 125 | -11.6 (1.6) | -9.7 (0.9) | -9.4 (0.5) | +1.9 | +0.3 |
| 250 | -11.3 (1.4) | -9.2 (1.0) | -9.2 (0.5) | +2.1 | 0.0 |
| 500 | -11.5 (1.4) | -8.9 (0.7) | -9.0 (0.2) | +2.6 | -0.1 |
| 1000 | -11.1 (1.0) | -7.8 (0.8) | -7.5 (0.4) | +3.3 | +0.3 |
| 2000 | -11.4 (1.4) | -9.0 (0.9) | -9.4 (1.3) | +2.4 | -0.4 |
| 4000 | -11.2 (1.8) | -9.5 (0.5) | -9.7 (1.4) | +1.7 | -0.2 |

Table 2. Averages, standard deviations and changes (Δ) of octave-band initial slopes in dB/dd for the measured factories.

| Band (Hz) | Empty | Fitted | Fitted+ Absorption | Δ(E→F) | Δ(F→F+A) |
|---|---|---|---|---|---|
| 125 | 2.2 (0.6) | 3.9 (1.3) | 4.5 (0.3) | +1.7 | +0.6 |
| 250 | 2.1 (0.6) | 3.8 (1.3) | 4.8 (0.4) | +1.7 | +1.0 |
| 500 | 2.2 (0.5) | 3.5 (1.1) | 5.0 (0.2) | +1.3 | +1.5 |
| 1000 | 1.9 (0.5) | 3.4 (1.1) | 4.8 (0.2) | +1.5 | +1.4 |
| 2000 | 2.1 (0.6) | 3.4 (1.2) | 4.0 (0.5) | +1.3 | +0.6 |
| 4000 | 2.6 (0.6) | 4.3 (1.4) | 4.3 (0.6) | +1.7 | 0.0 |

# "DETECTSOUND" and "dBOHS": A software package for the analysis of health and safety in noisy workplaces

**Chantal Laroche[1], Raymond Hétu[2], Hung Tran Quoc[2], Jean-Marc Rouffet[3]**
[1]Sonométric Inc., 5757 Decelles Ave., Suite 406, Montréal (Québec) H3S 2C3
[2]Groupe d'Acoustique de l'Université de Montréal, C.P. 6128, Succ. A, Montréal (Québec) H3S 2C3
[3]01 dB, 113, rue du 1er mars, Villeurbanne, France

## 1. Introduction

Every year serious injuries occur in noisy workplaces because a warning signal is not heard. Very few practical tools allowing direct prediction of the ability to detect acoustic signals in noisy environments are available. The Groupe d'Acoustique de l'Univesité de Montréal (GAUM) has developped a computerized model called DETECTSOUND which runs on an IBM-PC compatible and which can predict the capability of workers to detect auditory warning signals in noise. To run DETECTSOUND, it is necessary to obtain 1/3 octave band levels at each work station. dBOHS was designed to obtain this information from a recording made on the site using a digital audio-tape recorder and a hand-held controller. The following paragraphs present the main characteristics of each software.

## 2. DETECTSOUND software

DETECTSOUND allows user to:

1) Specify the characteristics of warning sounds to be installed in a workplace;

2) Evaluate the effectiveness of the warning sounds in use in a workplace.

The foundations of the model have been presented in a previous paper [1].

DETECTSOUND takes into account the following information:

- the background noise at each workstation (1/3 octave band levels from 25 to 12 500 Hz);
- the hearing protectors worn by a standard individual or by specific individuals (attenuation in dB from 63 to 8000 Hz);
- the audiogram of a standard individual or the actual individuals assigned to a workstation (hearing thresholds from 125 to 8000 Hz);
- all warning sounds that can be heard at the station (1/3 octave band levels from 25 to 12 500 Hz).

A standard individual refers to five different stages of hearing loss, stage 0 meaning normal hearing for a 50 years old man and stage 4 meaning an advanced level of noise-induced hearing loss.

The loss of frequency selectivity is also taken into account in the software. It is statistically related to the loss of sensitivity. In fact, the user do not have to enter this information. It is automatically computed based on the hearing thresholds.[2]

When these informations are entered in their specific table forms and computed together, the results are displayed in a graphic or a table form. Figure 1 presents an example of a graphic display.

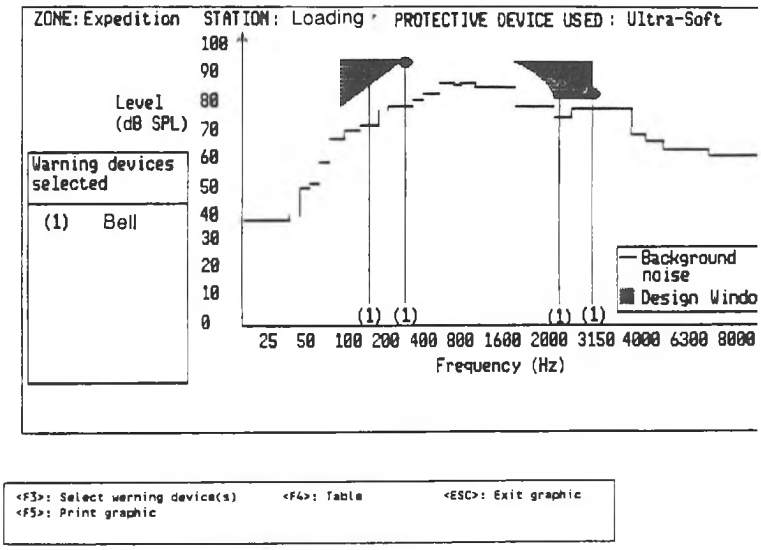


Fig.1 Graphical display of the design window for a particular workstation.

The frequency content is presented on the x axis and the level of each 1/3 octave band of the noise or the warning sound is on the y axis. The full horizontal line corresponds to the background noise level at the loading workstation of the expedition zone. The vertical lines correspond to the spectral content of the bell heard at this workstation. The dark zone represents the design window, i.e. the spectral and level region in which at least two spectral lines of a warning sound should be in order to attract attention and be recognized among different warning sounds. In this example, the bell should be well recognized by 50 years old workers (stage 0 has been used in this example) because each of the four lines are inside or at the borders of the design window. If all the spectral lines would have been below the design window, this would have meant that the spectral content of the warning sound should have been changed or the level increased . If the lines would have been over the design window, this would have meant that the warning sound level would have been too high and could have caused hearing damage, interference with communication or a startle reaction.

## 3. dBOHS software

dBOHS has been developped to help health and safety professionnals to make complete, rapid and automated noise measurements. It gives directly and simultaneously the noise dosis, the temporal evolution (short $L_{eqs}$, $L_p^{\Delta}$) and the spectral content (in octave and 1/3 octave band levels) of the background noise and of the warning sounds. The temporal evolution of each 1/3 octave band levels is also available. These parameters are useful to evaluate the risk of acquiring hearing loss and the audibility of warning sounds in workplaces.

Recordings of background noise and warning sounds are made with a special controller plugged into a digital audio-tape recorder (DAT) at each workstation. A type 1 microphone is plugged into the controller which sends signals (calibration, sampling, pause) to the second channel of the DAT . These signals are later used by dBOHS to automatically analyse the recordings. This method is presently used by Hydro-Quebec to evaluate the noise emitted by transformer stations[3,4] and saves a lot of time to the user.

The values given by dBOHS can be directly transferred to DETECTSOUND and synthetized on a personnalized form like the one presented on figure 2.

## 4. Conclusion

The ultimate goal of DETECSOUND and dBOHS is to supply practical, reliable and rapid means for health and safety personel to assess the audibility of warning sounds and the risk of acquiring hearing loss. Both software run on IBM-PC compatibles and are user-friendly. GAUM is now working on an upgraded version of DETECSOUND to allow users to enter individual data on frequency selectivity.

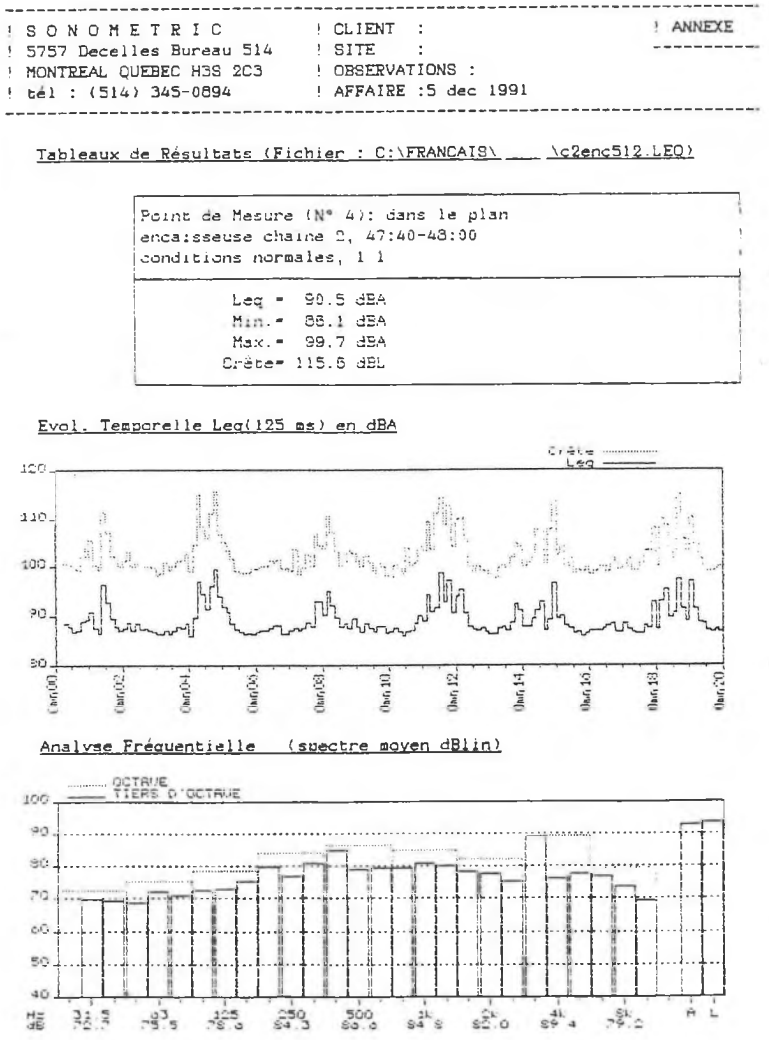


Fig.2 Example of a dBOHS form. Table of results, temporal evolution and spectral content.


### Acknowledgments

DETECSOUND development has been funded by IRSST .


### References


1. Laroche, C., Tran Quoc, H., Hétu,R. and McDuff, S. (1991). "Detectsound": A computerized model for predicting the detectability of warning signals in noisy workplaces. Applied Acoustics 32, 193-214.

2. Laroche, C., Hétu, R., Tran Quoc, H., Josserand, B., Glasberg, B. (1992). Frequency selectivity in workers with noise-induced hearing loss. Submitted for publication.

3. Gosselin, B., Fortin, J., L'Espérance, A. (1992). Measurement of noise emitted by electrical substations- Part I: Measurement method. Inter-Noise, Toronto, 771-774.

4. Laroche, C., Rouffet, J.M., Gosselin, B., Fortin, J. (1992). Measurement of noise emitted by electrical substations- Part II: Measurement system. Inter-Noise, Toronto, 775-78.

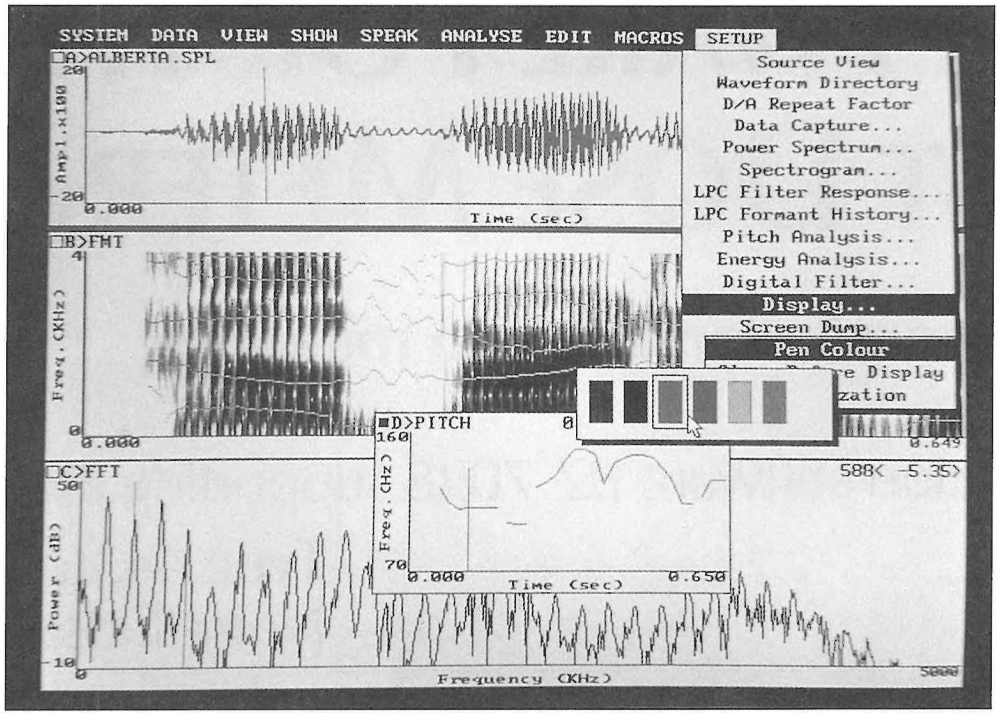


# Turn your PC into a powerful speech analysis system.

If you have an IBM®PC AT, or compatible computer, Kay Elemetrics has the speech analysis system for you.

Introducing the *CSL™, model 4300 computerized speech lab*.....the most powerful computerbased system available for speech acquisition, analysis and playback. CSL is a highly flexible speech analysis system that is designed for both the new and sophisticated user.

CSL comes complete with all hardware (except for the computer) and comprehensive software. The software operates in a "windows" type environment using pull-down menus. These menus can be customized to user's needs. The hardware consists of two input channels (50 kHz sampling at 16 bits), digital anti-aliasing filters, a 40 MHz digital signal processor and digital output filters.

With its two on-board DSP processors, the CSL provides speedy spectrograms, formant trace, pitch extractions, power spectrum analysis, selective filtering, LPC analysis and many other analysis functions. In addition, the CSL can interface to many other programs providing users with added flexibility. Other features include: file management, graphics and numerical display, audio output and signal editing.

***CSL with IBM compatible computer, monitor, microphone and mouse.***

The CSL is also designed as an ideal companion for Kay's DSP Sona-Graph speech workstation, model 5500. The DSP Sona-Graph's true real-time processing and scrolling graphics can be used to acquire, analyze and preview signals. These stored signals can be easily shared with the CSL to accommodate more than one user. Conversely, signals acquired using CSL can be easily uploaded to the 5500 making these two systems highly complementary - a perfect combination for your speech laboratory.

*To find out how the* ***CSL*** *can turn your IBM®PC AT or compatible into a speech analysis system* ***call one of Kay's Product Specialists today at 1-800-289-5297.***

**KAY**

Kay Elemetrics Corp
12 Maple Avenue
Pine Brook, NJ 07058
Tel: 201/227-2000
TWX: 710-734-4347
FAX: 201/227-7760

# THE BEST SOFTWARE FOR THE BEST DOSE METER.

## Permanent records in two minutes.

Application software BZ 7028 supporting the

Type 4436
Noise Dose Meter
makes for an unbeatable combination.

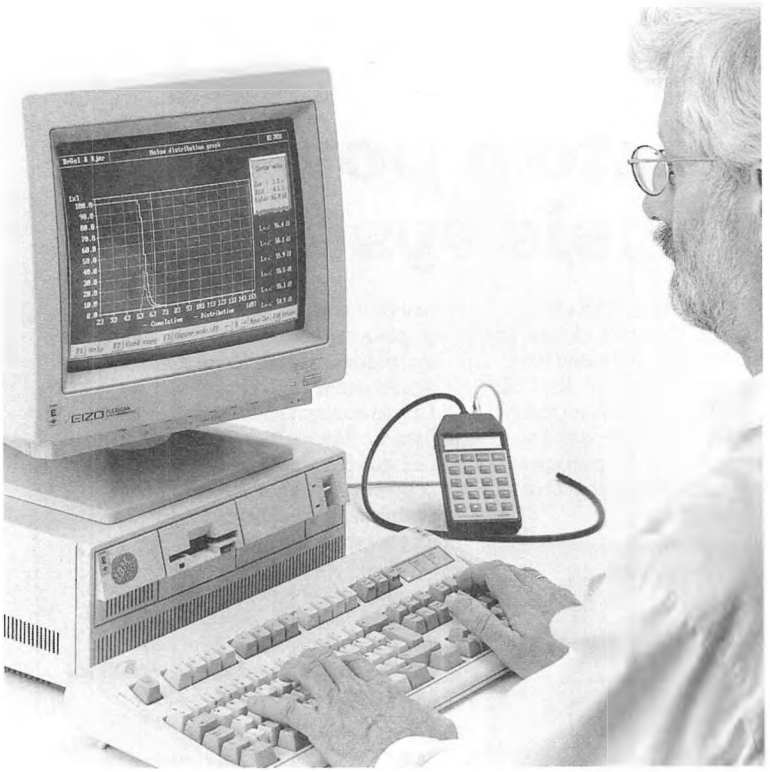

**This dynamic new product provides:**

- permanent records in two minutes or less.
- color graphs and tables
- time history
- statistical analysis
- cumulative distribution
- level distribution

In short, these are the tools with which you can quickly pinpoint problem noise exposures and provide full documentation.


**BRUEL & KJAER CANADA LTD.**

90 Leacock Road, Pointe Claire, Quebec H9R 1H1
Tel.: (514) 695-8225 Fax: (514) 695-4808 Telex: 05-821691 b k pcir

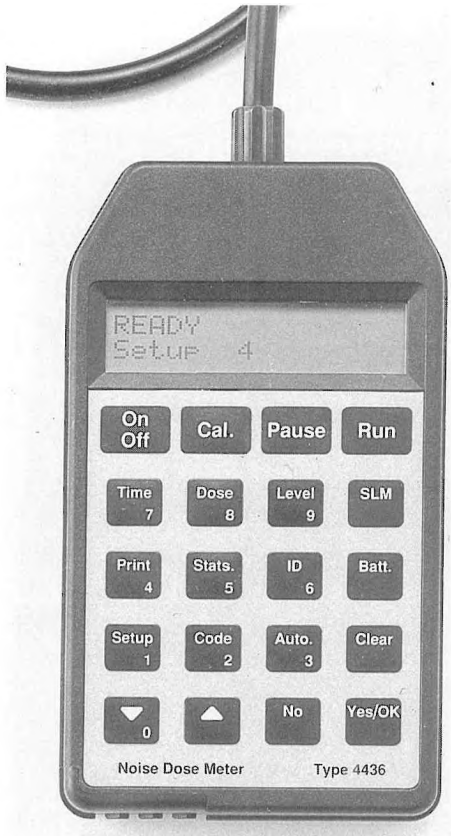


# A SOUND DECISION!

## This dose meter withstands the rigors of the modern industrial environment, yet provides accurate and dependable readings.

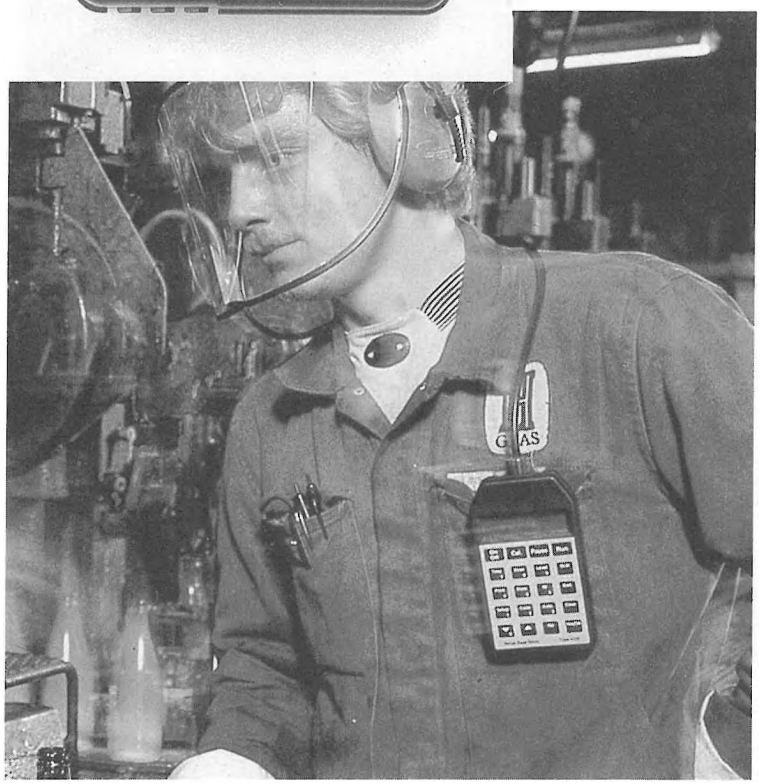

*The Type 4436 dose meter can be used as a Type 2 integrating sound level meter.*

Put the latest sound technology in your pocket and protect your employees from damaging noise exposure with a dose meter. The Type 4436 incorporates the latest technology and yet is rugged enough to withstand the most hostile industrial environments.

Bruel & Kjaers's Type 4436 microphone is protected inside the instrument casing where the hazards of the workplace cannot reach it. A strong, flexible rubber tube attached to the instrument, guides sounds to the microphone.

Specially-created software, known as the BZ 7028, allows information to be downloaded into a PC for analysis or data logging.

**BRUEL & KJAER CANADA LTD.**

90 Leacock Road, Pointe Claire, Quebec H9R 1H1
Tel.: (514) 695-8225 Fax: (514) 695-4808 Telex: 05-821691 b k pcir

# ACOUSTICAL INTERFACE™ SYSTEM

**precision acoustical measurements with your FFT, scope or meter**

## PS9200 POWER SUPPLY

■ Dual Channel ■ 9V "Radio" Battery
■ Portable ■ 50 Hours Operation
■ Low Noise ■ LED Status Indicator

## 7000 SERIES MICROPHONES

■ Type 1 Performance ■ ¼, ½ and 1 Inch Models

## 4000 SERIES PREAMPLIFIERS

■ 2Hz to 200kHz ± 0.5db ■ Removable Cable ■ PS9200 and 7000 Series Compatible

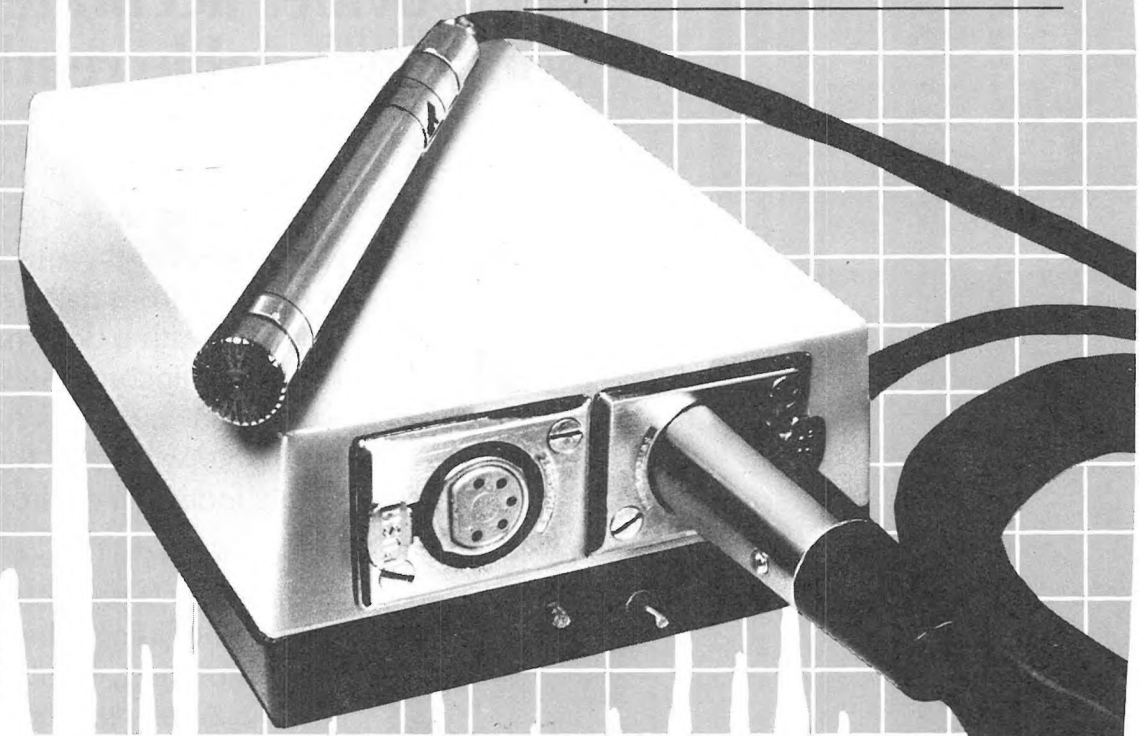

# NEW LOW COST PRECISION MEASUREMENTS

■ **SINGLE CHANNEL SYSTEM UNDER $1,200**
■ **DUAL CHANNEL SYSTEM UNDER $2,000**
(½ or 1 inch microphones)

**ACO Pacific, Inc.**
2604 Read Avenue
Belmont, CA 94002
(415) 595-8588



ACOUSTICS BEGINS WITH ACO

# CONTINUED DEVELOPMENT OF AN IMELDA BASED VOICE RECOGNITION SYSTEM FOR PERSONS WITH SEVERE DISABILITIES

**Gary E. Birch[1], Dariusz A. Zwierzynski[2], Claude Lefebvre[2], and David Starks[3]**

[1]Neil Squire Foundation
4381 Gallant Avenue
North Vancouver, B.C.
Canada
V7G 1L1

[2]Neil Squire Foundation
Speech Research Centre
National Research Council of Canada
Building U-61, Montreal Road
Ottawa, Ontario
K1A-OR6

[3]Canadian Marconi Company
415 Legget Drive
P.O. Box 13330
Kanata, Ontario
K2K-2B2

## INTRODUCTION

The Neil Squire Foundation is a Canadian non-profit organization responsive to the needs of individuals who have severe physical disabilities. Through direct interaction with these individuals we research and develop appropriate innovative services and technology. To date the Foundation has worked on a one-to-one basis with well over 3500 persons with disabilities from all over Canada. In almost every case we have been involved in assessing and recommending the most appropriate interface to computer based assistive devices. The concept of direct speech input to control assistive devices is often an appealing option and hence the Foundation has always worked to keep abreast of and, indeed in most cases, test commercially available speech recognition systems. We estimate that we have had well over 1500 hours of direct individual involvement with severely disabled persons who were utilizing speech input. Through this experience we have encountered several limitations with currently available systems which have resulted in simply too much frustration for a majority of our clients. These limitations, particularly in control applications, have been related to interference from background noise, varying degrees of speaker stress and/or emotion, fatigue and generally unfriendly and complicated user application/training software. Similar findings regarding the use of speech input systems were also reported by researchers at the University of Tennessee, Centre of Excellence for Computer Applications [1]. As indicated in [2], this experience with speech input lead the Foundation to become involved in a joint project with the Speech Research Centre at the National Research Council of Canada (NRC) and the Canadian Marconi Company (CMC) to research and develop a speech input system that will ultimately overcome these limitations. In 1990, the IMELDA system that had been designed and tested on a mainframe computer at NRC was implemented in stand-alone hardware by CMC and the initial results are very promising. The most dramatic test and evaluation to date has been through a project called "Fly-by-Voice".

## BACKGROUND

The general design of our speech recognition system is such that the acoustic features are first extracted from the speech signal in the front-end component. Subsequently, these features are passed on to the back-end component where they are compared with stored templates through the technique of dynamic programming.

The front-end processing in our speech recognition system is a mel-scale fast-fourier-transform based spectral filter-bank analysis followed by a linear transformation [3]. This linear transformation, which is called IMELDA, was developed and tested in our laboratory and is based on linear discriminant analysis [3,4]. Comparisons with other systems indicate that it is the "state of the art" for front-end processing in a robust speech recognition system, outperforming other transforms and recognition systems, particularly in degraded speech [2].

## OVERVIEW OF THE FLY-BY-VOICE PROJECT

In the "Fly-by-Voice" project a vocabulary was set up that would enable a pilot to fly a Bell 205A helicopter completely by voice commands. This project was undertaken to demonstrate the feasibility of speech recognition in an extremely adverse environment and it was not intended to suggest that flights could be controlled by voice. It does, however, point to the important potential of controlling secondary features in the cockpit, such as the control of navigational information.

The project used four male speakers whose voice was recorded in the helicopter cockpit under two of the most demanding flight regimes: at the hover and in the cruise. The test data consisted of each speaker recording 280 words and digits in both of the test flight regimes. This resulted in a total 560 tokens for each speaker (15 words and 10 digits). The words and digits were spoken in command strings. The reference templates for each speaker were derived from two passes of the vocabulary recorded in the helicopter in quiet and two passes with the main rotor at 70% maximum rpm. The manner and rate of speaking were chosen by each speaker individually to keep the procedure as natural as possible. Three major factors were found to impact the performance of the recogniser. The first factor involved syntax. A closed syntax that structured the sequence of command words with digits performed much better than an open syntax structure. The second factor was related to thresholding the speech input. It was found that performance was greatly improved when a thresholding technique was applied. This technique is based on the average spectral envelope of the speech for each speaker. This approach helps to preserve formant structure by providing more thresholding effect in the lower, noisier channels, and relatively less in the quieter upper channels. The third factor is related to the computation of the IMELDA transform. It was found that computing a user-specific transform, using examples of speech in both quiet and noisy backgrounds, provided the best performance in the severe conditions of a helicopter cockpit.

Overall, the recognition rate on the test data recorded in the cockpit for all four speakers is as follows: Speaker #1: 99.3%; Speaker #2: 99.6%; Speaker #3: 99.3%; Speaker #4: 99.3%. The hardware recogniser was also tested in actual flight by one of the speakers. In this test the recognition performance was 93.8% in hover and 94.8% in the cruise. Reasons for reduction in performance are mostly related to specific problems in integrating the recogniser into the cockpit, such as the presence of 400Hz aircraft power supply harmonics, variable microphone placement and audio-compression noise. For more details on the "Fly-by-Voice" project see [5].

The performance of the recogniser with the high level of background noise and inherent speaker stress in a helicopter cockpit environment is very encouraging for other applications. Of particular interest to the Neil Squire Foundation, is the expected carryover of these performance characteristics to other applications where persons with severe disabilities are using voice to control various aspects of their environment.

## EVALUATION OF SPEAKER INDEPENDENCE

Ideally, there are many applications for persons with disabilities where a speaker-independent system would be highly desirable. For example, a speaker-independent system, because it would avoid the need for any special training of the vocabulary by the user, would greatly simplify the set up procedures for a voice actuated home control system.

The laboratory implementation of the IMELDA speech recognition system has demonstrated good speaker-independent capabilities [2]. Until recently, however, the performance in the speaker independent mode has not been investigated using the stand-alone

hardware recogniser.

Work to assess the speaker independent capabilities of the hardware was carried out in three phases. In the first phase one set of data was used containing isolated and co-articulated digits (0-9). One thousand three hundred fifty co-articulated digits were extracted from triplets recorded by 9 male speakers of English from a pre-recorded database. Isolated digits were recorded on a magnetic tape in a quiet laboratory over a Shure SM-10 public address head-mounted microphone. The isolated digits were recorded 4 times for reference material by 14 speakers representing different accents of English (560 digits) and also 1530 isolated and 150 co-articulated digits were recorded by the same speakers for testing material. The digits and words were then processed for each speaker through the hardware recogniser to collect material for reference templates.

All the data were transferred onto a SUN SPARCstation for K-means clustering of the collected data examples. Three classes were computed for each digit, which was motivated by the limit of the vocabulary size in the hardware which at the time of the experiment was 39 tokens. An IMELDA transform and reference templates were computed and ported to the hardware. Two recognition experiments were conducted. The first test used data recorded for testing by the original 14 male speakers whose data were used for the reference material. The other test was truly speaker-independent, using data input live by 10 completely new male speakers. The overall recognition accuracy for all speakers with all digits (isolated and co-articulated) in the first test was 98.5% and 95.9% in the second test.

In the second phase, isolated and co-articulated digits were used along with 14 words appropriate for a home automation control application: help, next, menu, exit, up, scan, select, dial, number, answer, phone, auto, redial, hang (NSF lexicon). The digits were collected in the same way as in PHASE I, while the words were recorded by 14 speakers 4 times: 2 times for training, and 2 times for testing. K-means clustering was again used, with 2 classes computed for digits and 1 class for words. An IMELDA transform was computed with the entire material, including digits and words.

One recognition experiment was conducted. It used data recorded for testing by the original 14 male speakers whose data were used for the reference material. No test with new speakers was conducted, as it was decided to carry it out in PHASE III on a larger lexicon. The overall recognition accuracy for all speakers with all tokens and an open syntax (co-articulated digits and isolated words: 184 x 14 = 2576) was 97.2%.

In the third phase, isolated and co-articulated digits were used in this test along with 24 words: DME, ILS, MLS, VOR, UHF, VHF, channel, set, TACAN, transponder, normal, ident, squawk, emergency, guard, hijack, point, decimal, correction enter, fife, niner, oh, hundred (CMC lexicon). The digits and words were collected in the same way as in Phase II. K-means clustering was again used, with 1 class computed for digits and 1 class for words.

Two recognition experiments were conducted. One used data recorded for testing by the original 14 male speakers whose data were used for the reference material. The other test was truly speaker-independent, using data input live by 6 completely new male speakers. In the test with microphone input, the words from the CMC lexicon were used in combination with digits (e.g. DME 171.05). There were 40 such strings. The overall recognition accuracy for all speakers with all tokens and an open syntax (co-articulated digits and isolated words: 204 X 14 = 2856) was 95.1% in the first test and 81.1% in the second test. The experiment with microphone input in PHASE III (second test) was the most natural and difficult of all tests, as it comprised whole utterances rather than just lists of isolated words. For comparison, one of the speakers, whose voice was used for training, read through the microphone the list of 40 strings of words and co-articulated digits. In the test with tape input, 3 errors were detected for digits (3/156:98.1%), while with microphone 11 errors (11/129:91.4%) were detected. A similar trend was observed for words: 0/48:100% (tape) and 4/75:94.6% (microphone).

The following conclusions may be derived from these evaluations:

(a) even for a small number of speakers (14) and relatively small databases used for training, it has been possible to demonstrate speaker-independent performance at an accuracy rate of 96%. This is a result obtained for isolated and co-articulated digits, spoken by new speakers in an unconstrained way, with 3 classes of averaged digits as the reference templates.

(b) The inclusion of words in addition to digits did not degrade recognition accuracy. Words were on average recognised better than digits with both tape and microphone inputs with only 1 class of averaged words in each test. The performance of digits deteriorated in all conditions as the classes of averaged reference data were reduced from 3 to 2 and eventually to 1 only.

(c) The computation of more classes for both digits and words would improve recognition accuracy. The hardware recogniser will have to be modified to increase the vocabulary size. Work toward this end is currently being carried out and recently the vocabulary has been increased to 64 tokens.

(d) Automatic gain control (AGC) in the hardware should also contribute to increased recognition accuracy with the microphone. The input level from the tape was manually adjusted for each speaker.

## FUTURE WORK

Work in the future will continue in several areas. Work on developing a robust keyword activation algorithm which will allow a user to "hands free" switch the recogniser in and out of the recognition mode of operation will be performed. A method of AGC will be integrated into the hardware to allow a wider range of speaker levels and lessen the dependency on microphone positioning. Once the AGC and keyword activation have been implemented then a speaker-independent home control application will be field tested. In addition, the hardware will be redesigned to take advantage of newer DSP technology allowing for a single board implementation with greater working vocabulary capacity. Finally, as changes to the hardware are implemented the user interface application software will continue to evolve both to support the hardware changes and to improve its overall level of user friendliness.

## REFERENCES

1. V.A. Thomason, P.S. Chopra, S.M. Farajian, and M.A. Abazid, "Application of Voice Recognition Devices for Computer Access and Programming", Proc. RESNA, ICAART-88, Montreal, Canada, 1988, pp. 370-371.

2. Birch, G.E., Zwierzynski, D.A., Lefebvre C., and Starks, D.R., "An IMELDA Based Voice Recognition System: A Step Towards Effective Voice Recognition for Persons with Severe Disabilities", Proceedings of the Canadian Acoustical Association Conference, Edmonton, Alberta, October, 1991 pp. 111-112.

3. Hunt, M. and Lefebvre, C., "A Comparison of Several Acoustic Representations for Speech Recognition with Degraded and Undegraded Speech", Proc. IEEE Int. Conf. Acoustics, Speech, and Signal Processing, ICASSP-89, Glasgow, Scotland, Vol 27, No. 3, pp. 262-265, 1989.

4. Hunt, M. J. and Lefebvre, C., Distance measures for speech recognition, Aeronautical Note, NAE-AN-57, Ottawa, March, 1989.

5. Lefebvre, C.. Zwierzynski, D.A., Starks, D.R., and Birch, G.E., Further Optimization of a Robust IMELDA Speech Recogniser for Applications with Severely Degraded Speech, Proceedings of the International Conference on Spoken Language Processing, Banff, Alberta, Canada, October, 1992.

# Robust pitch detection for normal and pathologic voice

B. Boyanov†* , G. Chollet*
† Bulgarian Academy of Sciences, CLBA, Acad. "G. Bonchev" str. BLOC 105
Sofia 1113, Bulgaria
*TELECOM-Paris, CNRS URA-820
46, rue Barrault, 75 634 PARIS CEDEX 13, FRANCE

session **Speech, Hearing and Communication**

## Introduction

It is known that most of the laryngeal pathologies produce a change in the vocal quality of the patient. The pitch period (To) is significantly affected by these diseases. In most of the pathological voices there are present:

a) large deviations of To and in magnitudes of the peaks of the pitch;

b) deformation of the shape of pitch impulses;

c) abrupt changes in To and the magnitude of the peaks of the pitch;

d) interruptions of pitch generation during sustained vowel phonation - voice breaks;

c) noisy components having a significant amplitude.

In order to overcome these difficulties a method is proposed for calculating To by analysis of different domains of the signal.

## METHOD

The speech signal is analyzed by means of the following procedure:

### Preprocessing of segments.

The signal is divided into segments with a duration of 30ms. In order to minimize errors caused by low level signals [1] a verification of the signal's level is carried out:

a) search for at least 3 peaks: $A_m(t1)$, $A_m t2)$, $A_m(t3)$, (where: t3 > t2 > t1 ) fulfilling the following conditions:

$A_m(t1) > TR$, $A_m(t2) > TR$, $A_m(t3) > TR$, (1)

where: TR is 50% from the maximum possible value of the signal.

and

$$t2 - t1 > T_{hp} \text{ and } t3 - t2 > T_{hp} \quad (2)$$

The distances between these peaks have to be more than the highest To possible ($T_{hp}$) for the pathologic voice.

b) the signal in the segment is classified as a normal level and is processed if at least 3 peaks fulfilling these conditions are found. Otherwise the segment is rejected and the next one is processed.

### Pitch Period Evaluation.

The calculation of To is realized in parallel in 3 different domains:

1. PITCH EVALUATION IN TIME DOMAIN

1) To is calculated in the time domain using the autocorrelation function $R(\tau)$ [2,3]. The $R(\tau)$ is calculated over the center-clipped signal, allowing robust To detection from noisy speech [3]. However this method may give erroneous results due to [3] :

a) strong harmonics coinciding with the first formant;

b) strong harmonic and formant structure;

c) presence of several peaks in $R(\tau)$.

On the basis of the fact that $R(\tau)$t of a periodic signal is periodic the following procedure is used to minimize the above-mentioned errors:

1.1) Voiced-unvoiced detection by means of the algorithm described in[2];

1.2) In voiced segments the largest peak($R_{MAX}(\tau_{max})$) of the autocorrelation function in the range of To is found;

1.3) A threshold TR$\tau$ is calculated:

$$TR\tau = 0.6R_{MAX}. \quad (3)$$

This threshold is used because it was found [1] that for some pathological voices the peak in $R(\tau)$, corresponding to To is with reduced amplitude (nearly $0.6R_{MAX}$ );

1.4) Location of all the peaks ($R_p(\tau j)$) of $R(\tau)$ in the range of To greater than TR$\tau$;

1.5) Calculation of the differences (distances) between the lags of these peaks :

$$T(j) = \tau_{j+1} - \tau_j, \quad (4)$$

where: $\tau_0, \tau_1, \ldots \tau_J$ –successive lags of $R_p(\tau j)$,

j=0,1,...J,

J - number of the peaks,

$\tau_0$=0.

1.6) Calculation of the maximal difference ($\delta T$) found between T(j);

1.7) Calculation of the mean T(j) - $\overline{T}$;

1.8) The value of the pitch is obtained in the time domain as $To_{time}$ in the following cases:

1.8.1) If only one peak in $R(\tau)$ is found:

$$To_{time} = \tau_{max}. \quad (5)$$

1.8.2) The autocorrelation function is periodic i. e. the values of T(j) nearly constant:

$$To_{time} = \bar{T} \quad \text{if} \quad \delta T < 0.2\,To \qquad (6)$$

When no decision about $To_{time}$ it taken then all T(j) are saved as possible $To_{time}$ .

2. PITCH EVALUATION IN SPECTRAL DOMAIN

2.1) Calculation of the cepstrum (c(t));

2.2) Calculation of the smoothed spectrum by means of the group delay function (GDF) (the negative first derivative of the phase spectrum). The GDF is used because it was found [7] that it represents well the low and high energy spectral regions.

2.3) Coding the spectral components on the base of different thresholds for the low and high energy spectral regions:

a) For every spectral region are found the three largest peaks (X1(f1), X2(f2), X3(f3)), having a distance between them greater than the lowest fundamental frequency $F_{low}$ for pathological voices;

$$f2 - f1 > F_{low} \quad \text{and} \quad f3 - f2 > F_{low} \qquad (7)$$

b) Calculation of a threshold for the region:

$$TR_{spec} = lev[X1(f1) + X2(f2) + X3(f3)]/3,$$

where: lev=0.7. (8)

c) Coding the spectral components on the base of the different $TR_{spec}$ .

2.5) Calculation of a spectral autocorrelation function over the coded spectral components and evaluation of To using the procedure already described in the previous stage "analysis in time domain". If the segment is classified as voiced To is evaluated as $To_{spect}$ or no decision about To is taken and P possible values for $To_{spect}$ (where P-number of peaks in spectral autocorrelation function) are obtained

3. PITCH EVALUATION IN CEPSTRAL DOMAIN

To is evaluated in the cepstral domain using the robust method described in [2, 3]. The cepstral analysis is performed in order to compensate for inconveniances "b)" and "c)" of $R(\tau)$ [p. 405 in 3]. If the segment is classified as voiced the value of To is obtained in the cepstral domain - $To_{ceps}$.

4. OBTAINING THE PITCH PERIOD ESTIMATE

The calculated values of To are analysed for determination of To by means of the following procedure:

The segment is classified as unvoiced in the following cases:

a) In two domains it is classified as unvoiced;

b) In two domains there are no decision for the pitch period and in cepstral domain it is classified as unvoiced.

The difference between $To_{spect}$ and $To_{ceps}$ is calculated:

$$T11 = To_{ceps} - To_{spect} \qquad (9)$$

The segment is classified as unknown and is eliminated from future analysis if:

a) $T11 > 0.3.To_{spect}$ and $T11 > 0.3.To_{ceps}$,.

Here the results ($To_{ceps}$ and $To_{spect}$ ) from the most robust pitch detectors are.used.

b) In two domains no decision for the pitch period is obtained;

c) In one domain it is classified as unvoiced and in one domain no decision for the pitch period. is obtained

In all the other cases To is calculated as:

$$To = [To_{ceps} + To_{spect} + To_{time}]/3 \qquad (10)$$

As a result the erroneous values of To are eliminated almost in all the possible cases.

**Experimental research and results**

The vowel "a" and a control phrase pronounced by 45 patients (laryngeal pathology) and 28 normal speakers are analysed. Normal and pathologic voice signals were passed through a low-pass filter with a cutoff frequency of 5kHz and sampled at 16 kHz with 16 bits directly into the computer's memory. No large errors in the values of calculated To and no wrong classification of unvoiced segments as voiced were found. However 2% of voiced segments are classified as unvoiced and nearly 8% of the segments are rejected as no decision for To was obtained.

REFERENCES

1.Boyanov B. , Ivanov T. ,"Analysis the speech of patients with laryngeal diseases", Report 15/90, Bulgarian Academy of Sciences (In bulgarian).

2.Rabiner L., Shaffer R.,"Digital Processing of speech signals," Prentice Hall, NY, 1978.

3.Hess W.,"Pitch determination of speech signals", Springer Verlag. N.Y. 1983.

4.Lahat M., Niederjohn R.,Krubsack D.,"A spectral autocorrelation method for measurement of the fundamental frequency of noise-corrupted speech",IEEE Tr. Acoust. Speech, Signal Proc., ASSP-35, pp. 741-750,1987.

5.Laver J., Hiller S., Hanson R.,"Comparative performance of pitch detection algorithms of dysphonic voices," IEEE Proc. of ICASSP, pp.192-195,1982.

6.B. Boyanov, G. Chollet Pathological Voice Analysis using Cepstra, Bispectra and Group Delay Functions, Proc. Int. Conference on Spoken Language Processing, Banff, Canada, October, 1992. .

# ON NEUTRAL-TONE SYLLABLES IN MANDARIN CHINESE

Cao, Jianfen

Institute of Linguistics
Chinese Academy of Social Sciences
5 Jianguomennei Rd.
Beijing 100732, CHINA

## I. INTRODUCTION

One of the characteristic and hard to be grasped features in Mandarin Chinese is the so-called neutral-tone ( hereafter NT) syllables, which is neutralized from corresponding normal stressed syllables. Perceptually,The NT syllable sounds quite weak, and must be attached to other syllable as a dependent morpheme in polysyllabic words. However, it does not equal to the unstressed syllables in common, in stead, it forms an important morphophonemic contrast to the normal type one in bisyllabic words. Consequently, it might be of benefit to Chinese speech processing to clarify the phonetic nature of the NT syllables.

Many relevant approaches from different viewpoint [1][2][3] have been contributed before, this study is concerned in their phonetic characteristics. The discussion is based on a relevant acoustic measurements and anlysis [4] refered to a corpus of materials including over 200 of NT syllables,all of them are occurred as second morpheme in different category of neutral type bisyllabic words.

The hypothesis is that the perceptual feature of the NT syllables may be caused by a combination of multiple acoustic effects, in stead of any single factor. Therefore, this kind of syllables must own their special acoustic patterns.

## II. EXPERIMENTAL RESULTS AND DISCUSSION

### 2.1 The intensity of NT syllables

Perceptually, the stress of NT syllables is weaked, so people are often used to regard that it is a result of low intensity. However,The data obtained here illustrate that the intensity of NT syllable is not necessary lower than that of the syllable with normal stress. Table I offers a comparison on average intensity between normal syllables and the NT ones obtained from a set of duplicated bisyllabic words, in which two syllables with the same phonetic structure but different stress type. The corresponding figures show clearly that the intensity of NT syllable is lower than that of the normal one in general, but the situation is just reversed when it is preceded by a third tone syllable. This tendency also can be seen from Fig 1, so it seems to be a relational invariance in this area. Therefore, the stress of NT syllable is weaked,but not simplly related to its intensity.

Table 1. Comparison on averagy intensity(dB) between normal and NT syllables in duplicated neutral type bisyllabic words.

| Original tone category | intensity of normal syllable | | intensity of NT syllable | |
|---|---|---|---|---|
| | value | sd | value | sd |
| first tone | 15.20 | 1.95 | 7.46 | 0.96 |
| second tone | 12.77 | 2.99 | 9.87 | 1.35 |
| third tone | 9.38 | 1.38 | 10.05 | 0.94 |
| fouth tone | 15.85 | 0.64 | 7.08 | 1.88 |

### 2.2 The pitch of NT syllables

One of the most characteristic faetures of NT syllable is loss of its original tone pattern. Usually,people pay most of the attention to its short duration and relative pitch hight, while the dynamic range of pitch contour is often ignored[5].

According to the perceptual impression,the pitch hight is usually marked with the points of three or four levels[6][7], namely, the highest one occurred after a third tone syllable, then the ones occurred after the second tone and first tone syllable respectively, the lowest one is that occurred after the fourth tone syllable.

Based on the results obtained from relevant investigation, as it has been summarized in Fig.1 and Table II,the following findings have been made[4], though it is still remained as a controversial issue. First,it is obvious that there exist two different type of pitch contour among the NT syllables,and it is significantly distinguishable ($p<0.01$) determined by the tonal difference of preceding syllables, namely, a mid-level or slightly rising contour after a third tone syllable, and a mid-falling one after all of the other tone's syllables; Second, as what can be seen from Table II, the average pitch value at the onset of NT syllables in different tonal context is closed to one another, while the value at syllable offset does show a regular order, i.e, the highest value is held by the tokens occurred after the third tone syllable,and then is that of the tokens after second and first tone syllables, the lowest one is that occurred after the third tone syllables. This order is just matching to the four-level's distinction of perceptual impression mentioned above. Consequently, the dominant effects for the perceived impression of pitch height shouled be coming from the whole pitch contour, rather than a single point of pitch height, at least, it is more related to the later part of NT syllables, in stead of the pitch values at the onset as some approach[8] suggested. Actually,

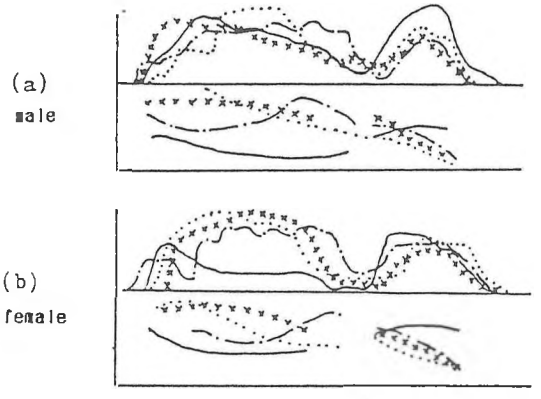


**** first tone, _._. second tone,
____ third tone, .... fouth tone.

Fig.1 Comparison on intensity and pitch height between NT syllable and preceding normal syllable: The top lines in both of (a) and (b) represent amplitude contours, and the bottom ones the pitch contours.

Table II. Average value of relative pitch hight(Hz) of NT syllables

| preceded tona context | pitch value at the onset | | pitch value at the offset | |
|---|---|---|---|---|
| | value | sd | value | sd |
| after 1st tone | 152.34 | 21.05 | 89.51 | 11.76 |
| after 2nd tone | 174.71 | 11.55 | 108.45 | 27.64 |
| after 3rd tone | 136.60 | 6.93 | 146.60 | 3.46 |
| after 4th tone | 123.45 | 15.19 | 75.30 | 11.59 |

Table III. Comparison on duration(ms) between normal(NM) type syllables and NT syllables

| original tone category | normal syllable | | NT syllable | | ratio of NM to NT syllables |
|---|---|---|---|---|---|
| | value | sd | value | sd | |
| first tone | 313.21 | 34.33 | 186.76 | 24.78 | 100:60 |
| second tone | 304.92 | 51.14 | 183.02 | 30.50 | 100:60 |
| third tone | 299.80 | 44.89 | 209.13 | 10.56 | 100:70 |
| fourth tone | 302.25 | 60.75 | 192.33 | 28.15 | 100:64 |
| plotted | 305.05 | 5.83 | 192.81 | 9.99 | 100:63 |

this finding has been revealed by a relevant test of the synthesis[9]. It idicates that, the NT syllables do have own regular pitch patterns and it is definitly contributed to the perception of NT syllables.

2.3 The duration of NT syllables

Generally, the NT syllable is systematically shorter than the syllable with normal stress, the average ratio between them is about 3:5 in isolation and 1:2 in running speech[10]. Of course, it is only a rough range, the specific realization of individual tokens is more complex. First, According to the average duration (see Table III) measured from a group of duplicated bisyllabic words in isolation, the durational realization of NT syllables seems also to be determined by tonal difference of the preceding syllables. Generally, a relatively longer duration is held by the tokens occurred after third tone syllables; second, the shorter duration of NT syllable is not just caused by a simple compression of the whole syllable, but a change of temporal distribution within the syllable. Generally, in the NT syllable, a relatively greater dgree of shortenning is taken place in the vowel, instead of the consonant of the syllable.

2.4 The sound quality of NT syllables

The sound qualities in NT syllables, especially for the syllable finals, are usually perceived as somewhat indistinct, it is due to the effect of neutralization. Specifically, the consonants are obviously shortened and reduced compare with that in corresponding normal syllables.In addition,it is most likely to become voicing; At the same time, the vowel qulity in NT syllable is neutralized and sounds close to that of the shwa. According to Fig. 2, however, their original sound quality is still identified. Fig. 2 shows a comparison in the

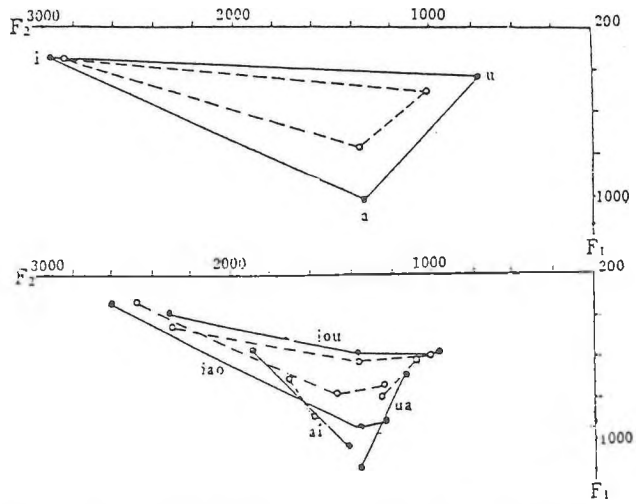


Fig 2. Comparison between NT and normal syllables in their acoustic vowel-chart

related acoustic vowel-chart between NT syllables and the normal ones. The top one represents the position of the monophthongs/I/,/a/,/u/, and the bottom one of diphthongs/ai/, /ua/,/iao/ and /iou/, here the solid line marks the vowel quality in normal syllables, and the dashed line marks that in NT syllables. As what can be observed from this Figure, the vowel quality of NT syllable in all cases are reduced just towards to the target of shwa compare with the original qualities in normal syllables,but still keep in discriminable one another.

III. CONCLUSION

The experimental results obtained from this investigation leads to following considerations:

(a) As the hypothesis made at the beginning of this paper,the perceptual feature of neutral-tone syllables is caused by the combined effect of neutrolization taken place in all the aspects of the syllable including intensity, pitch, duration and the sound quality, rather than any single factor;

(b) As a special morpheme and differentiate from the common unstressed syllables, the neutral-tone syllables in Mandarin Chinese do have some relatively fixed patterns in acoustic realization, and it is mainly determined by tonal difference of the preceding syllables.

REFERENCES


[1] Dong, Shaowen. An Introduction to Phonetics. Cultural & Educational Press, 1956, pp. 80-82.

[2] Lin, Maocan & Yan, Jingzhu. The acoustic characteristics of neutral-tone syllables in Standard Chinese. Fangyan, No.3, 1980, pp.166-178.

[3] Lin, Tao. Experimental approach on neutral-tone syllables in Standard Chinese. The Collections of Linguistics papers, Vol.10,1982, pp.16-37.

[4] Cao, Jianfen, Analysis of neutral-tone syllables in Standard Chinese. Applied Acoustics, 5:4, 1986, pp.1-6.

[5] Chao, Yuanren. A Grammar of Spoken Chinese, University of California Press, 1968.

[6] Chao, Yuenren. On the Language, Commercial Press, 1980, pp.59-83.

[7] Luo, Changpei & Wang, Yun. An Outline of General Phonetics, Commercial Press, 1981, pp. 133-135.

[8] Wu, Zongji & Lin, Maocan ed. An Outline of Experimental Phonetics, Higher Educational Press, Beijing, 1989.

[9] Yang, sun-an. Preliminary synthesis of neutral-tone syllable in Standard Chinese. PL-ARPR/1988, pp.81-91.

[10] Cao, Jianfen. Temporal structure in bisyllabic words frame: An evidence for relational invariance and variability from Standard Chinese. The Proceedings of ICSLP92, Alberta, Canada, 1992.

# QUATRE VISAGES DE LA VOIX

**Daniel Leduc**

Université de Montréal
15 rue Waterman app. 606
Saint-Lambert, Québec, Canada J4P 1R7

**introduction**

La voix humaine, à travers l'art sonore, peut prendre quatre formes différentes, selon qu'elle soit porteuse de sens ou non, et qu'elle soit issue ou non des ressources du langage. A l'aide du mélodrame électroacoustique il est possible de retrouver ces divers visages de la voix à travers ce que l'on peut nommer une mélodie principale. Toutefois, elle devient aussi, à certains moments, partie intégrante de l'organisation musicale pour former un tout.

**le mélodrame électroacoustique**

Le mélodrame électroacoustique détermine à la fois le genre et la forme d'une réalisation et est issue d'un art encore tout récent: l'acousmatique (du terme grec 'akousma': ce qu'on entend, perception auditive). De nos jours l'art acousmatique définit une musique des sons fixés à écouter sans voir. Parmi les penseurs contemporains de cette forme d'art sonore, nous retrouvons Michel Chion qui a tenu ces propos sur le mélodrame électroacoustique en 1986:

> "Le mélodrame électroacoustique est une pièce de musique électroacoustique de caractère dramatique, sur un texte ayant le statut d'un livret, et avec un seul personnage principal (...). Une des règles du genre est qu'il n'y a jamais de dialogue entre deux ou plusieurs personnages qui se parleraient entre eux par-dessus les sons. S'il y a dialogue, c'est celui du personnage avec les sons" (CHICON 1986: 12)

**musique et communication**

Le mélodrame électoacoustique, dans sa perspective d'écoute acoustique, se présente comme un art sonore très proche du médium radiophonique. Le penseur et chercheur canadien dans le domaine des communications, Marshall McLuhan, qualifie le médium radiophonique d'intime puisqu'il touche les auditeurs justement dans leur intimité: "c'est là le côté direct de la radio. C'est une expérience privée" (McLUHAN 1972: 327 et 328). L'une des manifestations de cette volonté est le hörspiel.

Le terme hörspiel provient de la fusion en allemand des mots oreille et jeu, et son concept évoque l'union de genres variés. Littérature, musique et art d'interprétation s'y fondent et marient des textes lyriques, narratifs, dramatiques et d'essai combinant le langage, le son et la musique. "Au temps où la radio n'avait pas encore été détrônée par la télévision, théâtre et musique <<pour l'oreille>> faisaient chanter les ondes" (FRISIUS 1989: 112). Art issu des techniques modernes, (tout comme le cinéma), le hörspiel propose des oeuvres à caractère singulier, où la présence du langage, qu'il soit dans sa forme concrète ou abstraite, est souvent requise.

Ce sonore organisé tel qu'on le retrouve en dramatique radiophonique, se présente sensiblement de la même façon dans le mélodrame électroacoustique. Selon Danielle Cohen-Levinas, "que la voix appartienne 'naturellement' à l'univers abstrait de la musique, cela semble être une affirmation définitivement acquise" (COHEN-LEVINAS 1987: 35). Un peu comme en musique mixte, "syntaxe musicale et syntaxe vocale s'unissent (...) sans jamais se confondre" (COHEN-LEVINAS 1987: 25).

**quatre visages de la voix**

Ainsi, la voix peut suivre quatre différentes avenues. C'est pourquoi nous parlerons ici de voix porteuse de sens ou non et issue ou non d'un langage.

*sens / langage*

Cette première avenue possible, sans doute la plus facile à concevoir parce que nous l'utilisons quotidiennement, est celle du langage porteur de sens. C'est bien sûr celui qui hante presque toute la production vocale, chantée ou parlée. Si nous observons le répertoire classique occidental, il appert que la voix porteuse de sens et se référant à un langage précis se traduit, musicalement parlant, par la ligne mélodique.

*non-sens / langage*

Cette deuxième avenue est celle de la voix porteuse d'un langage impossible à décoder lorsque l'on ne connait pas les clefs de celui-ci. Ce phénomène est souvent observable en musique traditionnelle avec l'abondance de textes incompréhensibles pour de simples questions de culture. En effet, un individu étranger à une langue ne pourra pas goûter la beauté d'un texte original.

*sens / non-langage*

Contrairement à la voix qui utilise un langage mais qui peut ne pas être significative, nous abordons maintenant une troisième avenue peu usitée en musique vocale classique ou traditionnelle. Il s'agit de la voix porteuse de sens mais sans le recours au langage. Cette voix va beaucoup plus loin que le langage onomatopéique, sans toutefois l'exclure totalement. Il faut constater combien cette facette vocale occupe une place timide dans notre vie musicale occidentale. Cette absence s'explique aisément dans notre civilisation où le langage organisé domine presque toutes nos façons de communiquer. Ces sons que nous produisons spontanément n'utilisent pas un langage organisé aux articulations défines. Toutefois ils seront habituellement compris par des gens de cultures et de langues différentes. Nous pouvons ici parler de langage universel, au même titre d'ailleurs que le langage du corps, puisqu'il est propre à l'être humain.

*sans-sens / non-langage*

Enfin, notre dernière avenue possible est celle de la voix dans son expression la plus instrumentale possible. La voix devient ainsi un corps sonore, au même titre qu'un instrument de l'orchestre. Elle laisse plutôt une empreinte vocale, sans chercher à se faire comprendre ou à vehiculer un langage.

**musique et langage**

Mais une question important se pose. La musique, et plus spécifiquement l'électroacoustique, est-elle un langage? Cette question, Pierre Schaeffer l'a posée dans le *Traite des objets musicaux*. Voici comment Michel Chion pose la question dans son *Guide des objets sonores*, veritable cornac de cet ouvrage fondamental:

> "On en vient alors à la fameuse interrogation contemporaine que la Traité n'elude pas, mais qu'il passe au crible de sa critique. Si la Musique est un langage, répond-il, ce n'est certes pas au même titre que le langage proprement dit: car la structure musicale se trouve liée indissolublement aux qualités sensibles de son matériau, qui n'est pas interchangeable." (CHION 1983:77)

Cette question est très ancienne. Il nous semble que la musique n'est pas un langage. Toutefois, il n'en reste pas moins que nous pouvons la considérer malgré tout comme étant un très efficace moyen de communication. En effet, la chaine compositeur-interprète et auditeur nous semble en tous points correspondre au

profil émetteur et récepteur propre à tout phénomène de communication.

En fait, si la musique n'est pas un langage, il n'en reste pas moins qu'elle demeure une forme de communication très proche du langage en tant que tel, sans toutefois le rejoindre. La musique, et plus particulièrement dans le cas qui nous intéresse celle de type électroacoustique, possède des similitudes avec un alphabet, un vocabulaire et plusieurs règles syntaxiques qui nous permettent d'établir un certain rapprochement avec le langage. Toutefois, nous croyons qu'elle le transcende puisqu'elle est de compréhension à la fois universelle et multiple à travers ses évocations et significations diverses. Reste à savoir, et cela est une interrogation très en vogue depuis la parution du révolutionnaire ouvrage de Schaeffer, s'il sera possible de fixer un jour les règles de la syntaxe électroacoustique, comme cela existe ailleurs en musique dans les traditionnels traités d'harmonie et de contrepoint. Il s'agirait alors de ce fameux "traité des organisations musicales" (SCHAEFFER 1977: 663) auguel Pierre Schaeffer a fait lui-même allusion.

**conclusion**

Bref, la voix possède quatre visages différents. Toutefois, la plupart des grilles d'analyses d'oeuvres musicales référant à la voix, comme celle de Stacey (Stacey 1989), ignorent ces différents aspects. Malgré tout, il est facile de démontrer, par le mélodrame électroacoustique, comment ces quatre visages de la voix se retrouvent inconsciemment présents dans la vie de tous les jours, et ce, à travers des aspects poétique (musique, organisation sonore, etc.) ou pratiques (communication radiophonique, échange verbal, perception sonore, etc.).

**sources documentaires**


- CHION, Michel et coll. *Michel Chion*, Arras, Acousmonium Noroit, 1986, 18 pages.

- CHION, Michel. *Guide des objets sonores*, Paris, INA/GRM - Buchet/Chastel, 1983, 186 pages.

- COHEN-LEVINAS, Danielle. *La voix au delà du chant*, Paris, Michel de Maule, 1987, 122 pages.

- FRISIUS, Rudolf. "La voix des ondes". *Le Monde de la musique*, Paris, septembre 1989, no. 125, pp. 112 et 113.

McLUHAN, Marshall. *Pour comprendre les médias*, Montréal, HMH, 1972, 390 pages.

- SCHAEFFER, Pierre. *Traité des objets musicaux*, Paris, Seuil, 1977, 711 pages.

- STACEY, Peter F. "Towards the analysis of the relationship of music and text in contemporary composition". *Contemporary Music Review*, vol. 5 (1989), pages 9 à 27.

# ACOUSTIC MEASUREMENTS OF VOCALIC NASALITY IN MANDARIN CHINESE

**Bernard L. Rochet and Yanmei Fei**
Department of Romance Languages, University of Alberta, Edmonton, T6G 2E6

## 1. INTRODUCTION

The assimilation of nasality onto vowels spoken in the context of nasal consonants has been documented by research using various methods (aeromechanical, acoustical, biomechanical, perceptual). The research reported here used acoustical analog recording and digital analysis techniques to quantify assimilation nasality patterns in Mandarin Chinese as a function of vowel height, place of articulation of the following nasal consonant, and tonal characteristics of the vowel.

## 2. PROCEDURES

### 2.1. Subjects/Speech Sample

Subjects were 8 young adult native speakers of Mandarin Chinese, with normal hearing, voice qualities and articulation patterns. They read aloud Chinese words in which the vowels /i, e, o, a, u/ were embedded in the contexts CVN and NVN, where V= one of the target vowels, C= a non-nasal obstruent and N= /m/, /n/, or /ŋ/.

### 2.2. Data Collection/Analysis

The oral and nasal acoustical signals corresponding to subjects' productions of the test words were transduced separately by means of a Kay Elemetrics Nasometer 6200. The Nasometer microphone signals were recorded simultaneously on separate channels of an FM tape recorder, low-pass filtered at 4.8 kHz and digitized at 10 kHz via CSpeech (Milenkovic 1990). The vowel portion of the oral and nasal component of each digitized signal was isolated, converted to an rms value, and the degree of nasalance computed by comparing rms amplitudes of corresponding oral and nasal data across the duration of the vowel in 5 ms steps, according to the formula: % nasalance = (nasal rms/(nasal + oral rms)) x 100. Data analysis focussed on three dependent measures: 1) degree of nasal resonance, using 0.5, or 50% nasalance as an arbitrary threshold, 2) percentage (%) of the vowel with nasalance values above 0.5, and 3) absolute duration (ms) of the vowel with nasalance above 0.5.

## 3. RESULTS

### 3.1. CVN data

Fig. 1 illustrates a common nasalization pattern for CVN signals. In the first portion of the vowel, the nasalance level remains below the threshold value of 0.5; in the last portion of the vowel, opening of the velopharyngeal port in anticipation of the following nasal consonant leads to an increase in the nasalance level.

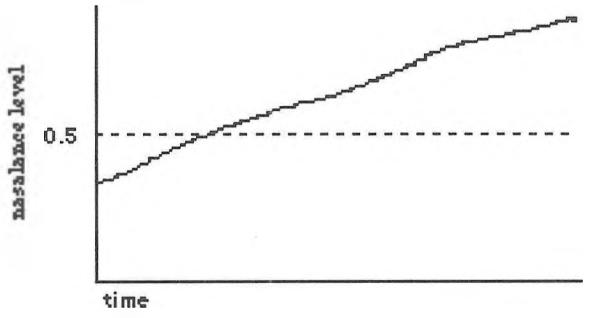


**Fig. 1: Common pattern of nasalization in CVN signals.**

In a number of cases, however, the nasalance level exhibits a value above the threshold of 0.5 for the entire duration of the vowel, i.e., from the very beginning of the vowel, as represented in Fig. 2.

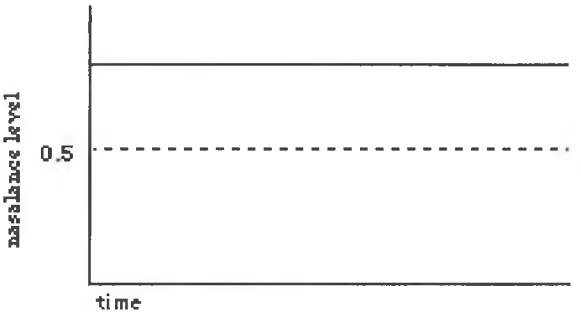


**Fig. 2: Nasalization of the entire vowel.**

Fig. 3 shows that the percentage of tokens with a nasalance level above 0.5 for the entire duration of the vowel is higher for the high vowels than for the mid vowels; there were no cases in which low vowels exhibited a nasalance level above 0.5 for the entire duration of the vowel. On the other hand, for 2% of the low vowels, the nasalance level remained below the 0.5 threshold for the entire duration of the vowel. Such a pattern was not observed for the high or the mid vowels.

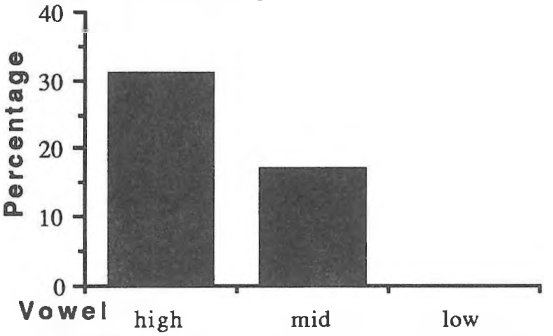


**Fig. 3: Percentage of vowels nasalized for their entire duration.**

Among tokens characterized by the nasalization pattern represented in Fig. 1, the high vowels exhibit more influence of the nasal consonant than the other vowels.

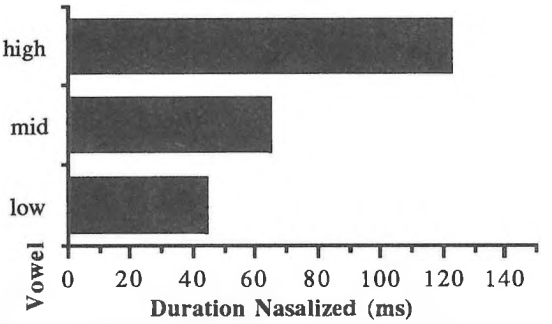


**Fig. 4: Duration of nasalized portion of vowel.**

This is true if we consider the absolute duration of the portion of the vowel with a nasalance level above 0.5 (Fig. 4). A one-way ANOVA showed that vowel height had a significant effect on the duration of the nasalized portion the vowel ($F(2,384)=129.172$, $p<0.0001$). A Sheffé test revealed that nasalization of the high vowels, with a mean duration of 123 ms, was significantly longer than for mid and low vowels, and that nasalization of the mid vowels (mean duration of 65 ms) was significantly longer than for the low vowels (44 ms; $p<0.01$).

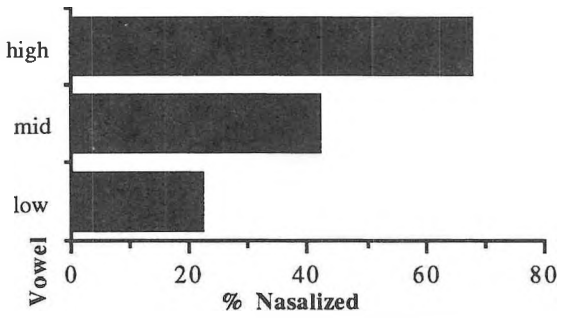


**Fig. 5: Percentage of vowel nasalized (CVN).**

The same is true if we consider the proportion of the vowel nasalized instead of its absolute duration (Fig.5; $F(2,384)=279.652$, $p<0.0001$). The differences among the three vowel categories--68% for the high vowels, 42% for the mid vowels, and 22% for the low vowels--are also significant (Scheffé, $p<0.01$).

On the other hand, no significant differences were observed in the duration of anticipatory nasalization in terms of the place of articulation of the following nasal consonant, or of the tonal characteristics of the vowel.

### 3.2. NVN data

Fig. 6 illustrates the pattern of nasalization characteristic of NVN signals. The nasalance level is above 0.5 in the initial portion of the vowel, as the result of carryover nasalization from the preceding consonant, and in the last portion of the vowel as the result of nasalization in anticipation of the following consonant. It is not uncommon, however, for the central portion of the vowel to remain at or above the 0.5 nasalance level (Fig. 2).

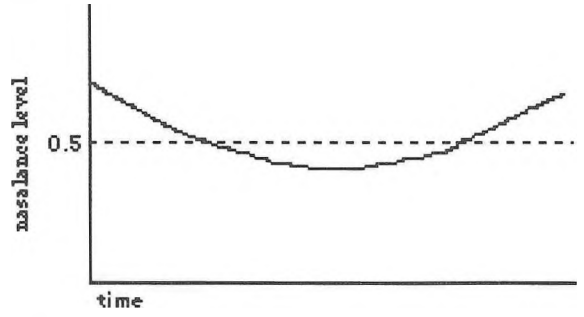


**Fig. 6: Common pattern of nasalization in NVN signals.**

In the case of high vowels, 98% of the tokens followed the pattern of nasalization represented in Fig. 2 (with a mean nasalance of 0.77), and 2% followed the pattern of nasalization represented in Fig.6. For the mid vowels, 13% exhibited a nasalance level above the 0.5 threshold (mean nasalance of 0.64), 77% followed the pattern of nasalisation represented in Fig. 6, and 10% were characterized by a level of nasalance below the 0.5 threshold (mean nasalance of 0.32). As for the low vowels, a mere 1% exhibited a nasalance level above the 0.5 threshold (mean nasalance of 0.58), 92% followed the pattern of nasalisation represented in Fig. 6, and 7% were characterized by a level of nasalance below the 0.5 threshhold (mean nasalance of 0.34).

As in the case of the CVN signals, these results suggest that the level of vocalic nasalance is positively correlated with the height of the vowel. On the other hand, no relationship was observed between degree of nasalance and consonantal place of articulation or tonal characteristics of the vowel.

## 4. SUMMARY/DISCUSSION

The results of this study indicate that, in Mandarin Chinese, the degree of vowel nasalization in a nasal consonant context varies with the height of the vowel: High vowels exhibit more assimilation nasality than mid and low vowels. These results are in keeping with those of Rochet and Rochet (1991) for Canadian English and Standard French. The apparent contradiction between these findings and those of Clumeck (1976) may be related to his use of the term "nasalized" to describe articulatory gestures of the velum, and to the fact that the biomechanical behavior of the velopharynx cannot be assumed to be monotonically related either to the perception of nasal resonance or to the acoustical consequences of nasal coupling during speech production. The acoustic attributes of nasal resonance are ultimately a function of the relative acoustic impedances of the oral and nasal cavities, as well as of the formant frequency values of the vowel in question. Curtis (1968) has shown that the spectral envelopes of /i/ and /u/ are more markedly affected by small degrees of nasal coupling than vowels with a more open tract configuration. This is consistent with listeners' judgements that the amount of nasal coupling necessary for the perceptual identification of nasalization is almost three times as much for low vowels as for high ones (House and Stevens 1956).

## 5. CONCLUSIONS

**5.1.** The higher levels and longer durations of assimilation nasality observed for the high vowels in Mandarin Chinese--as well as in both French and English--appear to be related to the acoustic impedance of the vocal tract for the production of these vowels. There is no obvious articulatory or physiological reason for the earlier lowering of the velum observed by Clumeck (1976) for low vowels in the CVN context. It may simply be that such lowering can take place because it does not have an undesirable acoustic effect, and does not lead to excessive detectable nasalization of these vowels. Later lowering of the velum for high vowels, however, may ensure that their spectral envelopes are not too markedly affected by extraneous nasal resonance.

**5.2.** In order to help understand and reconcile the apparent discrepancies among studies of assimilation nasality based on various methods of observation, further research is recommended by means of simultaneous multidimensional sampling methods that could consider biomechanical, perceptual and acoustical parameters of vowel production in a large number of languages.

## 6. REFERENCES

Clumeck, H. (1976), "Patterns of soft palate movement in six languages." *Journal of Phonetics 4,* 337-351.

Curtis, J. (1968), "Acoustics of speech production and nasalization." In D. C Spriestersbach & D. Sherman (eds.),*Cleft Palate and Communication.* New York: Academic.

House A., and K. Stevens, (1956) "Analog studies of the nasalization of vowels." *Journal of Speech & Hearing Disorders 21,* 218-232.

Milenkovic P. (1990) Department of Electrical & Computer Engineering, University of Wisconsin, Madison, WI 53705 U.S.A.

Rochet, A. P., and B. L. Rochet (1991) "The effect of vowel height on patterns of assimilation nasality in French and English." *Actes du XIIème Congrès International des Sciences Phonétiques* (19 août 1991- Aix-en-Provence, France). Aix-en-Provence: Université de Provence, Service des Publications (1991). Vol. 3, pp. 54-57.

# SOUND POWER DETERMINATION USING SOUND INTENSITY SCANNING TECHNIQUE

**G. Krishnappa**
Institute for Mechanical Engineering
National Research Council, Ottawa, Canada

## Introduction

Sound intensity is the primary quantity required to compute the sound power of sources, which is given by the surface integral of the product of the normal component of the sound intensity and the associated elemental area over any surface fully enclosing the source. The two methods that are currently being used to sample the sound field are based on:

a) measurements at discrete points distributed on the surface
b) sound intensity probe scan over the surface

In the discrete point method, the normal component of the sound intensity over an elemental area is independently measured on a large number of points distributed over an initial measurement surface. This method has been found to be complex and very time consuming, and particularly not well suited for large size sources operating in complex acoustic fields. In the scanning method, the probe is moved continuously along one or more prescribed paths on the surface. The surface average value of the normal component of sound intensity is obtained in a few scans, instead of independent measurements at several points. This method is relatively quick and easy to perform and gives good results for measurements requiring engineering grades of accuracies.

The measurement accuracy of the scanning technique mainly depends on the acoustic field conditions and the scanning parameters. the acoustic field condition can be expressed by the value of the indicator $F_{PI}$, based on two difference the average values of surface sound pressure level and sound intensity level. The scanning parameters include, speed of scanning, density of scanning and scanning patterns.

The study reported in this paper was undertaken to examine the range and effect of some of the major parameters associated with the scanning technique, for providing guidance to the user and to the standardization of the procedure.

## Experimental Details

Experimental sound source consisted of two 18 cm diameter loudspeakers, placed 0.5 meter apart, mounted in a 1 x 1 x 1/3 meter wooden box. The two loudspeakers were energized by white noise signals, with 6 dB difference in power levels, and 180° phase difference. This arrangement produces complex sound field with non uniform distribution of sound pressure and intensity, with recirculating regions of sound energy. Sound power levels from several horizontal surfaces directly above the source, covering an area of 1 x 1 meter, were estimated based on point measurements, and mechanical and hand scanning. The probe scanning on the measurement surface was performed on equally spaced eight horizontal lines. Both hand and mechanical scanning was done by moving the probe continuously at a constant speed along each line from one end to the other, back and forth.

## Results and Discussion

At 25 cm from the source, scanning measurements showed an accuracy, within 1 dB difference, in the frequency range 160 Hz to 3150 Hz for the scanning speeds in the range, 0.06 m/sec to 0.50 m/sec. Manual scans tended to show better results than the mechanical scans, due to extraneous noise generated by the probe traversing gear, especially at low frequencies. The sound field pressure intensity indicated values were all within 4 dB, for the point and mechanical scan measurements, both under free field and reflecting acoustic environments. Under reflecting environment, this indicator generally showed higher values.

On several measurement surfaces, it was observed that, for the measurement accuracies to be within 1 dB, the pressure intensity values are to remain less than 5 dB. In all the measurements, the dynamic capability index was higher than 10 dB. When pressure intensity index increased to 6 dB or higher, the measurement error was higher than 2 dB. This clearly demonstrated a need for another indicator in addition to the pressure intensity indicator.

## Conclusions

The experimental results show that the sound power of noise sources can be determined using sound intensity scanning technique. Both mechanical and manual scanning give good accuracy for engineering grade of measurements. The measurement distances from the source should be at distances greater than 25 cm. The pressure intensity indicator values were less than 5 dB for accuracies within 1 dB. The results also indicate a need for developing an additional indicator to assess the measurement accuracies.

## References

ISO 9614-1, *Acoustics - Determination of the Sound Power Levels of Noise Sources Using Sound Intensity - Part 1- Measurement at Discrete Points (1990).*

# A State-of-the-Art Advance from Larson Davis Labs!


## *The Model 2800 Realtime SLM:*

*A Precision Sound Level Meter and a 1/1, 1/3 Octave/FFT Realtime Analyzer with statistical analysis capability and on-board room acoustics software in a lightweight, notebook-size package including:*

- *Battery Operation*
- *256 KB CMOS memory*
- *External 3 1/2" floppy disk drive, MS-DOS® compatible*
- *RS 232 Interface*

## *The Model 2900 Handheld Dual Channel Analyzer:*

*All of the features of the Model 2800 plus a tachometer input and cross-channel measurement capability for:*

- *Acoustic Intensity*
- *Frequency Response*
- *Coherence*
- *Impulse Response*

LARSON•DAVIS LABORATORIES

Dalimar Instruments Inc.

89, boul. Don Quichotte · suite #12
ILE PERROT (QUÉBEC) J7V 6X2
(514) 453-0033 Fax (514) 453-0554

# PRECAUTIONS AND PROCEDURES FOR PRECISION PHASE MATCH OF MICROPHONES

**George S. K. Wong,**
Institute for National Measurement Standards
National Research Council Canada, Ottawa, Ontario, K1A 0R6.

## 1. INTRODUCTION

Since the publication of the measurement data obtained with the NRC three-port coupler [1] for the precision phase match of condenser microphones, an effort has been made to extend the high frequency performance of the device to cover the phase response of 1/4 inch microphones. The aim here is to present our current research data, and to discuss some often encountered but less familiar aspects of precision measurement and instrumentation that are necessary to ensure precision phase match.

## 2. PRECAUTIONS

The theory of the phase match procedure had been described [1]. However, there are several important basic precautions :

Before any meaningful readings can be taken, and with the microphones inserted into the coupler, instruments for the phase match such as measuring amplifiers and preamplifier should be powered-on for several hours for temperature stabilization. It is essential that the microphones be at the same temperature as the acoustical coupler. With the microphones and the preamplifiers inserted into the microphone adaptors (or holders), the physical positions of the adaptors inside the coupler should be repeatable after the inter-change of microphones. It is not realistic to expect precision phase match data when the measurements are performed during rapidly changing barometric pressure. It has been noticed that the small barometric pressure variation produced by opening doors of the laboratory has some influence on the level readings of the measuring amplifiers. Best results are usually obtained with the apparatus warmed-up over night.

## 3. PROCEDURES

The general measurement procedures are as follows :

With microphone (A) connected to Channel (A) of the measuring system, microphone (B) connected to the second channel (B), and with the driver of the coupler excited with sine waves over the one-third-octave frequency range of interest, the phase differences between the two channels were measured with a precision phase meter.

With microphone (A) connected to Channel (B), and microphone (B) connected to Channel (A), i.e. inter-changing the microphones, the phase readings were repeated, with special care given to repeat the measuring amplifier gain settings at each of the one-third-octave frequencies that had been used in the first measurement described above.

With the above two sets of phase measurements, it has been shown [1] that the phase difference of the microphones under test, and the phase difference between the instruments (preamplifiers, measuring amplifiers, one-third-octave filters) of the two channels can be deduced.

Since the phase between the instruments in the two channels (excluding the microphones), can be measured very precisely by applying a common electrical signal to both channels of the system, the performance of the coupler can be verified by comparing the phase difference of the measuring instrument channels calculated from information supplied by the coupler method, with the corresponding phase difference obtained with direct electrical measurements. In other words, the measuring method described above has a self checking mechanism.

## 4. PHASE MATCH OF 1/4 INCH CONDENSER MICROPHONES

With the Direct Method [2], the coupler arrangement has two independent electronic channels i.e. two preamplifiers, two measuring amplifiers and two one-third-octave filters (Brüel and Kjær 2639, 2636 and 1617, respectively). The test microphones (Brüel and Kjær 4136) were not matched in sensitivity or phase and they were selected at random from the existing measurement microphones of the laboratory. For this experiment, whether the microphones are of the free-field or the pressure type is irrelevant since the physical dimensions of both types of measuring microphones are identical.

The phase difference between two ¼ inch microphones over the high frequency region is shown here. The measurements were made with and without the protective grids. In the figure shown below, it can be seen that with the protective grids in place, the phase difference between the microphones is larger than the corresponding readings obtained without the protective grids. The difference between the two curves was approximately 0.01 degrees at 2500 Hz, and increased to approximately 1.2 degrees at 8000 Hz. Similar observations were obtained with ½ inch microphones : The corresponding phase difference increases were 0.2, 0.5 and 0.6 degrees at frequencies of 4000, 5000 and 6300 Hz, respectively.

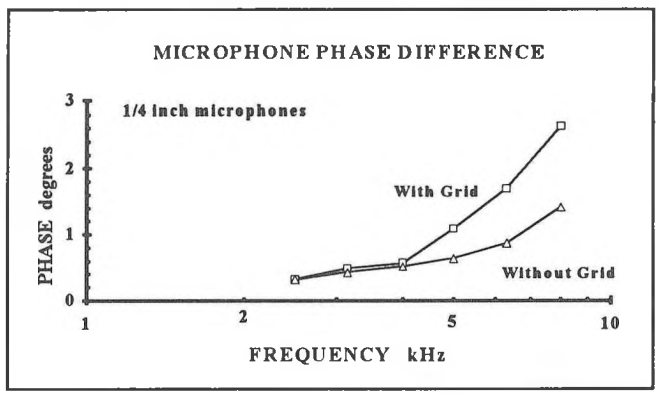


## 5. CONCLUSION

Special precautions have to be taken during precision phase match of microphones. Depending on the applications of the matched microphones, the protective grids have some influence on the phase match data.

## 6. REFERENCES

[1] G. S. K. Wong, "Precision method for phase match of microphones," J. Acoust. Soc. Am. **90**, September (1991).

[2] G. S. K. Wong, "Microphone phase response measurement methods," Inter-noise91 Proceedings, **2**, 1045-1048, Sydney (1991).

# EFFECT OF NOISE FIELD AND ARRAY CONFIGURATION ON MATCHED-FIELD PROCESSING IN UNDERWATER ACOUSTICS

*Peter Brouwer*[1] *John M. Ozard*[2]

[1]Datavision Computing Services Ltd., 1545 Pandora Ave., Suite 203 Victoria B.C. V8R 6R1
[2]Defence Research Establishment Pacific, FMO Victoria B.C. V0S 1B0

## ABSTRACT

The performance that can be achieved using Matched-Field Processing (MFP) depends on the nature of the ambient noise and the array configuration used to measure the field. In this paper, computer simulations were used to estimate MFP performance for an underwater source in different ambient noise fields and for different array configurations. Best MFP performance was obtained in a thermal ice cracking noise field and poorest performance in a fishing boat noise field. For arrays with fewer than 40 sensors in a surface noise field, best localization was obtained with a vertical array geometry. With more than 40 sensors, billboard arrays (composed of multiple vertical line arrays) outperformed horizontal line arrays which in turn outperformed vertical line arrays.

## 1. INTRODUCTION

Matched-Field Processing (MFP) may be employed for the passive detection and localization of underwater acoustic sources [1, 2, 3]. In MFP, the measured or predicted acoustic field due to a source is matched with a replica of the field for all possible source positions.

In this paper, we describe the results of computer simulations used to evaluate MFP performance in different ambient noise fields and for different array configurations. Models have been developed to represent three types of ambient noise field: noise generated by surface waves over an infinite half space [4], 'modal noise' generated by a large number of fishing boats in a shallow water waveguide, and Arctic noise generated by thermal ice cracking in a waveguide.

## 2. THEORY

### 2.1. Noise Modeling

The acoustic field generated by surface waves was modeled using the classical surface noise model developed by Cron and Sherman [4]. This model was used as a reference for comparison with the other two noise models.

Ambient noise, as might be generated by a large number of fishing boats, was modeled by including 100 widely distributed sources at a depth of 1 m in all simulations. The Arctic thermal ice cracking noise model was similar to the fishing boat noise model, except that the noise sources were impulsive.

### 2.2. Signal Processing

Matched-Field Processing (MFP) consists of matching the measured noisy field and a model or replica of the field at a single frequency. This is achieved by forming the covariance matrix of the data after Fourier transformation. The eigenvalues and eigenvectors of the covariance matrix are used for the matching or beamforming. A Minimum Variance (MV) beamformer, which is characterized by low sidelobes and high resolution, was employed.

## 3. GEOACOUSTIC MODEL

A range-independent geoacoustic model was used in this study to represent a shallow water Arctic environment with a high speed (2000 m/sec) bottom and a water depth of 500 m. The water was covered by a 6-m ice layer and had an upward refracting sound speed profile.

A normal mode model was used to represent the acoustic propagation for all cases simulated except the surface noise. Normal modes are a good approximation for signals whose ranges are large compared with the depth of the waveguide. The waveguide supported 12 modes at a source frequency of 24 Hz.

## 4. SIMULATION CONDITIONS

MFP was performed on simulated data for a source in the shallow water waveguide described in Section 3. For N sensors the simulations employed 3N averages to form the covariance matrix at a signal-to-noise ratio (SNR) of -10 dB. A 24-Hz target at 151 m depth and 25 km range was used for simulation. Ambient noise due to surface waves, fishing boats or thermal ice cracking was also included. Spatially white noise (at 20 dB below the signal level) was added to the simulations as a realistic component usually present which also stabilizes the covariance matrix for processing.

## 5. SIMULATION RESULTS

The ambiguity surfaces for a 16-element equispaced vertical line array (VLA) in three different noise fields are shown in Figure 1. The VLA extended from a depth of 50 m to the bottom of the waveguide. The target at a depth of 151 m and a range of 25 km can be readily recognized in the plots for the surface and thermal ice cracking ambient noise fields. For the fishing boat ambiguity surface, the target peak is masked by sidelobes or matches with the localized ambient noise sources i.e. fishing boats. Array gain for the array in fishing boat noise was 10 dB below that for

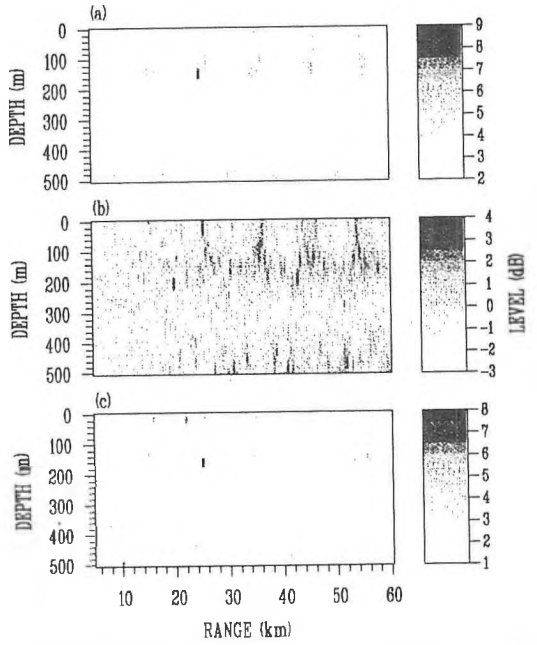


Figure 1. MV ambiguity surfaces for a 475-m-long 16-sensor equispaced VLA in: (a) surface noise, (b) fishing boat noise, and (c) thermal ice cracking noise.

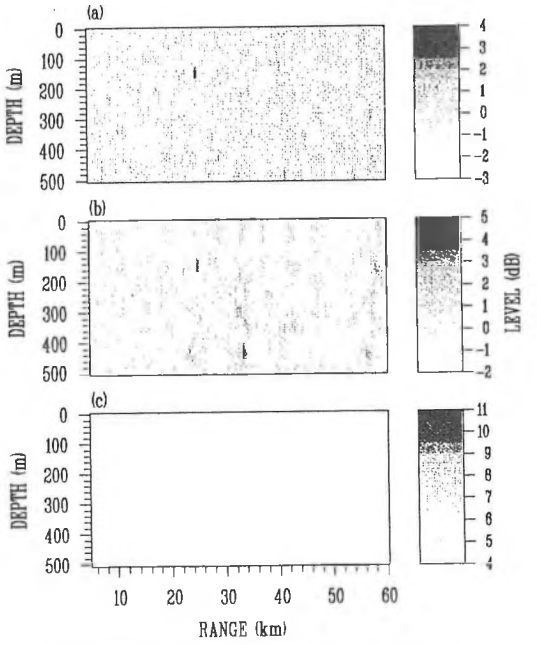


Figure 2. MV ambiguity surfaces for a 16-km-long 16-sensor equispaced HLA in: (a) surface noise, (b) fishing boat noise, and (c) thermal ice cracking noise.

the other two noise fields. Better MFP performance was obtained for thermal ice cracking noise than for fishing boat noise because the former is comprised of impulsive noises which last only for a single snap-shot in time. The impulsive nature and the infrequency of the impulses reduces the contributions to the cross-terms of the covariance matrix that are present in the other two models.

The ambiguity surfaces for a 16-km-long bottom-mounted horizontal line array (HLA) with 16 sensors, with the target at 45° to broadside, and for the same conditions as for Figure 1 is shown in Figure 2. Best performance for the HLA is achieved in thermal ice cracking noise. Because the HLA is able to discriminate noise in bearing, which is not discernable from a range-depth ambiguity plot, higher gains were obtained in the horizontally anisotropic fishing boat noise and thermal ice cracking noise fields than with the VLA.

MFP performance of vertical, horizontal and billboard arrays in surface noise was evaluated as a function of the number of sensors. The billboard arrays (BBA) were constructed from multiple 16-sensor VLAs and spanned a horizontal distance of 4 km. For high SNRs or large time-bandwidth products vertical array performance (array gain and peak-to-sidelobe ratio) reached a maximum at 16 sensors and remained constant beyond 16 sensors, indicating that the modes are properly sampled with a 16-sensor VLA. The performance of horizontal arrays continued to increase as more sensors were added: array gain increased by about 3 dB for each doubling of the number of sensors. For arrays of fewer than about 40 sensors, better localization was obtained with a vertical array geometry than with either a horizontal geometry or billboard geometry. BBAs with more than 40 sensors outperformed HLAs which in turn outperformed VLAs.

Simulations showed a degradation in vertical array performance with a decrease in array length. Similarly, performance of horizontal arrays and billboard arrays deteriorated with a decrease in horizontal array span.

## 6. CONCLUSIONS

Simulations showed that the best MFP performance was obtained in a thermal ice cracking noise field and poorest performance in a fishing boat noise field. Performance was evaluated for billboard, horizontal line arrays and vertical line arrays for MV processing in surface noise. With fewer than 40 sensors, best localization was obtained with a vertical array geometry. With more than 40 sensors, billboard arrays outperformed horizontal line arrays which in turn outperformed vertical line arrays.

## REFERENCES

[1] H. P. Bucker, "Use of calculated sound fields and matched-field detection to locate sound sources in shallow water", J. Acoust. Soc. Am. **59**, 368-373 (1976).

[2] J. M. Ozard, "Matched-field processing in shallow water for range, depth, and bearing determination: Results of experiment and simulation", J. Acoust. Soc. Am. **86**, 744-753 (1989).

[3] P. Brouwer, "MFP performance for various array configurations", DREP Contractors Rep. Ser. 91-19 (June 1991).

[4] B.F. Cron and C.H. Sherman, "Spatial-correlation functions for various noise models", J. Acoust. Soc. Am. **34**, 1732-1736 (1962).

# TRAINS, PLANES, & FISHING BOATS: A GEOPHONE SENSOR FOR UNDERWATER ACOUSTICS

**David M.F. Chapman**
Defence Research Establishment Atlantic, P.O. Box 1012, Dartmouth, N.S., B2Y 3Z7

## 1. Introduction

Usually, ocean acousticians use hydrophones (i.e. pressure sensors) for very-low-frequency measurements, either placed on the seabed or suspended in the water. Occasionally, we use transducers that sense the particle velocity associated with the acoustic wave in the water. In recent years, some investigators[1] have been using geophones (i.e. velocity sensors) coupled to the seabed itself. Geophones measure the motion at the seabed, which can be different from that in the adjacent water mass. In particular, geophones—unlike hydrophones—can sense the propagation of shear waves in the seabed. Seismologists have been using geophones in their Ocean Bottom Seismometer (OBS) packages for years. This paper describes the configuration, testing, and calibration of an OBS for underwater acoustic experiments.

## 2. Description of the OBS package

The geophones are shown in Fig. 1, installed in a gimbal mount. The gimbals are suspended in a frame attached to one end-cap of the cylindrical pressure vessel that houses the OBS. The gimbals are necessary to ensure that the vertical geophone is aligned with the direction of gravity and that the horizontal geophone is aligned in a perpendicular direction, as the two sensors are constructed differently. Also shown are the slip-rings that carry the geophone signals to the geophone preamps and the printed circuit board containing the preamps. The principal component of these is the LT1028 operational amplifier chip, which has an extremely low noise level.

**Figure 1** *The geophones mounted in gimbals on the OBS endcap. Note the slip rings and the preamps.*

A typical geophone consists of an electric coil and mass suspended by a spring in a magnetic field that is fixed to the body reference frame. Relative velocity between the case and the mass/coil creates an EMF that drives a current through the output load. The mass/spring system has a resonance frequency, above which the response is flat and below which the response decreases rapidly. There is little natural damping in the system; the system Q is controlled by a shunt resistor in parallel with the input resistance of whatever amplifier is used.

## 3. Calibration and Testing

When simply measuring the time-of-arrival of an impulsive signal—a typical OBS task—the sensitivity and self-noise level are not major considerations. However, for underwater acoustic measurements of ambient noise and propagation loss, we must ensure that the sensor self-noise level is well below the ambient noise level and that we accurately calibrate the sensor sensitivity over the frequency band of interest.

During a previous OBS deployment, we used preamps that were too noisy and we could not measure ambient noise. Fig. 2 shows the noise level at the input of the new preamps for three cases: the amplifier input shorted; the geophone attached electronically but with the motion clamped; and the geophone sitting on land in a quiet state. We are satisfied that we can measure ambient noise with this new arrangement.

We calibrated the vertical geophone using a shaker table, an accurate voltmeter, and a reference B&K accelerometer. We kept the geophone in the gimbal and frame as shown in Fig. 1 in order to account for the transfer function of the mounting method. With a 1.8 kΩ shunt resistor across the coil outputs, the geophone sensitivity above the resonance frequency of 4.5 Hz is 31 dBV re 1 m/s. At resonance this rises slightly to 34 dBV. Below resonance the response falls off at 40 dB/decade.

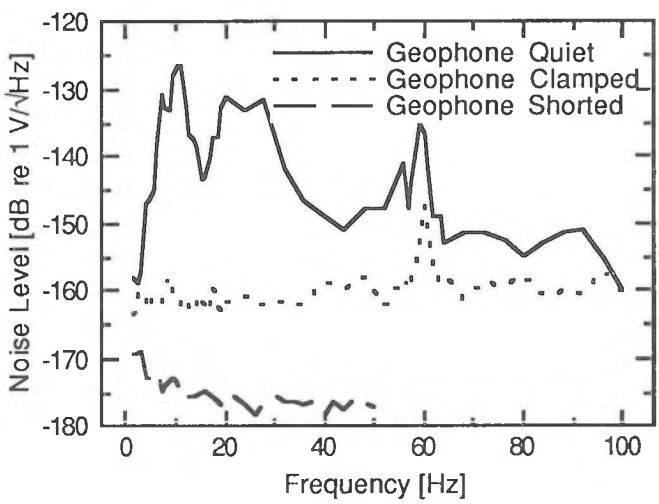


**Figure 2** *Noise levels at preamp input.*

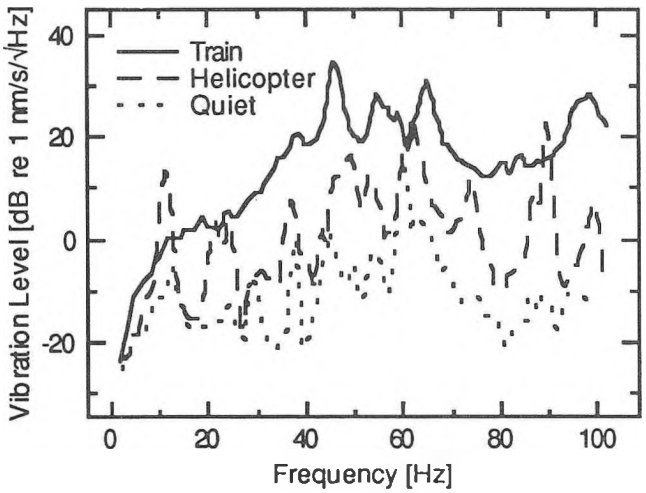


**Figure 3** *Noise spectra received at the vertical geophone from two sources of opportunity.*

## 4. Detection of Sources of Opportunity

While testing the OBS at a quiet location on land (the basement of a DREA building at 0600 one Sunday morning), we had the opportunity to observe signals from two sources of opportunity. The first was a train passing the sensor location at a distance of about 50 metres; the second was a low-flying helicopter at a range of several hundred metres. Fig. 3 shows noise spectra from the two sources, compared with a "quiet" noise spectrum. Note that the reference velocity is 1 nanometre per second and we have used a constant calibration factor of 31 dBV re 1 m/s.

The last example is from a deployment of the OBS on the seabed in 75 m of water. Although we experienced some difficulties on this trial (such as the failure of the horizontal geophone), we were fortunate to record signals from a stern trawler travelling at constant speed on a steady heading that brought it within 2 kilometres of the OBS. Also, there were several noisy whales in the vicinity. Fig. 4 shows a sonogram of the vertical geophone signals: the x-axis is frequency, the y-axis is time, and the grey level represents signal amplitude. One can see broadband noise (the curved swaths of grey) and narrowband signals (vertical lines) from the ship, and the whale sounds (short horizontal lines near 20 Hz).

## 5. Conclusions

Although the geophone sensors have presented us with some challenging electronic and mechanical problems to solve, these initial results are encouraging. We have been able to receive and record signals from several interesting sources. In future experiments we hope to compare the acoustic performance of geophone sensors with that of hydrophone sensors.


## Acknowledgment

Many thanks to Dave Heffler of the Atlantic Geoscience Centre, Bedford Institute of Oceanography, for the loan of the OBS.


[1] Jens M. Hovem, Michael D. Richardson, and Robert D. Stoll, *Shear Waves in Marine Sediments* (Kluwer Academic Publishers, Dordrecht, 1990).

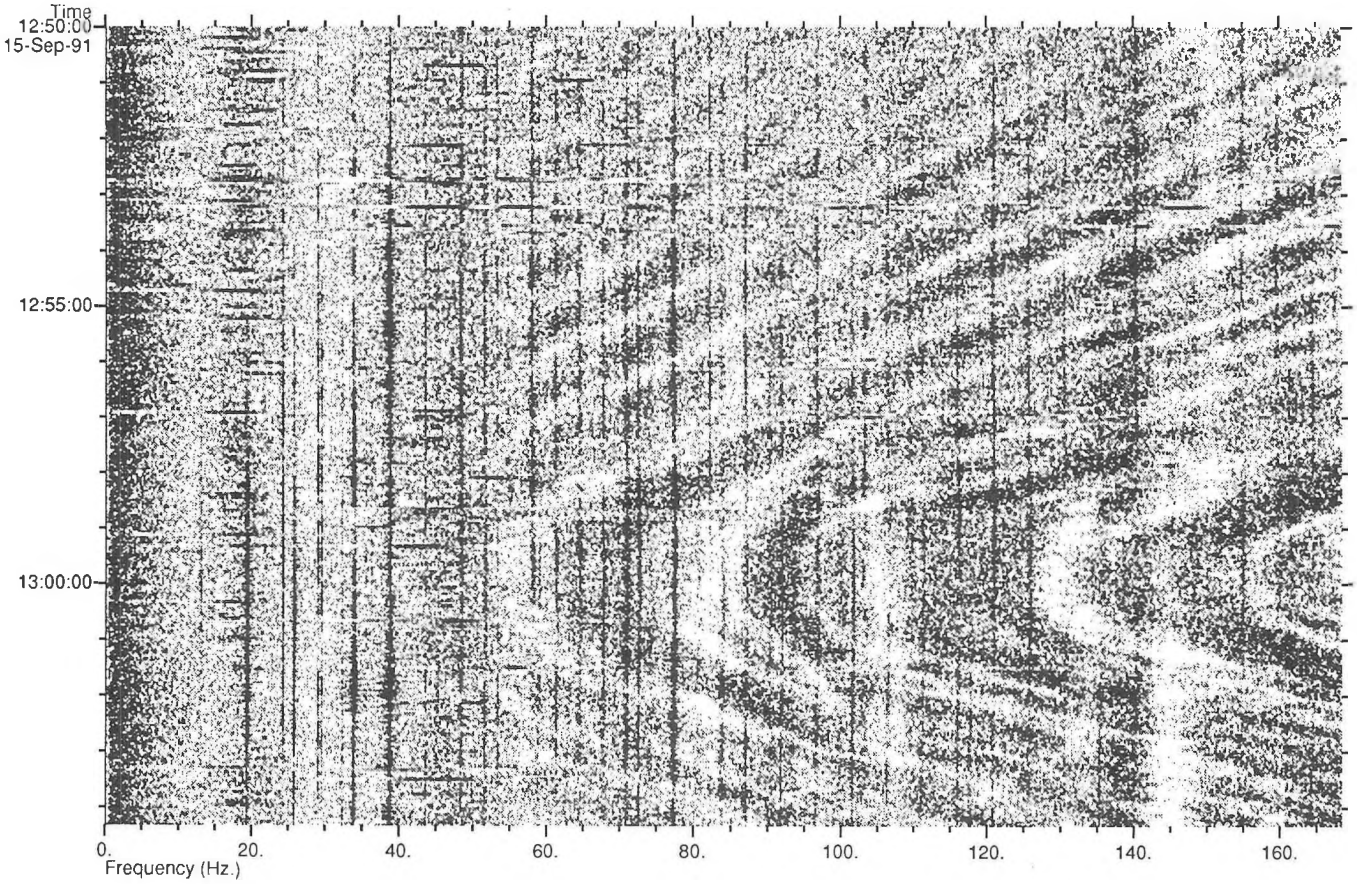


**Figure 4** *Sonogram of the signal received from a stern trawler at the vertical geophone on the seabed in shallow water.*

# Separation of Acoustic Multipaths in Saanich Inlet

Daniela DiIorio[1] and David M. Farmer[1,2]
1. Dept. of Physics, University of Victoria, Victoria, B.C., CANADA.
2. Institute of Ocean Sciences, Sidney, B.C., CANADA.

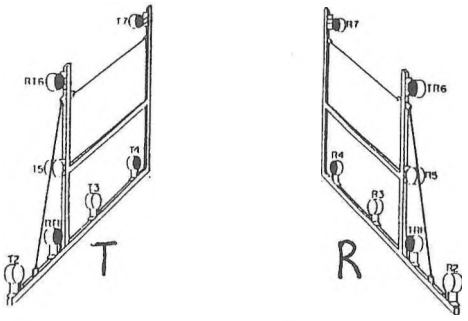


Figure 1: Acoustic array configuration deployed at 35 metres during the experiment.

## 1 Introduction

Acoustical scintillation measurements can provide a basis for determining the properties of ocean structure in coastal waters and can be used as a tool to remotely measure oceanographic processes (e.g. current and turbulent structure) which differ markedly from processes in the open ocean. A scintillation experiment in 1989 was carried out in a coastal environment in British Columbia, Canada in order to relate acoustic characteristics to the oceanography.

The experimental site was Saanich Inlet which is a deep (220 m), quiescent (maximum currents 10 $cm \cdot s^{-1}$) and stratified fjord. Our goal is to compare acoustic propagation through this relatively undisturbed, coastal environment with previous measurements in a turbulent tidal channel (Farmer *et.al.* [2]).

Figure 1 shows the two dimensional square array configuration used (2 metre spacing between darkened transducers). The arrays were deployed at 35 metres depth. Each transducer is directional with a beam width of 10 degrees at -3dB.

The 67 kHz acoustic signal used in the Saanich Inlet experiment made use of a 127 bit phase modulated pseudo-random-noise (PRN) code so as to improve the signal to noise ratio. The bit width of the code was chosen so that multipaths separated in arrival time by about $300\mu s$ ($20 cycles$) could be distinguished. The matched filter output of the PRN code produces a well known triangular peak shape.

The transmitter array cycles through all four transducers 5 times each second. The incoming signals at the receiver are filtered, amplified and then separated into in-phase ($I$) and quadrature ($Q$) components. Each is then correlated with a stored PRN template of the transmitted signal. The matched filter output shows a series of peaks corresponding to different signal paths. The amplitude ($A = \sqrt{I^2 + Q^2}$) and

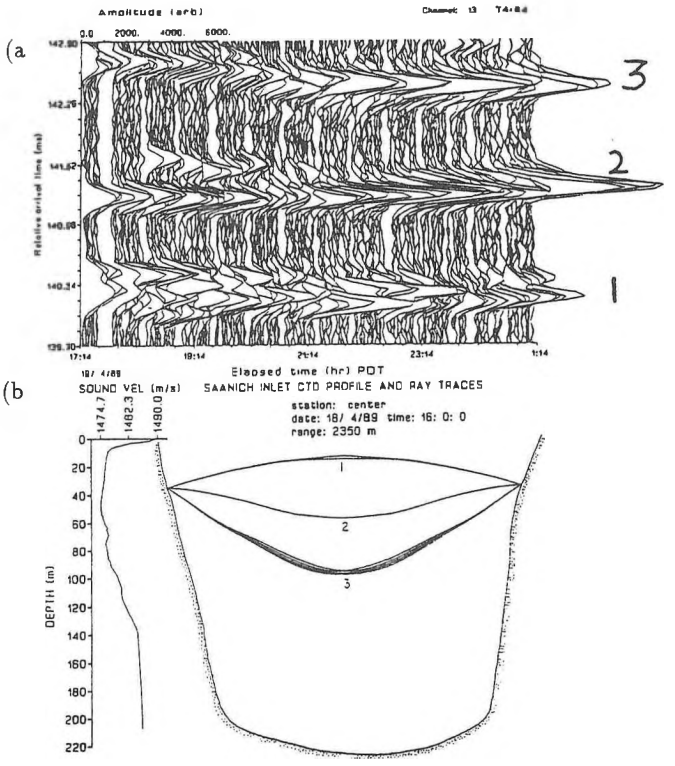


Figure 2: (a) Acoustic amplitude measured as a function of relative arrival time and as a function of elapsed time. (b) Averaged sound speed profile with the corresponding acoustic eigenrays.

arrival time ($\tau$) are determined using a maximum likelihood procedure. The phase $\phi$ is then defined as $\arctan[\frac{Q(\tau)}{I(\tau)}]$. The arrival time $\tau$ is used to resolve the $360^o$ phase ambiguity.

## 2 Multipath Analysis

The acoustic observations in Saanich Inlet show multipath propagation conditions. Figure 2(a) shows the measured amplitude (in arbitrary units) as a function of relative arrival time (3 ms total) and as a function of elapsed time. The figure represents 8 hours of sub-sampled data (75 second intervals). Three distinct acoustic paths are present and they correspond to the eigenrays shown in figure 2(b). These rays are obtained using a simple range independent ray tracing algorithm.

The first set of arrivals is refracted upwards into the near surface because of the shallow thermocline. The second ar-

rival, although appearing to have a well defined peak, is actually a superposition of several overlapping multipaths. It is this path that will be studied in closer detail. The third set of arrivals clearly show phase variations related to the internal tide that exists at 100 metres and beyond.

In order to separate the multipaths observed in the preliminary analysis, a maximum likelihood estimation algorithm is developed following Ehrenberg *et.al.* [1]. The mathematical model for the received signal $r(t)$ is,

$$r(t) = \sum_{i=1}^{N} A_i s(t - \tau_i) + n(t) \tag{1}$$

where $A_i$ and $\tau_i$ are the amplitude and arrival times for the $i^{th}$ path and $n(t)$ is the noise. The signal $s(t)$ is known since it is the matched filter output (c.f. Menemenlis and Farmer [3]):

$$s(t - \tau) = \sum_{n=0}^{9} a_n \left( \frac{t - \tau}{\tau_p} \right)^{2n}, \tag{2}$$

where $a_n$ are known coefficients and $\tau_p$ is the half-width of the correlation peak (= 1 bit = 3 samples). This function is triangular with a rounded apex.

The maximum likelihood estimation is derived as follows: minimize

$$Q = \sum_t \left[ r(t) - \sum_{i=1}^{N} A_i s(t - \tau_i) \right]^2, \tag{3}$$

$$= \sum_t r(t)^2 - 2 \left[ \sum_{j=1}^{N} A_j C(\tau_j) - \frac{1}{2} \sum_{j=1}^{N} A_j \sum_{k=1}^{N} A_k B(\tau_j, \tau_k) \right], \tag{4}$$

with respect to $A_i$ and $\tau_i$. Minimizing $Q$ implies that the second term on the right of the last equation should be maximized. That is,

$$\text{maximize} \quad P = \mathcal{C}^T \mathcal{A} - \frac{1}{2} \mathcal{A}^T \mathcal{B} \mathcal{A} \quad \text{w.r.t. } A_i \text{ and } \tau_i, \tag{5}$$

where $C(\tau_j) = \sum_t r(t) s(t - \tau_j)$ is the cross covariance between the received and modelled signal, and $B(\tau_j, \tau_k) = \sum_t s(t - \tau_j) s(t - \tau_k)$ is the auto covariance between the modelled signals. This maximization problem is written in matrix form where

$$\mathcal{A}^T = (A_1, A_2, ..., A_N), \tag{6}$$

$$\mathcal{C}^T = (C(\tau_1), C(\tau_2), ..., C(\tau_N), \tag{7}$$

$$\mathcal{B} = \begin{bmatrix} B(\tau_1, \tau_1) & B(\tau_1, \tau_2) & ... & B(\tau_1, \tau_N) \\ B(\tau_2, \tau_1) & B(\tau_2, \tau_2) & ... & B(\tau_2, \tau_N) \\ . & . & . & . \\ B(\tau_N, \tau_1) & B(\tau_N, \tau_2) & ... & B(\tau_N, \tau_N) \end{bmatrix} \tag{8}$$

Maximizing with respect to each of the $A_i$ yields,

$$\mathcal{A} = \mathcal{B}^{-1} \mathcal{C}. \tag{9}$$

Substituting into equation [5] gives the following maximization problem,

$$\text{maximize} \quad [\frac{1}{2} \mathcal{C}^T \mathcal{B}^{-1} \mathcal{C}] \quad \text{w.r.t. } \tau_i. \tag{10}$$

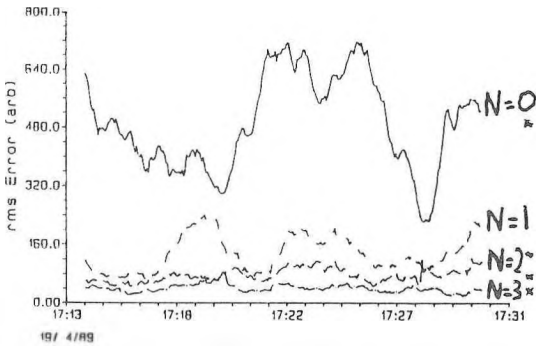


Figure 3: Integration of the noise for an assumed number of paths $N$. The integrated signal level is shown for $N = 0$. Averages are shown as an $*$ on the far right side.

Therefore, to determine the maximum likelihood estimate, equation [10] must first be maximized with respect to the arrival time estimates. This equation is in a quadratic form and is a function of N independent variables and so maximization occurs over an N dimensional space. Powell's quadratically convergent method [4] is used for this procedure. The resulting set of arrival time estimates are then used in equation [9] to obtain the amplitude estimates.

In deriving the maximum-likelihood estimate it is assumed that the number of paths $N$ is known and fixed. The number of paths chosen is $N = 3$. This is because the arrival time integration of the noise calculated for $N = 0, 1, 2, 3$ multipaths (see figure 3) gives the correct noise level for $N = 3$.

# 3 Conclusions

Now that we have separated the overlapping multipaths, we are in a position to use the amplitude and phase measurements in a variety of ways to contribute to our understanding of acoustic propagation in this environment. For example, the phase difference between vertical and horizontal receivers can be used to detect the angle of arrival of the acoustic waveform. Cross correlation techniques can be implemented in order to determine the current component perpendicular to the direction of propagation as well as give some indication of the coherence length scales.

# References


[1] Ehrenberg, J.E., Ewart, T.E. and Morris, R.D., "Signal processing techniques for resolving individual pulses in a multipath signal". *J.A.S.A.* **63**(6), 1978, pp. 1861-1865.

[2] Farmer, D.M., Clifford, S.F. and Verrall, J.A., "Scintillation Structure of a Turbulent Tidal Flow". *J. Geophy. Res*, **92**(C5), 1985, pp 5369-5382.

[3] Menemenlis, D., and Farmer, D.M., "Acoustical measurements of current and vorticity beneath ice". *J. Atmos. Oc. Technol.*, in press.

[4] Press, W.H., Flannery, B.P., Teukolsky, S.A. and Vetterling, W.T., Numerical Recipes - The Art of Scientific Computing. Cambridge University Press, 1986, pp 294-301.

# ON THE ACOUSTICAL INTENSITY OF BREAKING WAVES

Li DING[1,2]
1. Dept. of Electrical and Computer Engr.
University of Victoria
Victoria, B. C., Canada

David FARMER[2]
2. Institute of Ocean Sciences
Sidney, B. C., Canada

## INTRODUCTION

Breaking surface waves have been identified as the main source of wind-generated ambient sound in the ocean[1]. The sound radiated from breaking waves has been used to track these waves and measure their spatial and temporal statistics[2]. Recent laboratory work[3] has further suggested that the acoustic power released by breaking waves is correlated with the energy dissipation due to breaking. In this paper, we perform statistical analysis of the acoustic intensity of breaking waves measured in the open ocean and discuss the potential use of the result in remote measurement of wave energy dissipation.

## OBSERVATION

Our observations were made during the Surface Wave Process Program, in February/March 1990. Breaking waves were tracked with a hydrophone array deployed at a depth of 25 m beneath the ocean surface. For each tracked breaking wave, its position, velocity and duration were determined using the correlation technique discussed in Ref. 2. Previous analysis[4] has suggested that breaking waves radiate sound predominantly over the range 100 – 500 Hz. We therefore calculated a time series of acoustic power in this frequency band from one hydrophone, as shown in Fig. 1. Occurrences and locations of breaking waves during this period were simultaneously tracked. The horizontal bars on the top of the figure indicate the period of each tracked event, and the received acoustic intensity from each of these individual events can be found in this time series. However, the background noise intensity should be subtracted from the total intensity $I_A$, to obtain the actual received intensity from the event. Due to the nonstationarity of ambient noise over a longer period, the noise intensity must be estimated locally. For each event, we search for a local minimum within the neighbourhood of the instant of occurrence, and the corresponding noise intensity $I_N$ is estimated at the location of the minimum (Fig. 1). The actual received intensity from the event is given by $I = I_A - I_N$.

The acoustic intensity of breaking waves at 1 m distance is then calculated by assuming a dipole radiation pattern and neglecting aborption. Such calculations were performed over a period of 30 min in an area of radius 40 m. The estimated distribution of the source intensity (in dB) based on all the tracked events is given in Fig. 2. The source intensity is also shown against the travel speed of the breaking events in Fig. 3, where a low speed cutoff is imposed to reduce noise interference and the effect of swell advection on low event speeds. There is considerable scatter in the data (correlation coefficient r=0.37), possibly caused by lack of dipole radiation from a rough surface, or at least, tilting of dipole sources. The least squares fit is difficult to apply in this case. Nevertheless, a principal component analysis of these data shows that the two eigenvalues of the scatter matrix are $\lambda_1 = 1.37$ and $\lambda_2 = 0.63$ respectively, and that in the principal direction corresponding to $\lambda_1$ (as shown in Fig. 3), the source intensity is proportional to the 2.33 power of the breaking event speed.

## DISCUSSION

The travel speed of breaking waves represents the scale of breaking which can be related to energy dissipation due to breaking.[5] Thus the result in Fig. 3, within the limits of the low correlation, shows that the acoustic power released by individual breaking waves increases with the amount of dissipated energy. More direct evidence supporting the above observation comes from recent laboratory work using colliding plane waves that demonstrated that the acoustic power radiated by a breaking wave is proportional to the energy dissipated due to breaking[3]. The dissipated energy is proportional to the difference of the upstream and downstream surface displacement variances ($a_1^2$ and $a_2^2$ respectively) of the breaking wave. Note that the acoustic power radiated from a source is proportional to the source intensity at 1 m distance, $I_0$. Therefore, by accepting the laboratory observation, we

have

$$I_0 \sim E_{dis} \sim a_1^2 - a_2^2.$$

It is well known that the distribution of wave amplitude is closely Rayleigh[6], and hence $a^2$ is found to be exponentially distributed. Assuming $a_1^2$ and $a_2^2$ are independent with the same exponential distribution, it can be shown that $z = (a_1^2 - a_2^2) \geq 0$ is also exponentially distributed. Therefore we expect that $I_0$ has an exponential distribution[7]. In order to facilitate comparison between the data and this model, we make a transformation $x = 10 \log_{10} I_0$ to reduce the dynamic range of $I_0$. The resulting distribution of $x$ is found to be

$$f_x(x) = \alpha e^{-\alpha\beta} \exp\{\alpha x - e^{\alpha(x-\beta)}\} \qquad (1)$$

where $\alpha = \ln 10/10$ and $\beta = 10 \log_{10} \bar{I}_0$.

Equation (1) is then fitted to the data in Fig. 2, where the resulting curve is also plotted. It can be seen that the fit is fairly good in general, though deviations from the curve due to statistical errors must exist. Consequently this result appears to support the hypothesis that the acoustic power released by breaking waves is proportional to the dissipated wave energy.

In summary, observations of the acoustic intensity statistics of individual breaking waves in the ocean appear to be consistent with the dependence of the radiated acoustic power on the dissipated wave energy obtained for the special case of colliding plane waves in the laboratory. This suggests that energy dissipation by wave breaking at the ocean surface may be probed by using ambient sound.

*Acknowledgement:*This work was funded by the Canadian Panel on Energy Research and Development and the U.S. Office of Naval Research. Li Ding was supported by a University of Victoria Fellowship.

## References

1. Kerman, B. R., 1984: *J. Acoust. Soc. Am.* 75, pp149-165
2. Ding, L. and D. M. Farmer, 1992: *J. Atmos. Oceanic Technol,* Vol. 9, No. 4.
3. Loewen, M. R. and W. K. Melville, 1991: *J. Fluid Mech.* 224, pp601-623
4. Farmer, D. M. and L. Ding, 1992: *J. Acoust. Soc. Am.* 92, pp397-402
5. Phillips, O. M. 1991: *J. Fluid Mech.* 156, pp505-531
6. Longuet-Higgins, M. S., 1980: *J. Geophys. Res.* Vol 85, C3, pp1519-1523
7. Ding, L. and D. M. Farmer, 1992: *Proceedings of the 14th International Conference on Acoustics*, Beijing, September 3-10

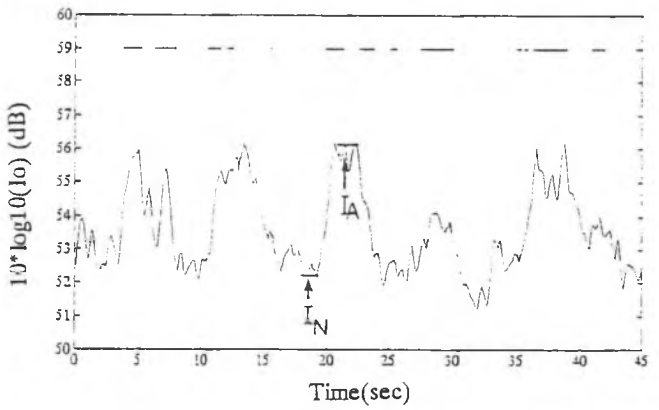


Figure 1: Time series of acoustic power in arbitrary unit. The horizontal bars indicate the occurrences of breaking waves.

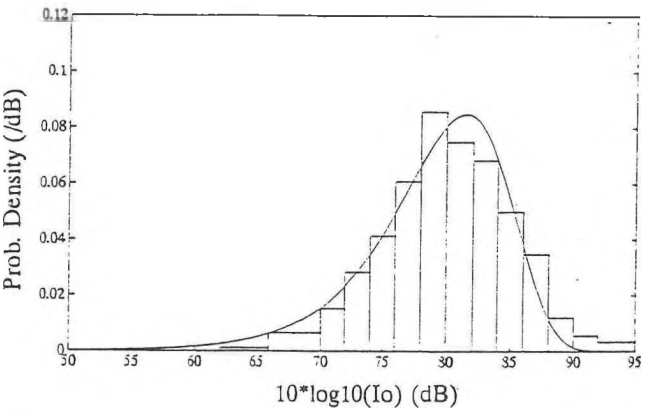


Figure 2: Probability distribution of acoustic source intensity of breaking events. The curve is Eq. (1) with $\beta$ obtained using the least squares fit.

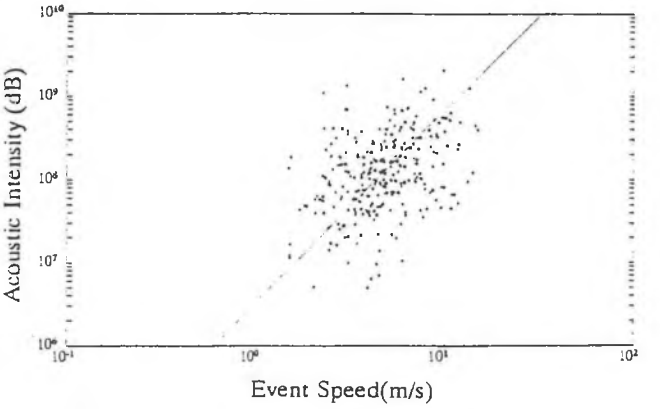


Figure 3: Acoustic source intensity of breaking events against the event speed. The straight line is in the principal direction corresponding to the higher eigenvalue.

# IT'S A SMALL WORLD: UNDERWATER SOUND TRANSMISSION FROM THE SOUTHERN INDIAN OCEAN TO THE WESTERN NORTH ATLANTIC

**Ian A. Fraser and Peter D. Morash**
Defence Research Establishment Atlantic, P.O. Box 1012, Dartmouth, N.S., B2Y 3Z7

## 1. Introduction

Sounds transmitted through the air are rarely detectable more than a few kilometres from their source. Beneath the sea, however, acoustic signals at frequencies less than a few hundred Hertz can often be detected at ranges of several thousand kilometres. In this paper we show that low-frequency acoustic signals entering the ocean near Heard Island in the southern Indian Ocean can be detected off the east coast of North America and that relatively crude modelling is sufficient to reproduce the signal levels observed, despite the long path length of approximately 17,000 km (17 Mm).

## 2. Experimental Details

Although the main purpose of the Heard Island Feasibility Test (HIFT) was to evaluate the concept of using travel-time variations of sound over long base lines in the ocean as a sensitive test of global warming, this topic is adequately covered elsewhere (e.g., in Ref. 1). In this initial look at the east-coast Canadian data we are primarily concerned with the measurement and modelling of signal levels. The measurements were performed using a research array of hydrophones towed behind the Defence Research Establishment Atlantic (DREA) research vessel CFAV QUEST while in transit to its home port of Halifax. The measurement sites are denoted by the solid circles in Fig. 1.

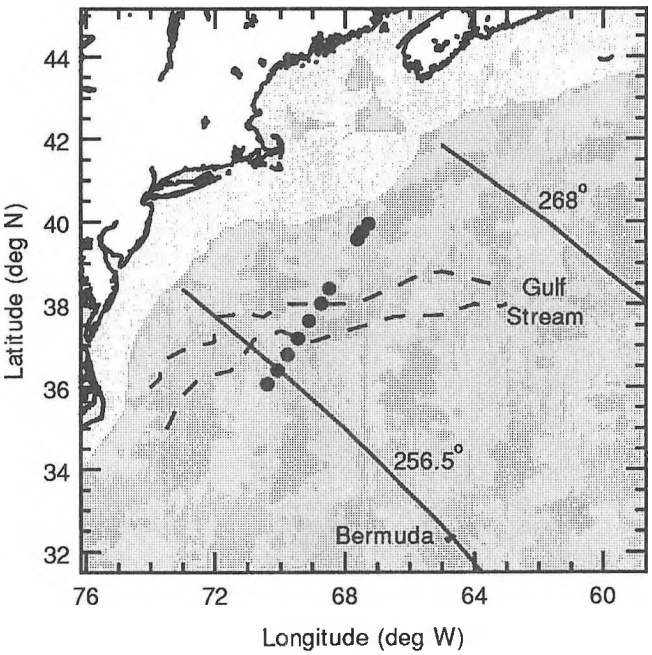


Figure 1 *Experimental area and ray paths from Heard Island.*

Figure 1 also includes the location of the Gulf Stream (dashed lines) and two ray paths from the 57 Hz source near Heard Island (the noted angles refer to emission angles at the source for these two rays). The lighter of the two grey levels denotes shallow water (less than 200 m deep). Because of shadowing by Bermuda, South America, and Africa, significant signal levels from Heard Island were expected to be found only between the two limiting rays shown in Fig. 1.

Vertical profiles of sound speed obtained from temperature measurements by QUEST are presented in Fig. 2 as a function of range along ray paths from Heard Island measured from the nominal northern boundary of the Gulf Stream. The distance of each profile from the boundary is denoted by the vertical bar near the bottom of the figure. The sound-speed scale at the top of the figure is the same for each profile, with a reference value of 1.5 km/s located directly above the range marker in each case. On crossing the Gulf Stream, the sensors moved from the warm water of the Sargasso Sea into much colder "slope" water. The dashed line shows the rapid decrease in depth of the sound speed minimum as the boundary was crossed.

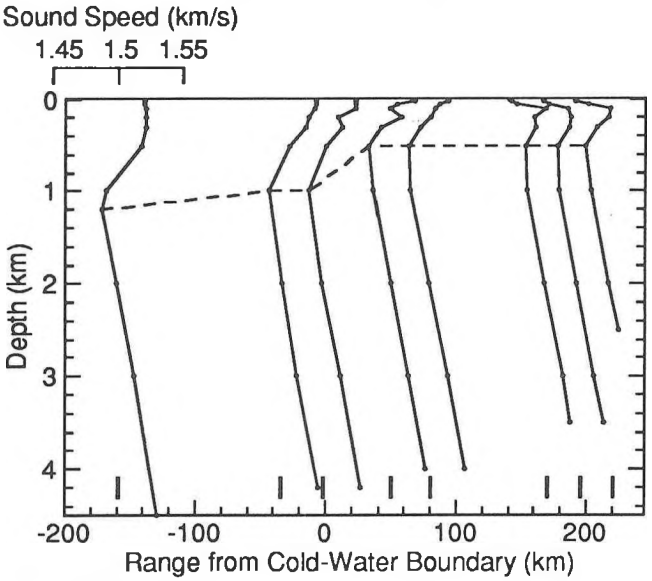


Figure 2 *Sound speeds measured near and in the Gulf Stream.*

Acoustic energy above the sound-speed minimum in Fig. 2 is refracted downward and energy below the axis is refracted upward, thereby creating a "sound channel". Sound trapped in this channel tends to follow the sound-channel minimum towards shallower depths north of the Gulf Stream. Since the sensors were being towed at depths close to 200 m, one would expect the detected signals to be stronger to the north of the Gulf Stream.

## 3. Transmission-Loss Modelling

The DREA normal-mode sound-transmission model PROLOS[2] was used to predict the strength of the 57 Hz Heard Island signal at the receiver. Since this model is "adiabatic" (i.e., no mode coupling is allowed), it works best in slowly changing environments. The environmental inputs for most of the acoustic path were obtained from bottom-contour charts and from a compendium of sound speeds[3]. More accurate environmental information was required near both ends of the track. Data on the source and on the nearby environment were supplied by Dzieciuch[4]. Environmental data at the receiver ranges were

collected by QUEST. Model estimates of transmission loss (decrease in signal level at the receiver range relative to the level 1 m from the source) for receiver depths of 200 and 900 m are compared in Fig. 3. (Note the change in horizontal scale at 16.6 Mm, near the cold-water boundary of the Gulf Stream.)

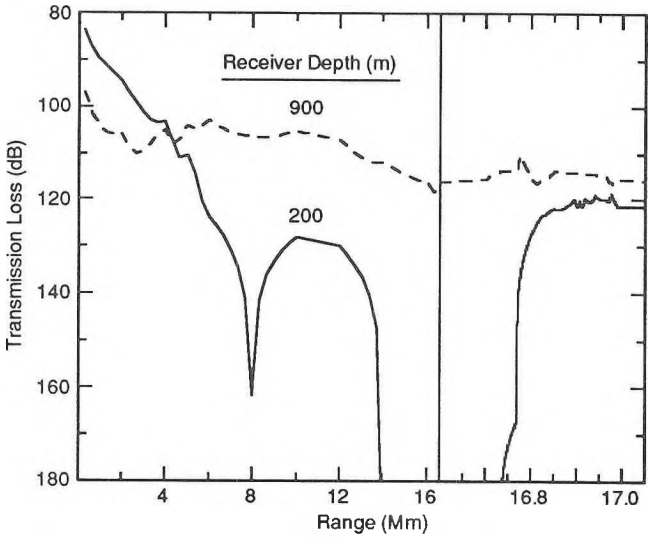


Figure 3 *PROLOS[2] model estimates of transmission loss.*

For the sensor depth of 200 m used in the experiment, the predicted transmission-loss (TL) increases rapidly at 14 Mm where the warm waters of the North Atlantic are first encountered. Between 16.7 and 16.8 Mm (near 0 km in Fig. 2), TL decreases again to levels comparable to simple "cylindrical spreading" as the receiver enters the cold water north of the Gulf Stream. The dramatic changes in TL predicted for a shallow receiver are not present at 900 m (dashed line in Fig. 3), since this depth lies much nearer the sound-channel minimum, where the signals propagating to long distances are concentrated.

The model estimates are compared with the measured TL values in Fig. 4, where the dots represent experimental data and the horizontal bars represent PROLOS-model estimates.

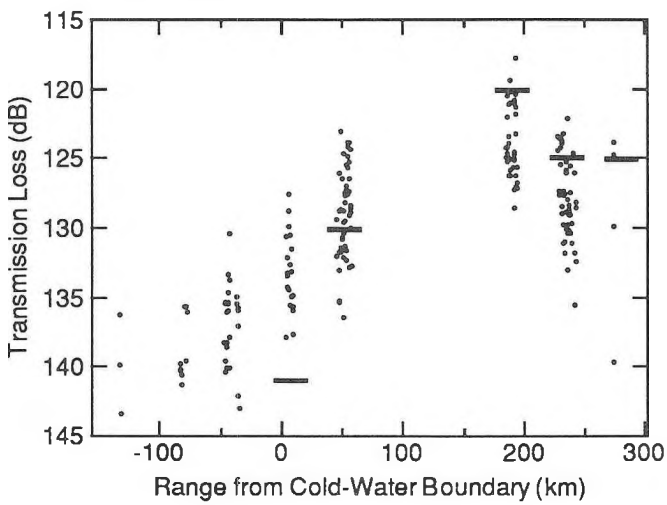


Figure 4 *Measured transmission loss.*

The maximum spectral-analysis resolution was 0.031 Hz; the resulting signal-to-noise ratio of the 57 Hz signal was typically about 10 dB. In the cold water north of the Gulf Stream (positive ranges in Fig. 4), the model and experimental mean values agree to within 3 dB. In and to the south of the Gulf Stream, the model values of TL increase rapidly, but the experimental data do not follow suit. The more gradual increase in experimental TL at negative ranges in Fig. 4 is believed to arise from the scattering of signal power from low-order modes concentrated near the sound-channel axis to higher-order modes that have significant amplitudes at the receiver depth. The scattering is attributed to interaction with the seabed, surface, and volume inhomogeneities along the sound path. PROLOS does not allow for this modal coupling, so it errs towards TL values that are too high. At still shorter ranges (not shown in Fig. 4) the 57 Hz HIFT signal was not detected, probably because of shadowing by Bermuda or South America (see Fig. 1).

## 4. Discussion

The good agreement between experimental and model transmission losses north of the Gulf Stream depends on the assumption of typical seabed properties at the source site. In that sense, then, we are examining the sea-bed acoustic properties near Heard Island by listening at a location southwest of Nova Scotia. Interaction with the seabed and surface in the intervening 17,000 km appears to become a significant factor only in and to the south of the Gulf Stream, where the receiver depth is ensonified only by boundary-scattered sound.

The HIFT projector source level of 200-210 dB re 1μPa@1m was at least 100 to 1000 times stronger than that normally generated by noisy merchant ships. Since ships usually control the ambient noise field near 57 Hz in the North Atlantic, and since absorption precludes long-range transmission at significantly higher frequencies, we can probably ignore contributions from the southern ocean to ambient noise in the North Atlantic.

## 5. Summary

The 57 Hz signals generated in the vicinity of Heard Island in January 1991 were readily detected near and in the Gulf Stream southwest of Nova Scotia at a depth near 200 m. The adiabatic normal-mode model PROLOS[2] provided good agreement with the experimental transmission loss over a 17 Mm path ending in the cold water north of the Gulf Stream. In warmer water, the model was unable to account for the relatively strong observed signal, probably because it does not include mode coupling.

## Acknowledgments

Our appreciation is extended to W.H. Munk for inviting DREA to participate in the Heard Island Feasibility Test.

---

[1]W. H. Munk, "The Heard Island Experiment," Naval Research Reviews **43**, No. 1, 2-22 (1991).

[2]D.D. Ellis, "A two-ended shooting technique for calculating normal modes in underwater acoustic propagation," Defence Research Establishment Atlantic, Dartmouth, NS, Canada Report 85/105, Sept 1985.

[3]*World Ocean Atlas Vol. 2: Atlas of the Atlantic and Indian Oceans,* edited by S.G. Gorshkov (Pergamon, New York, 1985).

[4]M.A. Dzieciuch (private communication).

# A TWO-COMPONENT ARCTIC AMBIENT NOISE MODEL

*Michael V. Greening*[1] *Pierre Zakarauskas*[2]

[1]Jasco Research Ltd., 9865 West Saanich Rd., Sidney B.C. V8L 3S1
[2]Defence Research Establishment Pacific, FMO Victoria B.C. V0S 1B0

## ABSTRACT

Short term Arctic ambient noise spectra over the frequency band 2 - 200 Hz are presented along with a two component noise model capable of reproducing these spectra. The model is based on the measured source spectrum and the spatial, temporal and source level distributions of both active pressure ridging and ice cracking. Modelled ambient noise levels are determined by summing the input energy of the distributions of ice cracking and pressure ridging events and removing the propagation loss. Both modelled and measured spectra show that ice cracking may dominate the spring-time ambient noise to frequencies as low 40 Hz with active pressure ridging dominating below this. Modelled results also show that over 80% of the total noise energy above 40 Hz produced by ice cracking is generated within 30 km of the receiving hydrophone while over 50% is generated within 6 km.

## 1. INTRODUCTION

The long term averaged ambient noise spectrum of the Arctic Ocean over the frequency band of 1 - 1000 Hz exhibits two broad peaks centered near 15 Hz and 300 Hz [1]. Two important factors for many sonar applications are the short term variability of the ambient noise spectrum and the spatial distribution of sources which comprise the ambient noise. This paper examines the short term fluctuations (2 min) of Arctic pack ice ambient noise spectra over the frequency band 2 - 200 Hz and relates these fluctuations to environmental conditions. A two component noise model incorporating both ice cracking and active pressure ridging is presented which is capable of reproducing the measured ambient noise spectra. This model shows the relative importance of each source term over the frequency band examined. Also shown is the maximum range required to model 80% (within 1 dB) and 50% (within 3dB) of the ambient noise created by ice cracking, thus indicating whether ambient noise generated by ice cracking is produced at close or far range.

## 2. AMBIENT NOISE MEASUREMENTS

The data analyzed in this paper were collected on the pack ice off the northern coast of Ellesmere Island over several days during April 1988. Details on the experimental setup and environmental conditions are available in other papers by the authors [2, 3].

A set of 69 two-minute samples of ambient noise were recorded approximately every 1.5 hours over 100 hours. At the end of this data collection period, a pressure ridge built itself approximately 2 km from the experimental site. Continuous ambient noise measurements were recorded for several hours during the time of this ridge building event.

The 69 two-minute samples of ambient noise recordings were separated into four distinct classes by examining their power spectra. Class one indicated a peak with a level of approximately 86 dB//$\mu$Pa at 8 Hz and a fall-off to 48 dB//$\mu$Pa at 200 Hz. Class two contained the same peak near 8 Hz but the fall-off at higher frequency had two stages with a rapid decrease in level out to 35 Hz and a slower decrease beyond 35 Hz to a level of 57 dB//$\mu$Pa at 200 Hz. Class three contained a weaker and broader peak at 4 Hz with a fall-off at higher frequency to 58 dB//$\mu$Pa at 200 Hz. Class four showed a continual but slow decrease in noise level with increasing frequency from a level of 85 dB//$\mu$Pa at 2 Hz to 66 dB//$\mu$Pa at 200 Hz. The minimum number of data sets used in any class was 14.

The four classes of ambient noise spectra are compared to environmental conditions and the number of detected ice cracking events occurring per minute. The noise level above 35 Hz was found to be highly correlated with both a falling temperature and the rate of detected ice cracking events. This is consistent with previous observations of thermal ice cracking. The strong peak at 8 Hz was found to be highly correlated with wind speed and barometric pressure.

## 3. MODEL

The goal of the two component ambient noise model described below is to accurately model the ambient noise spectra observed in the Arctic pack ice over the frequency band 2 - 200 Hz. For these frequencies, the ambient noise is assumed to be produced mainly by ice cracking and active pressure ridging. Thus, by summing the acoustic field generated by the distribution of these events, the ambient noise can be reproduced and the relative contributions of each noise source at the receiver can be determined.

### 3.1. Pressure Ridging

Measurements by SEASAT SAR give pan sizes for ice floes of 10 - 100 km. Pans are defined as groups of ice floes which move together. Because of the large spatial separation of active pressure ridges, the component of ambient noise caused by pressure ridging may be dominated by single or few events occurring at some large distance from the

array. Thus, examining a single pressure ridging event as a function of range may provide insight into the role of pressure ridging on the ambient noise. This requires only knowledge of the source spectral level and the propagation loss.

The source spectral level of active pressure ridging was reported in a previous paper [2] and shown to be monotonously decreasing. When this spectral level is corrected for propagation loss, the resulting spectrum of a very distant ridging event exhibits a broad infrasonic peak as found in the ambient noise [2].

### 3.2. Thermal Ice Cracking

In order to develop the thermal ice cracking component of the ambient noise model, the spatial, temporal and source level distributions along with the source spectrum and directivity of thermal ice cracking must be known. The spatial distribution of events over the entire 69 two minute samples was found to be uniform. This gives some justification to the proposed model of determining an average input energy per unit area. Note however that two forms of short term fluctuations of the average input energy can occur. The first is a strength fluctuation in the overall input level applied to all locations as the rate of ice cracking changes. The second is a random statistical fluctuation in the spatial distribution which may cause local areas of weak or intense ice cracking. These random statistical fluctuations have more effect on the ambient noise when occuring at close range and thus are applied only within 1 km of the hydrophone.

For the 2 - 200 Hz frequency band observed, the source directivity of thermal ice cracking was found to be well described by a monopole in the ice while the source spectrum was found to be relatively flat [3]. Thus, the source strength distribution of these events does not depend on frequency for this frequency band. Source levels of detected events were measured in the range of 110 - 180 dB//$\mu$Pa at 1m and approximated a linearly decreasing function on a log-dB scale of the number of events versus source level [3]. The decrease in occurring events with increasing source level is proportional to $10^{-\alpha SL}$ with $\alpha \approx 0.08$ for source levels below 160 dB//$\mu$Pa and $\alpha \approx 0.12$ for source levels above.

Using the source level distribution along with the fact that the events are spatially uniform, the mean energy input into the ice per square kilometer as a function of source power can be determined as:

$$E(P) = \delta t \; N(P) \; P$$

where $N(P)$ is the mean number of events occurring at source power $P$ per square kilometer per minute, and $\delta t$ is the mean time duration in minutes of an event. From our data, $\delta t$ was found to be approximately 0.1 seconds. The total average energy entering the ice per square kilometer is then obtained by summing over all source powers as:

$$E = \delta t \sum_{P=Pmin}^{Pmax} N(P) \; P.$$

This gives an average energy input into the ice of 116.6 dB/km$^2$//$\mu$Pa at 1 m. Using the average energy input per square kilometer calculated above, the average energy received at a hydrophone from a given source location is simply the average input minus the propagation loss associated with that location.

Finally, the thermal ice cracking model outlined above is capable of determining the relative contribution of close versus far range events in producing the ambient noise. Over 80% (within 1 dB) of the total noise energy produced from all thermal ice cracking events was generated within 30 km of the hydrophone while over 50% (within 3 dB) was generated within 6 km range.

## 4. RESULTS

The two-component noise model reproduced all four classes of measured real spectra within 1.5 dB for all frequencies above 3 Hz. The model showed that the measured ambient noise spectra can be reproduced by a single active pressure ridging event, along with a distribution of thermal ice cracking events. For frequencies below 40 Hz, the ambient noise spectrum may be determined by the range and level of the strongest received active pressure ridge. For frequencies above 40 Hz, the ambient noise spectrum is determined by thermal ice cracking, with overall levels and spectral shape dependent on the intensity of ice cracking and the relative strength of local to average events. For purposes of our model, local events are considered to be within 1 km of the hydrophone.

It was also noted that all of the data files used in classes 1 and 2 for real data occurred during a 66 hour span within the middle of the experiment while all except one of the data files used in classes 3 and 4 occurred before or after this time. This suggests that active pressure ridging was occurring at approximately 40 km range during the entire 100 hours of ambient noise measurements and that for a 66 hour span of time in the middle of the experiment, a much stronger active pressure ridge built itself at a range of approximately 70 km.

## REFERENCES


[1] I.Dyer, "The song of sea ice and other Arctic Ocean melodies", in *Arctic Technology and Policy*, eds: I.Dyer and C.Chryssostomidis, McGraw-Hill, New York, 1984.

[2] M.V.Greening and P.Zakarauskas, "Pressure ridging source spectrum level and a proposed origin of the infrasonic peak in Arctic ambient noise spectra," submitted to J.Acoust.Soc.Am.

[3] M.V.Greening and P.Zakarauskas, "Spatial and source level distributions of ice cracking in the Arctic Ocean," Submitted to J.Acoust.Soc.Am.

# Reciprocal Travel Time Scintillation Analysis

Dimitris Menemenlis[1] and David M. Farmer[1,2]
1. Electrical Engineering, University of Victoria, Victoria, B.C., CANADA.
2. Institute of Ocean Sciences, Sidney, B.C., CANADA.

## 1 Introduction

During a study of the arctic boundary layer, Menemenlis and Farmer [4] used acoustical reciprocal transmissions to obtain line-averaged velocity measurements along 200 m horizontal paths in the mixed layer beneath ice. The present discussion is motivated by a desire to interpret the observed high frequency velocity fluctuations in terms of the advection and evolution of turbulent velocity fine structure.

Kaimal *et al.* [2] discussed the problem of line-averaging in the context of extending the useful range of sonic anemometers to scales shorter than the acoustic paths. They derived transfer functions that relate measured and ideal one-dimensional power spectra. We investigate the asymptotic behaviour of the spectral transfer functions, as the length of the measuring baseline is increased, and derive analytic expressions.

The spectral transfer functions are shown to vary with dimensionless wavenumber and with angle between the measuring baseline and the mean velocity. The analysis is extended to anisotropic and inhomogeneous flows. Finally, some experimental data taken in the boundary layer beneath ice is compared with the theory.

## 2 Theory

Consider a stationary and homogeneous random velocity field advected by the mean flow past a long measuring baseline. The spectral transfer function, $T(k_1\ell, \theta, p)$, is defined as the ratio between the line-averaged one-dimensional spectrum and the ideal streamwise one-dimensional spectrum. It indicates the spectral attenuation due to line-averaging as a function of streamwise wavenumber $k_1$, pathlength $\ell$, orientation of the measuring baseline relative to the mean velocity vector $\theta$, and spectral slope $-p$.

Kaimal *et al.* [2] solved the spectral transfer function numerically for an isotropic inertial subrange, $p = 5/3$, and a measuring baseline perpendicular to the mean flow, $\theta = 90°$. When the measuring baseline is long compared to the scales of interest, an analytic solution can be found,

$$T(k_1\ell, \theta, p) = \frac{K(p)\sin^p\theta}{k_1\ell}\left(\frac{(p+1)(\cos^4\theta + \sin^4\theta) + 1}{2}\right),$$

where $K(p) = 2\Gamma(1/2)\Gamma(p/2 + 1/2)/\Gamma(p/2)$.

### 2.1 Axisymmetric Turbulence

McPhee [3] reports that heat and momentum flux under ice is typically caused by turbulent eddies that are of order 10-20 m in horizontal extent and a few meters in vertical extent. Therefore, in a given wavenumber range, the flow is more likely to be axisymmetric about the vertical axis rather than isotropic.

Herring [1] introduced a simple and useful formalism for describing axisymmetric turbulence in terms of an anisotropy parameter $a$, where $0 \le a \le 1$, and $a = 1/2$ implies isotropy. Once again, when the measuring baseline is long compared to the scales of interest, an analytic solution can be found,

$$T_a = \frac{K(p)\sin^p\theta}{k_1\ell}\left(\frac{b(\cos^4\theta + \sin^4\theta) + 2a\cos^2\theta\sin^2\theta}{(b+ap)\cos^2\theta + (a+bp)\sin^2\theta}\right)(p+1),$$

where $b = (p+2)(1-a)$. For $a = 0$, *i.e.* when all the kinetic energy is contained in the horizontal mode of motion, the spectral transfer function is at most 16% higher than for the isotropic case.

### 2.2 Anisotropic Turbulence

Consider a baseline of length $\ell$ that is split in two pieces of length $\alpha$ and $\beta$ so that $\ell = \alpha + \beta$. The line-averaged velocity $\tilde{u}$ is related to $\tilde{u}_\alpha$ and $\tilde{u}_\beta$, the velocities averaged along $\alpha$ and $\beta$ respectively, by $\tilde{u} = (\alpha\tilde{u}_\alpha + \beta\tilde{u}_\beta)/\ell$. We define $\tilde{F}_\alpha(k_1)$ and $\tilde{F}_\beta(k_1)$ to be the line-averaged one-dimensional spectra associated with $\tilde{u}_\alpha$ and $\tilde{u}_\beta$ respectively. For $k_1\alpha$ and $k_1\beta$ sufficiently large, $\tilde{u}_\alpha$ and $\tilde{u}_\beta$ are statistically independent and in that wavenumber range

$$\tilde{F}(k_1) = \frac{\alpha^2\tilde{F}_\alpha(k_1) + \beta^2\tilde{F}_\beta(k_1)}{\ell^2}.$$

Assuming homogeneity, this equation can only be satisfied when $\ell\tilde{F}(k_1) = \alpha\tilde{F}_\alpha(k_1) = \beta\tilde{F}_\beta(k_1)$, *i.e.* the measured spectra are inversely proportional to the averaging length. Using $k_1$ to non-dimensionalize $\ell$, we conclude that $\tilde{F}(k_1) \propto F(k_1)/\ell k_1$, *i.e.* for a sufficiently long baseline, the measured spectral slope is one unit less than the true spectral slope.

### 2.3 Inhomogeneous Turbulence

We use the same notation and paradigm as above, but now $\alpha$ spans an isotropic region with one-dimensional spectrum $F_\alpha(k_1)$ and similarly $F_\beta(k_1)$ is the spectrum associated with

$\beta$. Using the spectral transfer functions for isotropic turbulence derived earlier, we obtain

$$\tilde{F}(k_1) = T(k_1\ell, \theta, p)\left(\frac{\alpha F_\alpha(k_1) + \beta F_\beta(k_1)}{\ell}\right),$$

*i.e.* at sufficiently high wavenumbers, line-averaged measurements provide a true weighted average of the turbulent kinetic energy spectrum.

# 3 Experiment

During a coordinated study of the boundary layer beneath ice in the Arctic, Menemenlis and Farmer [4] deployed an acoustical instrument to measure path-averaged horizontal current and vorticity. A triangular acoustic array of side 200 m was used to obtain reciprocal transmission measurements at 132 kHz, at 8, 10 and 20 m beneath an ice floe. Pseudo random coding and real-time signal processing provided precise acoustic travel time and amplitude for each reciprocal path.

Mean current along each acoustic path is proportional to travel time difference between reciprocal transmissions. Horizontal velocity normal to the acoustic paths is measured using scintillation drift. The instrument measures horizontal circulation and average vorticity relative to the ice, at length scales characteristic of high frequency internal waves in the region. The rms noise level of the measurements is less than 0.1 mm/s for velocity and 0.01 $f$ for vorticity, averaged over one minute. Except near the mechanical resonance frequency of the moorings, the measurement accuracy is limited by multipath interference.

The sensitivity of the path-averaging acoustical current meter is such that it allows detection of kinetic energy at frequencies associated with the advection and evolution of turbulent velocity fine structure. In addition to the acoustical instrument, clusters of high resolution mechanical current meters were deployed roughly at the center of the acoustic array by McPhee [3].

The underside surface of the ice is irregular and contains keels that extend down to 10 m depth in the vicinity of the acoustic array. Because of the passage of internal waves and tides under the ice camp, steady current flow in one direction is rarely achieved for periods long enough to obtain good statistical averages. For these reasons, we expect departure of observed properties from the predictions made by the theory.

Fig. 1, is a spectral comparison of line-averaged and locally measured horizontal velocity fluctuations at 20 m depth on April 13, 1989. The spectra are a six hour average, during a period when the mean flow relative to the ice was 15 cm/s in a northward direction. The line-averaged data corresponds to a sonic path that forms angle $\theta = 76°$ with the mean flow. A straight line with $-5/3$ spectral slope is fitted to the high wavenumber region of McPhee's data. A second line with $-8/3$ slope is also drawn based on the analytic transfer function derived earlier. This prediction is seen to fall well within the 95% confidence interval of the line-averaged spectrum.

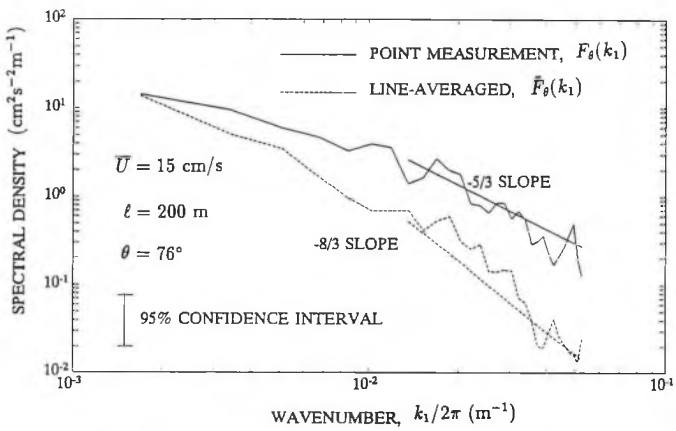


Figure 1: Comparison of energy spectra for point and line-averaged horizontal velocity measurements obtained 20 m beneath floating ice in the arctic boundary layer, on April 13, 1989.

# 4 Conclusions

For measuring baselines long compared to the scales of interest analytic expressions for the transfer function between true and line-averaged one-dimensional spectra have been derived for isotropic and axially symmetric turbulence. Line-averaged measurements are most sensitive to velocity fine structure when the mean velocity is perpendicular to the measuring baseline. The error incurred by assuming isotropy instead of axial symmetry is unlikely to exceed 16%.

For homogeneous turbulence and a sufficiently long baseline, the slope of line-averaged measurements is one unit less than the true spectral slope, irrespective of the form of the spectral density tensor. At sufficiently high wavenumbers, line-averaged measurements through regions of locally homogeneous turbulence provide a true weighted average of the kinetic energy spectrum.

This theory explains high frequency fluctuations observed during an experimental study of the arctic boundary layer beneath ice, where reciprocal acoustical transmissions were used to obtain line-averaged velocity measurements along 200 m horizontal paths.

# References


[1] J. R. Herring. Approach of axisymmetric turbulence to isotropy. *The Physics of Fluids*, 17(5):859–872, May 1974.

[2] J. C. Kaimal, J. C. Wyngaard, and D. A. Haugen. Deriving power spectra from a three-component sonic anemometer. *Journal of Applied Meteorology*, 7:827–837, Oct. 1968.

[3] M. G. McPhee. Turbulent heat flux in the upper ocean under sea ice. *Journal of Geophysical Research*, 97(C4):5365–5379, April 15, 1992.

[4] D. Menemenlis and D. M. Farmer. Acoustical measurement of current and vorticity beneath ice. *Journal of Atmospheric and Oceanic Technology*, in press.

# Modelling Azimuthal and Vertical Directionality of Active Sonar Systems for Undersea Reverberation

**James A. Theriault**
Defence Research Establishment Atlantic, P.O. Box 1012, Dartmouth, N.S., B2Y 3Z7

## 1. Introduction

Traditional methods for modelling undersea reverberation where either the transmitter or receiver has azimuthal directionality approximate the azimuthal component by sector coverage. Often, the effects from other than a main lobe are ignored. In some cases, the width of the sector is chosen such that the azimuthally-integrated response is the same for the sectored coverage as the original sonar in the horizontal plane. Unfortunately, should the sonar have both azimuthal and vertical directivity (which is often the case), accounting for only the main lobe or using a simple azimuthal integration may lead to erroneous reverberation estimates. Historically, inclusion of the full directionality or beam pattern has been too computationally costly to consider, but with the proliferation of modern high-speed computers, this is no longer the case. The full directionality can and in many cases should be included.

This azimuthal-integration concept is not new or difficult to understand; yet, it is often ignored when considering beam patterns. The concept has been used in calculating an effective beamwidth or in calculating the scattering area. Ellis[1] considered an "effective vertical beam pattern" by assuming that either the transmitter or the receiver was azimuthally independent. Urick[2] considered the case where the transmit angle and the receive angle are the same. i.e. backscatter. This omits the "hybrid paths" shown by Ellis and Franklin[3] to be important in bottom reverberation estimates. Even if hybrid paths were included, the technique would not properly model the high-angle paths which dominate the reverberation at shorter ranges. Urick also indicates that it is generally too difficult to analytically perform the integration even for this simplified case. The following sections describe the equations and techniques for the azimuthal integration.

## 2. Theory

We restrict the problem to consider azimuthally symmetric environments with source and receiver horizontally co-located. However, they may be vertically displaced. Without loss of generality, we will assume that all of the scatterers lie on the same boundary, the seafloor. Reverberation effects from other scatterers may be computed and added to obtain the total reverberation. The reverberation intensity from an ocean boundary as a function of time may be written as[1]:

$$R(t) = I_0 \int_{A(t)} \sum_{s,r} H_s(\rho,\theta_s)\, B_s(\theta_s,\phi) \bullet H_r(\rho,\theta_r)\, B_r(\theta_r,\phi)\, S(\theta_s',\theta_r')\, dA, \quad (1)$$

where

| | |
|---|---|
| $t$ | time, |
| $I_0$ | source intensity, |
| $dA$ | elemental area, |
| $A(t)$ | area contributing to reverberation at time t, |
| $r,s$ | receiver and source, respectively, |
| $H_s, H_r$ | propagation loss to and from the scattering area, |
| $\rho$ | radial component in cylindrical coordinates, |
| $\phi$ | azimuthal angle, |
| $\theta$ | vertical angle measured from the horizontal at the sonar, |
| $\theta'$ | grazing angle at the seafloor, |
| $B_s, B_r$ | source and receiver beam patterns, and |
| $S$ | scattering function. |

Note that due to refraction effects, $\theta$ and $\theta'$ are not necessarily equal. The sumation over r and s indicate the inclusion of all combinations of relevent transmit and receive paths. i.e. hypbrid paths are included.

Furthermore, if one substitutes $dA = \rho\, d\rho\, d\phi$, the two-dimensional integration may be reduced and the sonar directivity (beam pattern) isolated:

$$R(t) = 2\pi I_0 \int_{\rho(t)} \sum_{s,r} H_s(\rho,\theta_s)\, H_r(\rho,\theta_r)\, S(\theta_s',\theta_r') \bullet D(\theta_s,\theta_r)\, \rho\, d\rho, \quad (2)$$

where D is defined by

$$D(\theta_s,\theta_r) = \frac{1}{2\pi} \int_0^{2\pi} B_s(\theta_s,\phi) B_r(\theta_r,\phi)\, d\phi\,. \quad (3)$$

$D(\theta_s,\theta_r)$ is an azimuthally-integrated beam pattern product function. In agreement with Urick, even in the case where $\theta_s = \theta_r$, this integral can not be generally solved using analytic tools. Of course, if one removes the azimuthal dependence, the integral is trivial.

Ellis considered the case in which either $B_s$ or $B_r$ was azimuthally independent. For discussion purposes, consider $B_s$ as being azimuthally independent; a case which may be easily characterized using existing reverberation models. $B_s$ may be entered in its usual form, while the $B_r$ is replaced by its "effective vertical beam pattern." Ellis defined the "effective vertical beam pattern" to be the azimuthally-integrated beam pattern similar to equation 3, but without $B_s$.

As long as one is willing and able to modify an existing reverberation model, Ellis' restriction is not necessary. Eigenray-based numerical models may be easily modified to accept $D(\theta_s,\theta_r)$ as input or alternatively to accept $B_s$ and $B_r$ and perform a numerical integration to arrive at $D(\theta_s,\theta_r)$. The NUSC Generic Sonar Model[4] has been modified to include a "Simpson's Rule" integration of the beam pattern product in order to produce the results in section 4.0.

## 3. Example Sonar System

To demonstrate this technique, we will use a simple sonar consisting of an 8-element horizontal line array receiver, spaced at 1/2 wavelength with rectangular weighting. Receiver sidelobes are cut-off at -35 dB.

For demonstration purposes, we shall choose three sources. An omni-directional source which has azimuthal and vertical independence; a four-element (1/2 wavelength spacing) vertical line array which gives vertical dependence while having azimuthal independence and a third which consists of the four-element vertical array rotated to be collinear with the receiving array. This yields a source with both vertical and azimuthal dependence. It is possible to properly model the first two source/receiver options using Ellis' technique (but not Urick's), but the third source requires the solution presented in the previous section. For simplicity, we shall choose the transmit parameters to be the same as those used by Ellis; namely a 0.33 s rectangular CW pulse at a frequency of 315 Hz. The source level, $I_0$, is 220 dB re 1 μPa at 1m. Transmitter sidelobes are cut-off at -20 dB.

## 4. Calculated Reverberation

To demonstrate the technique, we again turn to Ellis to supply the environment. We will assume a typical deep-water environment with no surface duct and a water depth of 5300 m. The source and receiver are collocated at 175 m.

Figure 1 shows the calculated reverberation including fathometer returns for each of the source options and the line array receiver. Each of the line-array sources is steered in the broadside direction. In each case, the receiver is steered in the broadside direction.

The results for the omni directional source show significant increases over the smoothly decaying reverberation due to the fathometer returns. The results for the horizontal source show the same maximum levels of the fathometer returns as with the omni source, with slightly lower levels in the smoothly decaying region. The fathometer-return levels are the same since the horizontal line array is steered in the broadside direction where it has unity response in the vertical direction. The fathometer-return levels for the vertical line source show a significant decrease since the array is steered in the horizontal direction (broadside) and does not insonify the higher angle paths to the seafloor which dominate the reverberation.

Analyzing these differences between source directionalities would be extremely difficult or impossible without considering the full azimuthal directionality of both the receiver and transmitter. Using alternate techniques that ignore the 2D dependence may produce misleading results.

## 5. Discussion

This paper shows a relatively straight-forward technique for including both azimuthal and vertical directionality in reverberation calculations for active sonar systems. Though the technique is not new or difficult to understand, this azimuthal integration concept is often ignored.

The resulting equations are easily incorporated in almost any reverberation model. Without any modification, most reverberation models accounting for vertical directionality may be used to model systems where either the source or receiver has azimuthal independence. The difficulty arises when both source and receiver have azimuthal and vertical dependencies. Though generally not difficult, changes are required in most numerical models to account for this case.

The included example indicates how the technique may be applied to the analysis of complicated sonar systems. Other than in very special cases, the azimuthal and vertical directionality of the source and receiver should be included to properly model reverberation.


[1] D.D. Ellis, "Effective Vertical Beam Patterns for Ocean Reverberation Calculations," IEEE JOE, Vol. 16, No. 2, April 1992.

[2] R.J. Urick, Principles of Underwater Sound, 3rd ed. New York; McGraw-Hill, 1983.

[3] D.D. Ellis, J.B. Franklin, "The importance of hybrid ray paths, bottom loss, and facet reflection on ocean bottom reverberation," in Progress in Underwater Acoustics, H.M. Merklinger, Ed. New York; Plenum, 1987, pp. 75-84.

[4] H. Weinberg, "Generic SONAR Model," in Oceans '82 Proceedings, pp. 201-205, 1982.


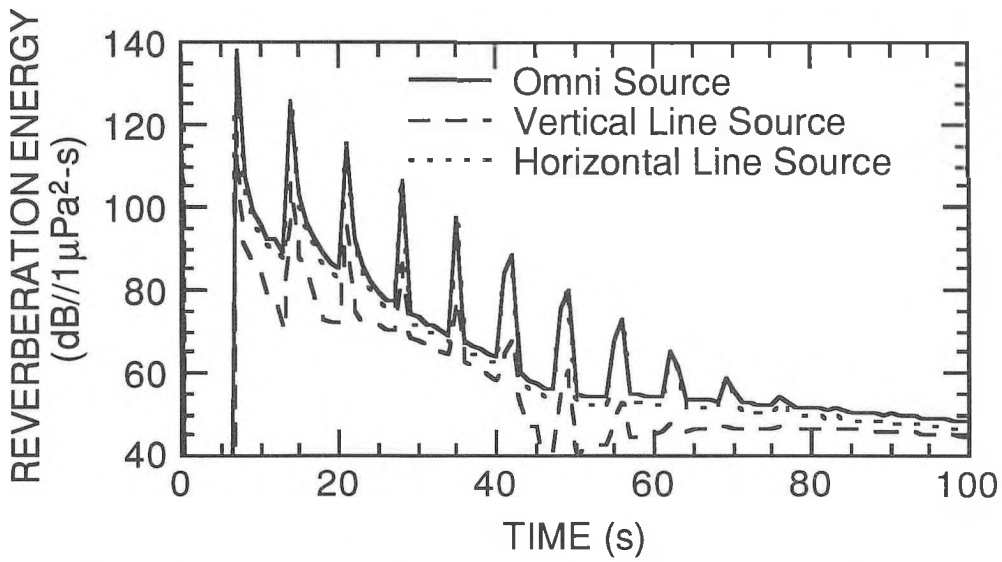


**Figure 1** *Example Reverberation versus Time Plot for Line Array Receiver and Three Sources.*

# A STATIONARY APPROXIMATION IN MATCHED-FIELD PROCESSING FOR A MOVING UNDERWATER ACOUSTIC SOURCE

Cedric A. Zala [1] John M. Ozard [2]

[1]Barrodale Computing Services Ltd., 8 – 1560 Church Ave., Victoria, B. C., Canada V8P 2H1
[2]Defence Research Establishment Pacific, F. M. O., Victoria, B. C., Canada V0S 1B0

## 1. INTRODUCTION

A normal-mode model for the acoustic field due to a moving source, derived by Hawker [1], was recently used in the development of procedures for applying matched-field processing (MFP) techniques to a moving source [2]. This approach involved matching "measured" array covariance matrices at multiple frequencies using replica matrices computed with a phase-expanded form of the Hawker model. Excellent results were obtained, but the technique was compute-intensive. In this paper, a procedure is described for using snapshot vectors at a single frequency to generate the replica matrices. By comparing the performance of the MFP techniques applied to simulated data, it is shown that this new stationary approximation procedure allows the position of a moving source to be estimated as acurately as, but much more efficiently than, the full multiple-frequency procedure.

## 2. SIMULATION OF MEASURED DATA

The simulated environment consisted of a 500-m channel with an Arctic upward refracting sound-speed profile, and a bottom consisting of a 60-m sediment layer with sound speed 2000 m/s and density 1.5 g/ml, and an underlying layer with sound speed 2600 m/s and density 2.5 g/ml. When these layers were modelled as fluids in the generation of a normal mode model at 20 Hz, 12 propagating modes were obtained.

Data were simulated for a vertical array spanning the water column. The array consisted of 20 sensors evenly spaced from 25 m to 500 m depth, with increments of 25 m. For each simulation a single source was present at a depth of 100 m and a velocity of 10 m/s outward along a radial from the array. The initial range of the source was set to either 20,000, 25,000, 30,000, 35,000 or 40,000 m. The time domain model of Hawker [1] was used in conjunction with the above 12-mode model to compute discrete noise-free time series for each sensor at a sampling rate of 51.2 Hz. Data segments of 10 s were Fourier transformed, giving a frequency resolution of 0.1 Hz, and array covariance matrices were computed for each of the seven discrete frequencies between 19.7 Hz and 20.3 Hz. These matrices were averaged over time for integration times of 10, 20, 50, 100, 200, 500, or 1000 s.

For the MFP procedure involving full matching of source motion [2], the set of seven time-averaged measured matrices $M(f_j)$ (one for each frequency $f_j$) for each simulation were stored and used directly. For the MFP procedures involving the conventional snapshot and our new stationary approximation, these matrices were averaged across frequency and the resulting time-and-frequency-averaged matrix $\overline{M}$ for that simulation was used.

## 3. MATCHED-FIELD PROCESSING

The 12-mode model was used to generate replica data for matching the simulated measured data. Depending on the input data and the type of matching to be performed, one of three forms of the generalized Bartlett beamformer (GBF) was used for the matching. In each case the GBF power was normalized with respect to both the measured and replica data so that it corresponded to the correlation coefficient for the match.

For the full matching of source position and velocity, including Doppler shifts, the following form was used:

$$P_{\text{full}} = \frac{\sum_j \text{Tr}\,[M(f_j)R(f_j)]}{\sum_j \lambda_N^M(f_j)\lambda_N^R(f_j)}, \tag{1}$$

where $P_{\text{full}}$ is the GBF power for the full source motion matching procedure, $M(f_j)$ is the measured covariance matrix for frequency $f_j$, $R(f_j)$ is the replica matrix for frequency $f_j$, and $\lambda_N^M$ and $\lambda_N^R$ are the largest eigenvalues of $M$ and $R$, respectively. $R(f_j)$ was generated by summation of outer product matrices formed from vectors computed using the phase-expanded form of the Hawker model (Eq. 2 of [2]). The summation was performed at 10-s intervals over the corresponding integration time. Here $R(f_j)$ is a function of source position, velocity, and frequency $f_j$.

For the stationary approximation matching of source position and velocity, in which Doppler shifts are not matched, the following form was used:

$$P_{\text{stat\_approx}} = \frac{\text{Tr}\,[\overline{M}\ \overline{R}]}{\lambda_N^{\overline{M}}\lambda_N^{\overline{R}}}, \tag{2}$$

where $P_{\text{stat\_approx}}$ is the GBF power for the stationary approximation matching procedure, and $(\overline{\cdot})$ denotes the time-and-frequency-averaged matrix. In this form, $\overline{R} = \sum_k \mathbf{r}(t_k)\mathbf{r}^*(t_k)$, where $\mathbf{r}(t_k)$ is the stationary snapshot vector at time $t_k$, and the summation is over the integration time as above. The snapshot vectors were generated using the standard form of the normal mode model. Here, $\overline{R}$ is a function of source position and velocity but is defined at only a single frequency.

Table 1: Normalized GBF power (correlation coefficient) for MFP of data simulated for a source moving at 10 m/s. The data were matched using the full matching procedure, the stationary approximation and the snapshot method.

| Integration Time (s) | Number of Averages | Source Motion (m) | Normalized GBF Power (Correlation Coefficient) | | |
|---|---|---|---|---|---|
| | | | Full Moving | Stationary Approximation | Snapshot |
| 10 | 1 | 100 | $1.0000 \pm 0.0000$ | $0.9970 \pm 0.0017$ | $0.9970 \pm 0.0017$ |
| 20 | 2 | 200 | $1.0000 \pm 0.0000$ | $0.9970 \pm 0.0017$ | $0.9943 \pm 0.0021$ |
| 50 | 5 | 500 | $1.0000 \pm 0.0000$ | $0.9966 \pm 0.0019$ | $0.8787 \pm 0.0065$ |
| 100 | 10 | 1000 | $1.0000 \pm 0.0000$ | $0.9966 \pm 0.0017$ | $0.7562 \pm 0.0121$ |
| 200 | 20 | 2000 | $0.9999 \pm 0.0001$ | $0.9970 \pm 0.0015$ | $0.6952 \pm 0.0209$ |
| 500 | 50 | 5000 | $0.9995 \pm 0.0003$ | $0.9989 \pm 0.0005$ | $0.6368 \pm 0.0034$ |
| 1000 | 100 | 10000 | $0.9994 \pm 0.0003$ | $0.9998 \pm 0.0002$ | $0.6879 \pm 0.0031$ |

For the conventional snapshot matching of source position, the following form was used:

$$P_{\text{snapshot}} = \frac{\mathbf{r}^* \overline{M} \mathbf{r}}{\lambda_N^{\overline{M}} |\mathbf{r}|^2}, \tag{3}$$

where $P_{\text{snapshot}}$ is the power for the conventional snapshot form of the GBF, and $\mathbf{r}$ is the stationary snapshot replica vector. Here, $\mathbf{r}$ is a function of source position only.

MFP was performed using the grid-search-optimization (GSO) technique. GSO involves the generation of a search grid of power values for various source positions, followed by identification of local maxima in this grid, which are then used as initial estimates in the optimization of source position. The result is a set of discrete estimates of the source position. Since the array was vertical and the environment was range-independent, the power only depended on source range and depth (not bearing). For the full and stationary approximation forms of the GBF (Eqs. 1 and 2), the source speed and heading were set to their known values.

The depth search region extended from 50 to 150 m, with increments of 25 m. The specification of the range search region depended on the form of the matching. For the full and stationary approximation forms, the region was set to $\pm 1000$ m from the known initial range of the source, with increments of 100 m. (Here, source position and velocity are matched for a given initial position.) For the snapshot form, which does not match velocity, the region was defined to be from 100 m before the initial range to 100 m beyond the final range for that simulation. The increments for the range search grid were 100 m for integration times from 1 to 200 s, 200 m for 500 s, and 250 m for 1000 s.

MFP was performed for three processors, seven integration times, and five initial source ranges. The maximum correlation in each set of GSO outputs was taken, and these were averaged across the five ranges to give means and standard deviations of the GBF power for each processor and integration time.

## 4. RESULTS

Table 1 shows the results of these analyses. As expected for the noise-free conditions here, the full matching procedure gave essentially perfect matches for all integration times.

The stationary approximation procedure also gave very high correlations for all conditions here; these correlations were only slightly less than unity. This was the case even though the data matrices were averaged in both time and frequency, and the matching did not take Doppler shifts into account. The high correlations indicate that simply matching the source track at the reference frequency provides an excellent means of estimating the position though not the direction of motion of the moving source, and that it is not necessary to model the Doppler effects. Using the stationary approximation requires an order of magnitude less computations than the full multiple frequency procedure.

The snapshot matching procedure gave multiple peaks of approximately equal correlation values at various positions along the source track. These correlation values rapidly decreased as the integration time, and corresponding extent of source motion, increased. For integration times of the order of a few minutes, the correlations decreased to less than 0.7, compared to values of greater than 0.99 for the stationary approximation procedure.

## 5. CONCLUSIONS

The use of the stationary approximation procedure provides a highly effective approach to the estimation of the position of a moving source. It is almost as effective as the use of the multi-frequency full matching method, and much more effective than matching with simple snapshot vectors. The stationary approximation procedure does not involve Doppler shifts and is substantially less compute-intensive than the full procedure, since it involves matching replicas generated at only the single reference frequency. It may also be adapted for use with precomputed grids of field values to yield further increases of speed.

## REFERENCES


[1] K. E. Hawker, "A normal-mode theory of acoustic Doppler effects in the oceanic waveguide," *J. Acoust. Soc. Am.*, vol. 65, pp. 675–681, 1979.

[2] C. A. Zala and J. M. Ozard, "Matched-field processing for a moving source," *J. Acoust. Soc. Am.*, vol. 92, pp. 403–417, 1992.

# The Canadian Acoustical Association
# L'Association Canadienne d'Acoustique

## MINUTES OF THE BOARD OF DIRECTORS MEETING

July 19, 1992, 10:00 a.m.
Inn on the Park Hotel, Toronto, Ontario

| | | | |
|---|---|---|---|
| Present: | W. Sydenborgh | J. Hemingway | E. Bolstad |
| | M. Hodgson | M. Roland Mieszkowski | F. Laville |
| | B. Dunn | J. Bradley | T. Embleton (part time) |
| | D. Chapman | C. Laroche | S. Abel (part time) |
| | A. Behar (part time) | | |
| Regrets: | L. Brewster | Absent: S. Forshaw | |

1. Report on Planning of INTER-NOISE 92 - Tony Embleton

Tony provided a written and oral report on conference activities. There were about 460 registrants and 269 papers. D. Chapman thanked Tony and the conference committee for the hospitality shown to the CAA BoD.

2. Report on St. Petersburg Conference - David Chapman

M.J. Crocker wrote to the CAA asking for support for the Int. Conf. on Noise and Vibration Control in St. Petersburg, June 1993. Murray Hodgson has published the information in Canadian Acoustics. Tony Embleton comments that the problem is that such a meeting fragments the noise control community (i.e. INTER-NOISE '93 in Leuven, Belgium). Motion of Alberto Behar: we are in favour of international acoustical activities but we are concerned about conflicts, so the CAA will not add its name to the list of sponsors for this one. We'll publicize all meetings but we will not endorse that one. Vote: all in favour.

3. Secretary's Report - Winston Sydenborgh

In addition to handling incoming mail, the secretary maintains the membership list. In response to the mail-out for renewals in the new year, 85% renewed, 15% did not renew. Some explained they had left the field of acoustics. There are 16 new members of which 7 are students. We do not anticipate a change in the total number of members next year. List will be published in December issue. Winston does not intend to re-offer as secretary. He recommends that the By-laws of CAA be reviewed, as they are 20 years old. They should be reviewed by the board of directors and published in both official languages. Secretary's budget of $1500 should probably be increased. Are membership fees adequate? Subscription fees for Canadian Acoustics? Student fees? Should there be a difference between foreign and domestic subscriptions? 1993 subscription fees have to be decided soon.

4. AWC Student Presentations - Alberto Behar

Everything went fine last year. AWC '92 Committee reports only two applications this year. Students should know because Bruce Dunn sent posters to many universities. Alberto will contact Doug Wicker to make sure late applications for student prizes will be accepted and students will be made aware of this possibility.

5. President's Report - Dave Chapman

Awards sub-committee was reorganized. Bruce Dunn is now chairman with Alberto Behar and Murray Hodgson as members. Alberto Behar put together the new rules and application format for the Student Presentation Awards. People who are currently points-of-contact for individual prizes will continue. ICS asked for $60 to maintain a list of all acoustical societies in the world. Dave Chapman will check with ICA why CAA was not asked to represent the acousticians of Canada. Sharon Abel accepted invitation to chair AWC'93 in Toronto. About 2000 copies of a 2 color letterhead at a cost of $180 will be available by next meeting.

6. Treasurer's Report - Eugene Bolstad

There was much discussion regarding the subscription, advertising, and member rates for Canadian Acoustics. Motion passed: The CAA Treasurer and Editor of Canadian Acoustics will review the financial state of the journal and make recommendations for alterations to prices if needed. Motion passed: Advertising editor of Canadian Acoustics should get in touch with Editor and Treasurer concerning the billing problem. Motion to accept Treasurer's report: proposed by Bruce Dunn, seconded by Marek. All in favour.

7. Postdoctoral Prize - Sharon Abel

No applicants this year. Suggestion that prize be maintained and more advertisements done next year. Eugene Bolstad: capital funds grow if prize not awarded.

8. Acoustics Week in Canada 1993 - Sharon Abel

It was proposed and accepted that the CAA not organize seminars for the Toronto meeting, but that independent companies could apply for permission to do so, provided that they accepted full responsibility. Location: Downtown Toronto, probably the Delta Chelsea.

9. Cost of Travel to CAA Meeting - Eugene Bolstad

The Treasurer has produced a form for applying for partial reimbursement of expenses to travel to the spring BoD meeting. The maximum amount of reimbursement is the amount of an APEX discount return airfare, a correction of the previous BoD minutes.

10. Editor's Report - Murray Hodgson

The CAA may need to increase the $12000 subsidy for Canadian Acoustics. We need more papers. Only 3 papers for December issue; none for later. Dave Chapman suggests that directors should solicit papers. Bruce Dunn proposed, John Hemingway seconded: report accepted.

11. Membership/Recruitment Report - John Bradley

John Bradley sent a letter asking CAA members to solicit new members. An increase of 30 followed the John Bradley action. Brochure will be updated: Marek will help John produce brochure by October meeting. Bruce Dunn proposed, John Hemingway seconded, report accepted.

12. Nomination Committee - Bruce Dunn

Two directors leaving: Lynne Brewster and Tony Embleton. Secretary will not be re-offering; John Hemingway volunteered for Secretary's position. (All Executive positions and 2 Directors are open for nomination of any member.) Three names suggested for replacement directors. John Hemingway proposed, Chantal Laroche seconded: report accepted.

13. Awards

- Director's Awards - Chantai Laroche

  The list of papers to be reviewed will be sent. There is a problem in determining age and status of authors.

- Postdoctoral Prize - see Item 7.

- Bell Speech Prize - Dave Chapman for Lynn Brewster.
  No applicants.

- Fessenden Prize - Dave Chapman
  There were 5 applicants. A winner was selected and notified. Motion: increase the prize to $500 and award it every year. Bruce Dunn moved, John Hemingway seconded; approved by all.

- Eckel award - Murray Hodgson
  No applicants.

- Science Fair - Dave Chapman for A. Cohen
  A winner was chosen at this year's fair in Sudbury; the details will be published in Canadian Acoustics. Next year Science Fair is in Rivière du Loup; Frédéric will talk to Annabel Cohen regarding finding a judge/presenter.

General Discussion on how to better publicize awards. Motion to accept reports: Eugene Bolstad moved, Marek Mieszkowski seconded, all approved.

14. Acoustics Week in Canada 1992 - Murray Hodgson for Doug Whicker

A written report was submitted. Eugene moved the acceptance of the report. Marek seconded, all accepted.

15. Acoustics Week in Canada 1994 - John Bradley

John Bradley will investigate the possiblity of an Ottawa meeting in 1994.

16. Other Business

Letter received from member interested in the creation of a CAA Service Certificate; the Board voted not to institute a routine certificate but would entertain occasional proposal to award a certificate to an outstanding individual. Discussion on protection (possibly better legislation) for workers exposed to excessive noise levels in the entertainment industry. Eugene Bolstad relates his own experience with this kind of legislation; he suggests education. Marek to investigate further and report in October.

17. Reviewing the By-laws

Dave Chapman will ask Winston if he is interested in assisting. A copy will be sent to everybody of the board for review, and the topic will be placed on the agenda for the next meeting.

Adjourn at 15:20; moved by John Bradley, seconded by Murray Hodgson, accepted by all.

# NEWS/INFORMATIONS

## CONFERENCES

**14th International Congress on Acoustics**: Beijing, China, September 3 - 10, 1992. contact: ICA Secretariat, Institute of Acoustics, P.O. Box 2712, Beijing 100080, China or FAX at 256-1457.

**1992 International Congress on Noise Control Engineering:** Toronto, Ontario, July 20 - 22, 1992. A four-page Announcement and Call for Papers for INTERNATIONAL NOISE 92 is now available from the Congress Secretariat. Contact: Congress Secretariat, P.O. Box 2469 Arlington Branch, Poughkeepsie, NY 12603, USA. Tel: (914) 462-4006, FAX: (914) 473-9325.

**6th International FASE - CONGRESS 1992:** Zürich, Switzerland, July 29 - 31, 1992. Contact: FASE Congress 1992, Swiss Acoustical Society, P.O. Box 251, 8600 Dübendorf, Switzerland. Tel: 0041-1-954 06 05 (Mrs. E. Rathe) FAX: 0041-1-954 33 48.

**Acoustical Society of America**: Memphis, Tennessee, October 19 - 23, 1992. Contact: Acoustical Society of America, 500 Sunnyside Blvd., Woodbury, NY 11797. Tel: (516) 349-7800 ext. 481.

**IEEE Ultrasonics Symposium**: Tucson, Arizona, USA, October 1992. Contact: Motorola Government Electronics Group, Attn: F.S. Hickernell, 8201 E. McDowell Rd., Scottsdale, AZ 85252.

**VDE - Kongress '92**: Köln, FGR, November 18 - 21, 1992. Contact: VDE-Zentralstelle, Tagungen und Seminare, Stresemannallee 15, D-6000 Frankfurt, 70, FGR.

**Tonmeistertagung 1992**: Bergheim, FGR, November 18 - 21, 1992. Contact: Bildungswerk des Verbandes Deutscher Tonmeister, Honniggasse 16, D-5010 Bergheim 12, FGR.

**XIIIth World Congress on Occupational Safety and Health**: New Delhi, India, April 4 8, 1993. Contact: National Safety Council, P.O. Box 26754, Sion, Bombay 400 022, India. Tel: 407-3285; 407-3694; 409-1285, FAX: +91-22-525-657, Telex: 011-74577 CLI-IN, Cable: NASACIL.

**International Noise and Vibration Control Conference**: St. Petersburg, Russia, May 31 - June 3, 1993. Contact: Noise Control Association Leningrad Mechanics Institute, Professor Nickolai Igorevich Ivanov, St. Petersburg, Russia.

**6th International Congress on Noise as a Public Health Problem**: Nice, France, July 6 - 9, 1993. Contact: Noise and Man '93, Inrets-Len, P.O. Box 24, 69675 Bron Cedex, France.

## COURSES

**Program in Acoustics and Signal Processing**: State College, PA, June, 1992. A unique four-week program, comprised of ten accredited graduate level courses in acoustics and signal processing, will be offered in June, 1992 by Penn State's Graduate Program in Acoustics in cooperation with the University's Applied Research Laboratory (ARL). Contact: Dr. Alan D. Stuart, Summer Program Coordinator, the Penn State Graduate Program in Acoustics, P.O. Box 30, State College, PA, 16804. Telephone (814) 863-4128 or FAX (814) 865-3119.

**Modal Analysis**: San Diego, California, USA, June 9 - 11, 1992. Contact: Scientific-Atlanta, Spectral Dynamics Products, 13112;.Evening Creek Drive South, San Diego, CA 92128, USA. For further information or to register, Telephone Bob Keifer at (619) 679-6351.

## CONFÉRENCES

**14e Congrès international sur l'acoustique**: Beijing, Chine, du 3 au 10 septembre 1992. Contacter: ICA Secretariat, Institute of Acoustics, P.O. Box 2712, Beijing 100080, Chine. Télécopieur 256-1457.

**Conférence Inter-Noise 92**: Toronto, Canada, du 20 au 22 juillet 1992. L'annonce de la conférence et l'appel aux auteurs sont maintenant disponibles auprès du secrétariat de la conférence. Contacter: Congress Secretariat, P.O. Box 2469, Arlington Branch, Poughkeepsie, NY 12603, USA. Téléphone (914) 462-4006, télécopieur (914) 473-9325.

**Congrès 1992 de la fédération européenne des sociétés d'acoustique (FASE)**: Zürich, Suisse, du 29 au 31 juillet 1992. Contacter: FASE Congress 1992, Swiss Acoustical Society, P.O. Box 251, 8600 Dübendorf, Suisse. Téléphone 0041-1-954 06 05 (Mme E. Rathe), télécopieur 0041-1-954 33 48.

**Acoustical Society of America**: Memphis, Tennessee, du 19 au 23 octobre 1992. Contacter: Acoustical Society of America, 500 Sunnyside Blvd., Woodbury, NY 11797. Téléphone (516) 349-7800, poste 481.

**Symposium de l'IEEE sur les ultrasons**: Tucson, Arizona, octobre 1992. Contacter: Motorola Government Electronics Group, attnetion F.S. Hickernell, 8201 E. McDowell Rd., Scottsdale, AZ 8252, USA.

**VDE - Kongress '92**: Köln, Allemagne, du 12 au 14 octobre 1992. Contacter: VDE-Zentralstelle, Tagungen und Seminare, Stresemannallsee 15, D-6000 Frankfurt, 70, Allemagne.

**Tonmeistertagung 1992**: Bergheim, Allemagne, du 18 au 21 novembre 1992. Contacter: Bildungswerk des Verbandes Deutscher Tonmeister, Honiggasse 16, D-5010 Bergheim 12, Allemagne.

**XIIIe congrès mondial sur la santé et la sécurité du travail**: New Delhi, Inde, du 4 au 8 avril 1993. Contacter: National Safety Council, P.O. Box 26754, Sion, Bombay 400 022, Inde. Téléphone 407-3285; 407-3694; 409-1285, télécopieur +91-22-525-657, télex 011-74577 CLI-IN, câble NASACIL.

**Conférence internationale sur la réduction du bruit et des vibrations**: St-Pétersbourg, Russie, du 31 mai au 3 juin 1993. Contacter: Noise Control Association, Leningrad Mechanics Institute, Professeur Nickolai Igorevich Ivanov, St-Pétersbourg, Russie.

**6e Congrès international sur le bruit comme problème de santé publique**: Nice, France, du 6 au 9 juillet 1993. Contacter: Noise and Man '93, Inrets-Len, Boîte postal 24, 69675 Bron Cedex, France

## COURS

**Program in Acoustics and Signal Processing**: State College, Pennsylvanie, juin 1992. Programme d'une durée de quatre semaines comprenant dix cours de 2e cycle en acoustique et en traitement des signaux, offert par le programme de 2e cycle en acoustique du Penn State College en collaboration avec le laboratoire de recherche appliquée (ARL). contacter: Dr. Alan D. Stuart, Summer Program coordinator, the Penn State Graduate Program in Acoustics, P.O. Box 30, State College, PA 16804, USA. Téléphone (814) 863-4128, Télécopieur (814) 865-3119.

**Modal Analysis**: San Diego, Californie, du 9 au 11 juin 1992. Contacter: Scientific-Atlanta, Spectral Dynamics Products, 13112;. Evening Creek Drive South, San Diego, CA 92128, USA. Téléphone (619) 679-6351 (Bob Keifer).

**Sound Intensity**: Cheswick, Pennsylvania, June 22 - 26, 1992. AVNC, Continuing Education Division, 250 Shagbark Drive, R.D. #1, Cheswick, PA 16094.

**ISVR - Short Courses 1992**: The University, Southampton, UK.

| | |
|---|---|
| Technical Audiology | Sept. 7 - 11 |
| 21st Advanced Course in Noise & Vibration | Sept. 14 - 18 |
| 11th Annual Engine Noise & Vibration Control Course | September |

Further information regarding the above courses may be obtained from: ISVR Conference Secretary, Institute of Sound and Vibration Research, The University, SOUTHAMPTON, SO9 5NH, UK/ Tel: 0703 0592310; FAX: 0703 593033.

**Certificate in Competence in Work Place Noise Assessment**: London. UK. October 12 - 15, 1992. Contact: Centre for Continuing Professional Education, Room n201, IoEE, South Bank Polytechnic, Borough Road, London SE1 0AA, UK.

## NEW PRODUCTS

**The American Institute of Ultrasound in Medicine's (AIUM)** Placement Referral Service efficiently and effectively disseminates career opportunity information and brings together suitable employers and emplyees.

For more information on AIUM's Placement Referral Service simply call, Phone: (301) 881-2486, FAX (301) 881-7303, or write to:

AIUM,
Marketing Department,
11200 Rockville Pike,
Suite 205,
Rockville MD 200852-3139

**Three Sound Intensity Congress Proceedings are Available**

In 1981, a seminal Congress on Acoustic Intensity was held at the Centre Technique des Industries Mécaniques (CETIM) in Senlis, France.

The second CETIM conference, entitled The 2nd International Congress on Acoustic Intensity, was held in Senlis on 1985 September 23 - 26. The Congress Proceedings contains 570 pages and 78 technical papers, 58 in English and 20 in French.

The Third International Congress on Intensity Techniques, held at CETIM on 1990 August 27 - 29, was devoted to this topic, and the Proceedings contain 472 pages and 59 technical papers.

All three of these volumes are now available in limited quantities from Noise Control Foundation. Indivuduals who wish to have copies of all three volumes, may order the set of three volumes at the special price of $150 (USD 150). The books will be shpped postpaid except that orders overseas which are shipped by air require additional airmail postage. The additional required postage for handling and shipping by air mail is $58 (USD 58) for all three volumes, and $23 (USD 23) for the proceedings of the third Congress. Overseas orders must be paid in United States Funds through a U.S. bank or through a bank that has a correspondent relationship in the United States. Orders for these volumes should be placed with Noise Control Foundation, P.O. Box 2469 Arlington Branch, Poughkeepsie, NY 12603, USA.

**Sound Intensity**: Cheswick, Pennsylvanie, du 22 au 26 juin 1992. Contacter: AVNC, Continuing Education Division, 250 Shagbark Drive, R.D. #1, Cheswick, PA 16094.

**ISVR - Short Courses 1992**: The University, Southampton, Grande-Bretagne. Technical Audiology, du 7 au 11 septembre; 21st Advanced Course in Noise & Vibration, du 14 au 18 septembre; 11th Annual Engine Noise & Vibration Control Course, septembre. Contacter: ISVR Conference Secretary, Institute of Sound and Vibration Research, The University, Southampton, S09 5NH, Grande-Bretagne. Téléphone 0703 592310, Télécopieur 0703 593033.

**Certificate in Competence in Work Place Noise Assessment**: Londres, Grande-Bretagne, du 12 au 16 octobre 1992. Contacter: Centre for Continuing Professional Education, Room n2102, IoEE, South Bank Polytechnic, Borough Road, Londres SE1 0AA, Grande-Bretagne.

## NOUVEAUX PRODUITS

**L'American Institute of Ultrasound in Medicine (AIUM)** offre un service de placement avec renseignements sur les possibilités d'emploi et contacts entre employeurs et employés potentiels.

On peut joindre le service de placement de l'AIUM par téléphone au (301) 881-2486 ou par télécopieur au (301) 881-7303, ou en écrivant à l'addresse suivante:

AIUM,
Marketing Department,
11200 Rockville Pike,
Suite 205,
Rockville MD 200852-3139

**Actes de trois conférences sur l'intensité acoustique**

Les actes des trois dernières conférences organisées par le Centre technique des industries mécaniques (CETIM) sont maintenant disponibles, en quantités limitées, auprès de la Noise Control Foundation.

Ces trois conférences ont eu lieu à Senlis, France. La première, en 1981; la deuxième, du 23 au 16 septembre 1985; et la troisième, du 27 au 29 août 1990. Les actes de la deuxième conférence, regroupés en 570 pages, contiennent 78 communications techniques sur l'intensité acoustique, dont 58 en anglais et 20 en français.

Ceux de la conférence de 1990 regroupent 59 communications en un volume de 472 pages.

La série des trois volumes est disponibe aux prix spécial de 150 $ (US). Les commandes seront envoyées port-payé. Pour les envois outremer, un montant de 58 $ (US) pour la série, ou de 23 $ (US) pour le troisième volume seulement, doit être ajouté pour les frais d'expédition par avion. Toutes les commandes outremer doivent être payées en argent américain par l'entremise d'une banque américaine ou d'une banque étrangère reliée à une banque américaine. Les commandes doivent être adressées à la Noise Control Foundation, C.P. 2469 Arlington Branch, Poughkeepsie, NY 12603, USA.

# The Canadian Acoustical Association
# l'Association Canadienne d'Acoustique

## ANNONCE DE PRIX

Plusieurs prix, dont les objectifs généraux sont décrits ci-dessous, sont décernés par l'Association Canadienne d'Acoustique. Quant aux quatre premiers prix, les candidats doivent soumettre un formulaire de demande ainsi que la documentation associée avant le dernier jour de février de l'année durant laquelle le prix sera décerné. Toutes les demandes seront analysées par des sous-comités nommés par le président et la chambre des directeurs de l'Association. Les décisions seront finales et sans appel. L'Association se réserve le droit de ne pas décerner les prix une année donnée. Pour certains des prix, les candidats doivent être membres de l'Association. La préférence sera donnée aux citoyens et aux résidents permanents du Canada. Les candidats potentiels peuvent se procurer de plus amples détails sur les prix, leurs conditions d'éligibilité, ainsi que des formulaires de demande auprès de: Le Secretaire, Association Canadienne d'Acoustique, C.P. 1351, Station F, Toronto, Ontario M4Y 2V9.

### Prix Post-Doctoral Edgar et Millicent Shaw en Acoustique

Ce prix est attribué à un(e) candidat(e) hautement qualifié(e) et détenteur(rice) d'un doctorat ou l'équivalent qui a complèté(e) ses études et sa formation de chercheur et qui désire acquérir jusqu'à deux années de formation supervisée de recherche dans un établissement reconnu. Le thème de recherche proposée doit être relié à un domaine de l'acoustique, de la psycho-acoustique, de la communication verbale ou du bruit. La recherche doit être menée dans un autre milieu que celui où le candidat a obtenu son doctorat. Le prix est de $3000 pour une recherche plein temps de 12 mois avec possibilité de renouvellement pour une deuxième année. Coordonnatrice: Sharon Abel. Les récipiendaires antérieur(e)s sont:

*1990 Dr. Li Cheng, Université de Sherbrooke*

### Prix Etudiant Alexander Graham Bell en Communication Verbale et Acoustique Comportementale

Ce prix sera décerné à un(e) étudiant(e) inscrit(e) dans une institution académique canadienne et menant un projet de recherche en communication verbale ou acoustique comportementale. Il consiste en un montant en argent de $800 qui sera décerné annuellement. Coordonnatrice: Lynne Brewster. Les récipiendaires antérieur(e)s sont:

*1990 Bradley Frankland, Dalhousie University*
*1991 Steven Donald Turnbull, University of New Brunswick*
*Fangxin Chen, University of Alberta*
*Leonard E. Cornelisse, University of Western Ontario*

### Prix Etudiant Fessenden en Acoustique Sous-marine

Ce prix sera décerné à un(e) étudiant(e) inscrit(e) dans une institution académique canadienne et menant un projet de recherche en acoustique sous-marine ou dans une discipline scientifique reliée à l'acoustique sous-marine. Il consiste en un montant en argent de $500 qui sera décerné annuellement. Ce prix a été inauguré en 1991. Coordonnateur: David Chapman.

### Prix Etudiant Eckel en Controle du Bruit

Ce prix sera décerné à un(e) étudiant(e) inscrit(e) dans une institution académique canadienne dans n'importe quelle discipline de l'acoustique et menant un projet de recherche relié à l'avancement de la pratique en contrôle du bruit. Il consiste en un montant en argent de $500 qui sera décerné annuellement. Ce prix a été inauguré en 1991. Coordonnateur: Murray Hodgson.

### Prix des Directeurs

Trois prix sont décernés, à tous les ans, aux auteurs des trois meilleurs articles publiés dans l'*Acoustique Canadienne*. Le premier auteur doit étudier ou travailler au Canada. Tout manuscrit rapportant des résultats originaux ou faisant le point sur l'état des connaissances dans un domaine particulier sont éligibles; les notes techniques ne le sont pas. Le premier prix, de $500, est décerné à un(e) étudiant(e) gradué(e). Le deuxième et le troisième prix, de $250 chaqun, sont décernés à des auteurs professionnels âgés de moins de 30 ans et de 30 ans et plus, respectivement. Coordonnatrice: Chantal Laroche.

### Prix de Presentation Etudiant

Trois prix, de $500 chaqun, sont décernés annuellement aux étudiant(e)s sous-gradué(e)s ou gradué(e)s présentant les meilleures communications lors de la Semaine de l'Acoustique Canadienne. La demande doit se faire lors de la soumission du résumé. Coordonnateur: Alberto Behar.

# The Canadian Acoustical Association
# l'Association Canadienne d'Acoustique

## PRIZE ANNOUNCEMENT

A number of prizes, whose general objectives are described below, are offered by the Canadian Acoustical Association. As to the first four prizes, applicants must submit an application form and supporting documentation before the end of February of the year the award is to be made. Applications are reviewed by subcommittees named by the President and Board of Directors of the Association. Decisions are final and cannot be appealed. The Association reserves the right not to make the awards in any year. For some awards applicants must be members of the Canadian Acoustical Association. Preference will be given to citizens and permanent residents of Canada. Potential applicants can obtain full details of the prizes and their eligibility conditions, as well as application forms and procedures from: The Secretary, Canadian Acoustical Association, P.O. Box 1351, Station F, Toronto, Ontario M4Y 2V9.

### Edgar and Millicent Shaw Postdoctoral Prize in Acoustics

This prize is made to a highly qualified candidate holding a Ph.D. degree or the equivalent, who has completed all formal academic and research training and who wishes to acquire up to two years supervised research training in an established setting. The proposed research must be related to some area of acoustics, psychoacoustics, speech communication or noise. The research must be carried out in a setting other than the one in which the Ph.D. degree was earned. The prize is for $3000 for full-time research for twelve months, and may be renewed for a second year. Coordinator: Sharon Abel. Past recipients are:

*1990 Dr. Li Cheng, Université de Sherbrooke*

### Alexander Graham Bell Graduate Student Prize In Speech Communication and Behavioural Acoustics

The prize is made to a graduate student enrolled at a Canadian academic institution and conducting research in the field of speech communication or behavioural acoustics. It consists of an $800 cash prize to be awarded annually. Coordinator: Lynne Brewster. Past recipients are:

*1990 Bradley Frankland, Dalhousie University*
*1991 Steven Donald Turnbull, University of New Brunswick*
*Fangxin Chen, University of Alberta*
*Leonard E. Cornelisse, University of Western Ontario*

### Fessenden Student Prize in Underwater Acoustics

The prize is made to a graduate student enrolled at a Canadian university and conducting research in underwater acoustics or in a branch of science closely connected to underwater acoustics. It consists of a $500 cash prize to be awarded annually. The prize was inaugurated in 1991. Coordinator: David Chapman.

### Eckel Student Prize in Noise Control

The prize is made to a graduate student enrolled at a Canadian academic institution pursuing studies in any discipline of acoustics and conducting research related to the advancement of the practice of noise control. It consists of a $500 cash prize to be awarded annually. The prize was inaugurated in 1991. Coordinator: Murray Hodgson.

### Directors' Awards

Three awards are made annually to the authors of the best papers published in *Canadian Acoustics*. The first author must study or work in Canada. All papers reporting new results as well as review and tutorial papers are eligible; technical notes are not. The first award, for $500, is made to a graduate student author. The second and third awards, each for $250, are made to professional authors under 30 years of age and 30 years of age or older, respectively. Coordinator: Chantal Laroche.

### Student Presentation Awards

Three awards of $500 each are made annually to the undergraduate or graduate students making the best presentations during the technical sessions of Acoustics Week in Canada. Application must be made at the time of submission of the abstract. Coordinator: Alberto Behar.

## INSTRUCTIONS TO AUTHORS
## PREPARATION OF MANUSCRIPT

**Submissions**: The original manuscript and two copies should be sent to the Editor-in-Chief.

**General Presentation**: Papers should be submitted in camera-ready format. Paper size 8.5" x 11". If you have access to a word processor, copy as closely as possible the format of the articles in Canadian Acoustics 18(4) 1990. All text in Times-Roman 10 pt font, with single (12 pt) spacing. Main body of text in two columns separated by 0.25". One line space between paragraphs.

**Margins**: Top - title page: 1.25"; other pages, 0.75"; bottom, 1" minimum; sides, 0.75".

**Title**: Bold, 14 pt with 14 pt spacing, upper case, centered.

**Authors/addresses**: Names and full mailing addresses, 10 pt with single (12 pt) spacing, upper and lower case, centered. Names in bold text.

**Abstracts**: English and French versions. Headings, 12 pt bold, upper case, centered. Indent text 0.5" on both sides.

**Headings**: Headings to be in 12 pt bold, Times-Roman font. Number at the left margin and indent text 0.5". Main headings, numbered as 1, 2, 3, ... to be in upper case. Sub-headings numbered as 1.1, 1.2, 1.3, ... in upper and lower case. Sub-sub-headings not numbered, in upper and lower case, underlined.

**Equations**: Minimize. Place in text if short. Numbered.

**Figures/Tables**: Keep small. Insert in text at top or bottom of page. Name as "Figure 1, 2, ..." Caption in 9 pt with single (12 pt) spacing. Leave 0.5" between text.

**Photographs**: Submit original glossy, black and white photograph.

**References**: Cite in text and list at end in any consistent format, 9 pt with single (12 pt) spacing.

**Page numbers**: In light pencil at the bottom of each page.

**Reprints**: Can be ordered at time of acceptance of paper.

## DIRECTIVES A L'INTENTION DES AUTEURS
## PREPARATION DES MANUSCRITS

**Soumissions**: Le manuscrit original ainsi que deux copies doivent être soumis au rédacteur-en-chef.

**Présentation générale**: Le manuscript doit comprendre le collage. Dimensions des pages, 8.5" x 11". Si vous avez accès à un système de traitement de texte, dans la mesure du possible, suivre le format des articles dans l'Acoustique Canadienne 18(4) 1990. Tout le texte doit être en caractères Times-Roman, 10 pt et à simple (12 pt) interligne. Le texte principal doit être en deux colonnes séparées d'un espace de 0.25". Les paragraphes sont séparés d'un espace d'une ligne.

**Marges**: Dans le haut - page titre, 1.25"; autres pages, 0.75"; dans le bas, 1" minimum; aux côtés, 0.75".

**Titre du manuscrit**: 14 pt à 14 pt interligne, lettres majuscules, caractères gras. Centré.

**Auteurs/adresses**: Noms et adresses postales. Lettres majuscules et minuscules, 10 pt à simple (12 pt) interligne. Centré. Les noms doivent être en caractères gras.

**Sommaire**: En versions anglaise et française. Titre en 12 pt, lettres majuscules, caractères gras, centré. Paragraphe 0.5" en alinéa de la marge, des 2 cotés.

**Titres des sections**: Tous en caractères gras, 12 pt, Times-Roman. Premiers titres: numéroter 1, 2, 3, ..., en lettres majuscules; sous-titres: numéroter 1.1, 1.2, 1.3, ..., en lettres majuscules et minuscules; sous-sous-titres: ne pas numéroter, en lettres majuscules et minuscules et soulignés.

**Equations**: Les minimizer. Les insérer dans le texte si elles sont courtes. Les numéroter.

**Figures/Tableaux**: De petites tailles. Les insérer dans le texte dans le haut ou dans le bas de la page. Les nommer "Figure 1, 2, 3,..." Légende en 9 pt à simple (12 pt) interligne. Laisser un espace de 0.5" entre le texte.

**Photographies**: Soumettre la photographie originale sur paper glacé, noir et blanc.

**Références**: Les citer dans le texte et en faire la liste à la fin du document, en format uniforme, 9 pt à simple (12 pt) interligne.

**Pagination**: Au crayon pâle, au bas de chaque page.

**Tirés-à-part**: Ils peuvent être commandés au moment de l'acceptation du manuscrit.

## WHAT'S NEW ??

| | |
|---|---|
| Moves | Retirements |
| Deaths | Degrees awarded |
| New jobs | Distinctions |
| Promotions | Other news |

Do you have any news that you would like to share with *Canadian Acoustics* readers? If so, fill in and send this form to:

## QUOI DE NEUF ??

| | |
|---|---|
| Déménagements | Retraites |
| Décès | Obtention de diplômes |
| Offre d'emploi | Distinctions |
| Promotions | Autres nouvelles |

Avez-vous des nouvelles que vous aimeriez partager avec les lecteurs de l'*Acoustique Canadienne*? Si oui, écrivez-les et envoyer le formulaire à:

Jim Desormeaux, Ontario Hydro, 757 McKay Road, Pickering, Ontario L1W 3C8

The Canadian Acoustical Association


l'Association Canadienne d'Acoustique

## SUBSCRIPTION INVOICE

Subscription for the current calendar year is due January 31. Subscriptions received before July 1 will be applied to the current year and include that year's back issues of Canadian Acoustics, if available. Subscriptions received from July 1 will be applied to the next year.

Check ONE Item Only:

| | |
|---|---|
| CAA Membership | $35 |
| CAA Student membership | $10 |
| Corporate Subscription | $35 |
| Sustaining Subscription | $150 |

Total Remitted $_____

INFORMATION FOR MEMBERSHIP DIRECTORY

Check areas of interest (max 3):

1. Architectural Acoustics _____
2. Electroacoustics _____
3. Ultrasonics & Physical Acoustics _____
4. Musical Acoustics _____
5. Noise _____
6. Psycho/Physiological Acoustics _____
7. Shock & Vibration _____
8. Speech Communication _____
9. Underwater Communication _____
10. Other _____

## FACTURE D'ABONNEMENT

L'abonnement pour la présente année est dû le 31 janvier. Les abonnements reçus avant le 1 juillet s'appliquent à l'année courante et incluent les ancient numéros (non-épuisés) de l'Acoustique Canadienne de cette année. Les abonnements reçus à partir du 1 juillet s'appliquent à l'année suivante.

Cocher la case appropriée :

| | |
|---|---|
| Membre individuel | |
| Membre étudiant(e) | |
| Membre de société | |
| Abonnement de soutien | |

Versement total

RENSEIGNEMENT POUR L'ANNUAIRE DES MEMBRES

Cocher vos champs d'intérêt (max. 3):

1. Acoustique architecturale _____
2. Electroacoustique _____
3. Ultrasons, acoustique physique _____
4. Acoustique musicale _____
5. Bruit _____
6. Physio/psychoacoustique _____
7. Chocs et vibrations _____
8. Communication parlée _____
9. Acoustique sous-marine _____
10. Autre _____

Telephone number (_____) _____ Numéro de téléphone
Facsimile number (_____) _____ Numéro de télécopieur
E-Mail number _____ Numéro de courier électronique

PLEASE TYPE NAME AND ADDRESS BELOW:

VEUILLEZ ECRIRE VOTRE NOM ET VOTRE ADRESSE CI-DESSOUS:

Faites parvenir ce formulaire à l'adresse suivante en prenant soin d'y joindre un chèque fait au nom de L'ASSOCIATION CANADIENNE D'ACOUSTIQUE:

Make cheques payable to THE CANADIAN ACOUSTICAL ASSOCIATION. Mail this form with payment to:

W.V. Sydenborgh
H.L. Blachford Ltd.
2323 Royal Windsor Drive
Mississauga, Ontario L5J 1K5

# The Canadian Acoustical Association
# l'Association Canadienne d'Acoustique

## SUSTAINING SUBSCRIBERS / ABONNES DE SOUTIEN

The Canadian Acoustical Association gratefully acknowledges the financial assistance of the Sustaining Subscribers listed below. Annual donations (of $150.00 or more) enable the journal to be distributed to all at a reasonable cost. Sustaining Subscribers receive the journal free of charge. Please address donation (made payable to the Canadian Acoustical Association) to the Associate Editor (Advertising).

L'Association Canadienne d'Acoustique tient à témoigner sa reconnaissance à l'égard de ses Abonnés de Soutien en publiant ci-dessous leur nom et leur adresse. En amortissant les coûts de publication et de distribution, les dons annuels (de $150.00 et plus) rendent le journal accessible à tous nos membres. Les Abonnés de Soutien reçoivent le journal gratuitement. Pour devenir un Abonné de Soutien, faites parvenir vos dons (chèque ou mandat-poste fait ou nom de l'Association Canadienne d'Acoustique) au rédacteur associé (publicité).

**Acoustec Inc**
935 rue Newton, suite 103
Québec, Québec G1P 4M2
Tél: (418) 877-6351

**Barman Swallow Associates**
1 Greenboro Dr., Suite 401
Rexdale, Ontario M9W 1C8
Tel: (416) 245-7501

**Barron Kennedy Lyzun & Assoc.**
#250-145 West 17th Street
North Vancouver, BC V7M 3G4
Tel: (604) 988-2508

**H.L. Blachford Ltd.**
Noise Control Products
Engineering / Manufacturing
Mississauga: Tel.: (416) 823-3200
Montreal: Tel: (514) 938-9775
Vancouver: Tel: (604) 263-1561

**Bolstad Engineering Associates**
9249 - 48 Street
Edmonton, Alberta T6B 2R9
Tel: (403) 465-5317

**Bruel & Kjaer Canada Limited**
90 Leacock Road
Pointe Claire, Québec H9R 1H1
Tel: (514) 695-8225

**BVA Systems Ltd.**
2215 Midland Avenue
Scarborough, Ontario M1P 3E7
Tel: (416) 291-7371

**J.E. Coulter Associates Engineering**
1200 Sheppard Avenue East
Suite 507
Willowdale, Ontario M2K 2S5
Tel: (416) 502-8598

**Dalimar Instruments Inc.**
P.O. Box 110
Ste-Anne-de-Bellevue
Québec H9X 3L4
Tél: (514) 453-0033

**Eckel Industries of Canada Ltd.**
Noise Control Products, Audiometric
Rooms - Anechoic Chambers
P.O. Box 776
Morrisburg, Ontario K0C 1X0
Tel:(613) 543-2967

**Electro-Medical Instrument Ltd.**
Audiometric Rooms and Equipment
349 Davis Road
Oakville, Ontario L6J 5E8
Tel:(416) 845-8900

**Environmental Acoustics Inc.**
Unit 22, 5359 Timberlea Blvd.
Mississauga, Ontario L4W 4N5
Tel: (416) 238-1077

**Fabra-Wall**
Box 5117, Station E
Edmonton, Alberta T5P 4C5
Tel: (403) 987-4444

**Hatch Associates Ltd.**
Attn.: Tim Kelsall
2800 Speakman Drive
Mississauga, Ontario L5K 2R7
Tel: (416) 855-7600

**Hugh W. Jones Ltd.**
374 Viewmount Drive
Allen Heights
Tantallon, Nova Scotia B0J 3J0
Tel: (902) 826-7922

**Industrial Metal Fabricators Ltd.**
Environmental Noise Control
288 Inshes Avenue
Chatham, Ontario N7M 5L1
Tel: (519) 354-4270

**Larson Davis Laboratories**
1681 West 820 North
Provo, Utah, USA 84601
Tel: (801) 375-0177

**Mechanical Engineering Acoustics and Noise Unit**
Dept. of Mechanical Engineering
6720 30th St.
Edmonton, Alberta T6P 1J3
Tel: (403) 466-6465

**MJM Conseillers en Acoustique Inc.**
**M.J.M. Acoustical Consultants Inc.**
Bureau 440, 6555 Côte des Neiges
Montréal, Québec H3S 2A6
Tél: (514) 737-9811

**Nelson Industries Inc.**
Corporate Research Department
P.O. Box 600
Stoughton, Wisconsin, USA 53589-0600
Tel: (608) 873-4373

**OZA Inspections Ltd.**
P.O. Box 271
Grimsby, Ontario L3M 4G5
Tel: (416) 945-5471

**Scantek Inc.**
Sound and Vibration Instrumentation
916 Gist Avenue
Silver Spring, Maryland, USA 20910
Tel: (301) 495-7738

**Spaarg Engineering Limited**
Noise and Vibration Analysis
822 Lounsborough Street
Windsor, Ontario N9G 1G3
Tel: (519) 972-0677

**Tacet Engineering Limited**
Consultants in Vibration & Acoustical Design
111 Ava Road
Toronto, Ontario M6C 1W2
Tel: (416) 782-0298

**Triad Acoustics**
Box 23006
Milton, Ontario L9T 5B4
Tel: (800) 265-2005

**Valcoustics Canada Ltd.**
30 Wertheim Court, Unit 25
Richmond Hill, Ontario L4B 1B9
Tel: (416) 764-5223

**Vibron Limited**
1720 Meyerside Drive
Mississauga, Ontario L5T 1A3
Tel:(416) 670-4922

**Wilrep Ltd.**
1515 Matheson Blvd. E.
Mississauga, Ontario L4W 2P5
Tel: (416) 625-8944